

Sources, Quality, and Fate of Organic Matter in Deep-Sea Sediments in the Larsen A
Embayment, Weddell Sea: Changes by Global Warming and Ice Shelf Melt

by

Megumi S. Shimizu

Marine Science and Conservation
Duke University

Date: _____

Approved:

Cindy L. Van Dover, Chair

Kai-Uwe Hinrichs

Dana E. Hunt

Nicolas M. Cassar

Dissertation submitted in partial fulfillment of
the requirements for the degree of Doctor
of Philosophy in Marine Science and Conservation in the Graduate School
of Duke University

2017

ABSTRACT

Source, Quality, and Fate of Organic Matter in Deep-Sea Sediments in the Larsen A
Embayment, Weddell Sea: Changes by Global Warming and Ice Shelf Melt

by

Megumi S. Shimizu

Marine Science and Conservation
Duke University

Date: _____

Approved:

Cindy L. Van Dover, Chair

Kai-Uwe Hinrichs

Dana E. Hunt

Nicolas M. Cassar

An abstract of a dissertation submitted in partial
fulfillment of the requirements for the degree
of Doctor of Philosophy in
Marine Science and Conservation in the Graduate School of
Duke University

2017

Copyright by
Megumi S. Shimizu
2017

Abstract

Ice shelf coverage in Antarctica is declining due to recent global warming. The northern part of Larsen Ice Shelf, the Larsen A in the Weddell Sea, has been decreasing since the 19th century and in 2000 finally disappeared. Ice shelf coverage decrease should dramatically enhance biological productivity in surface water and organic matter flux to the seafloor. This dissertation examines sources of organic matter to sediments, indicators of labile organic matter flux increase due to the ice-shelf collapse, and potential subsequent impacts of changing ocean productivity on the sedimentary microbial community in the sediment cores taken across a 170-year chronoseries of ice-shelf loss, five-transect stations. Characterizing lipid biomarkers, phytoplankton (rather than terrestrially derived organic material) was identified as the major source of organic matter in the sediments, as previously found in other nearshore Antarctic regions. The predominance of C₁₆, C₁₈, and C₂₀ fatty acids, 24-methylenecholesterol, sitosterol, and ¹³C-enriched sea-ice diatom biomarker (C_{25.2} HBIs) indicate the importance of organic matter inputs from sea-ice diatom communities that become more dominant as the prevalence of sea ice coverage once the ice shelf disappears. Bacterial and Archaeal lipids were second and third largest lipid sources. These lipids could be sourced from the water column and in situ production as well as former ice shelf and ice-rafted debris. Using the vertical lipid distributions, diagenetic models were applied to estimate the

pelagic lipid flux before and after the ice shelf collapse. The results suggest that the rapid increase in flux due to the ice shelf disintegration, but further characterization of degradation rates need to be undertaken to increase confidence in the magnitude of this increased flux. Lipid flux increase may induce a shift in the microbial community structure in the sediments. Multivariate analyses identified that the organic matter content and $\delta^{13}\text{C}_{\text{TOC}}$ values, relative abundances of labile and recalcitrant lipid biomarkers, and concentrations of nitrogen species are important factors that correlate with downcore and cross-shelf microbial community composition. Enriched organic matter content (electron donor) may influence the microbial community through the decreased availability of electron acceptors in the sediments. The quality of the organic matter may also influence the microbial community: microbes that use recalcitrant organic matter shift to phytodetritus degraders as more-labile organic matter is delivered to the seabed following ice-shelf collapse. These results will offer a new perspective on the potential impacts of the ice-shelf disintegration to the subseafloor environment. Further investigations are needed to quantify the flux increase and microbial degradation rates of organic matter to expand the knowledge on influences of glacier melt on biogeochemical cycle.

Dedication

This dissertation is dedicated to the memory of my grandfather, Ikuo Shimizu, who encouraged me starting this journey but passed away when I was in the research cruise in the Antarctica for this dissertation research.

I believe his spirit must have traveled to Antarctica.

Contents

Abstract	iv
List of Tables	xii
List of Figures	xiv
Acknowledgements	xviii
1. General Introduction	1
1.1 Global warming in polar environments and ice retreat.....	1
1.2 Ecological impacts of ice shelf melt	2
1.3 Lipid biomarkers in marine sediments	6
1.4 Research Objectives.....	8
2. Distributions and Sources of Lipid Biomarkers Across the Larsen A Embayment, Weddell Sea	10
2.1 Introduction.....	10
2.2 Materials and Methods.....	13
2.2.1 Sampling.....	13
2.2.2 Lipid Analysis.....	15
2.2.3 Total organic carbon contents and stable carbon isotope values	17
2.2.4 Compound-specific stable carbon isotope measurement of HBIs.....	18
2.2.5 Trapezoidal numerical integration	18
2.2.6 BIT Index.....	18
2.2.7 Statistical Analysis.....	19
2.2.8 Principal component analysis.....	19

2.3 Results and Discussion	20
2.3.1 General description of total organic carbon characteristics and lipid biomarkers.....	20
2.3.1.1 TOC (concentration and stable isotopic composition).....	20
2.3.1.2 Total lipid classes	26
2.3.1.3 Fatty Acids	26
2.3.1.4 Sterols	29
2.3.1.5 Hydrocarbons – Highly branched isoprenoids	32
2.3.1.6 Hydrocarbons – <i>n</i> -alkanes.....	34
2.3.1.7 Ketones	38
2.3.1.7 GDGTs and ARs.....	39
2.3.1.8 Branched GDGTs	40
2.3.2 TOC and lipid biomarker inventories across the transect.....	44
2.3.4 Principal component analysis.....	49
2.5 Conclusions	53
3. Increasing organic matter flux to the seafloor and reactivity in the sediments following the ice shelf collapse in the Larsen A Embayment, Antarctica.....	55
3.1 Introduction.....	55
3.2 Materials and Methods.....	59
3.2.1 Sampling.....	59
3.2.2 Lipid input estimation with diagenetic models.....	60
3.2.3.1 Parameters used in model calculations.....	65
3.2.3.2 Biodiffusion-advection-reaction model	65

3.2.3.3	Steady-state biodiffusion-reaction model.....	67
3.2.3.4	Non-steady-state biodiffusion-reaction model.....	69
3.2.3.2	First-Order Reaction (G) Model.....	71
3.2.3.3	Sensitivity Analysis	73
3.2.3.4	Lipid Flux Response.....	74
3.2.4	Statistical Analysis	76
3.3	Results	77
3.3.1	Pelagic lipid distributions and flux at Reference Station K.....	77
3.3.2	Total Pelagic Lipid Flux, Stations G – I post-ice-shelf collapse (biodiffusion zone).....	77
3.3.3	Reactivity (degradation rate constant)	82
3.3.4	Sensitivity Analyses	83
3.3.5	Potential increase in lipid flux following the ice shelf collapse	86
3.4	Discussion.....	92
3.4.1	Biodiffusion rate assumptions and uncertainties in Larsen A Embayment before and after the ice shelf disintegration	92
3.4.2	<i>Post-ice-shelf collapse lipid fluxes across the Larsen A Embayment</i>	94
3.4.3	Factors controlling organic matter reactivity in sediments.....	97
3.4.3.1	Quality of organic matter.....	97
3.4.3.2	Oxidation.....	98
3.4.4	Limitation of diagenetic models.....	99
3.4.5	Dramatic increase in flux response and ecological implications.....	100
3.5	Appendix: Flux modeling using TOC	102

4. Quality and sources of organic matter shape microbial community in sediments after the ice shelf collapse in the Larsen A embayment	104
4.1 Introduction.....	104
4.2 Materials and Methods.....	107
4.2.1 Sampling.....	107
4.2.2 Geochemical analyses	108
4.2.3 Microprobe analyses	109
4.2.4 DNA analysis.....	110
4.2.5 Statistical Analyses.....	111
4.2.5.1 Community diversity	111
4.2.5.2 Multivariate analyses – with all environmental variables	112
4.2.5.3 Multivariate analyses – with lipid biomarkers	113
4.2.5.4 Clustering Analysis	113
4.2.6 Metagenome prediction.....	114
4.3 Results and Discussion	115
4.3.1 Geochemical distribution	115
4.3.2 Bacterial and Archaeal Distributions and Diversity.....	119
4.3.3 Environmental Drivers of Bacterial and Archaeal Diversity	121
4.3.4 Source and Lability of Organic Matter Shape Microbial Community	123
4.3.5 Microbial functional clusters	127
4.3.5.1 Cluster I.....	129
4.3.5.2 Clusters IIa, IIb, and IIc.....	130

4.3.5.3 Cluster III.....	131
4.3.5.4 Clusters IVa and IVb	132
4.3.6 Metagenome prediction.....	138
4.4 Conclusions	144
5. Conclusions.....	146

List of Tables

Table 1: Sampling station positions and water depths	14
Table 2: TOC contents and $\delta^{13}\text{C}$, lipid concentrations, and relative abundance within fatty acids, sterols, hydrocarbons, ketones, and core GDGTs and ARs in surface (0-1 cm) (n = 3 replicate samples per analysis) and bottom (18-20cm) sediments (n=1 sample per analysis) at five sampling stations (G-K). \pm Standard deviation for %TOC, $\delta^{13}\text{C}$ TOC, and total concentrations. n.a.: not available	24
Table 3: List of lipid biomarker compounds and groups identified and their major sources	46
Table 4: Sediment conditions, stations and sediment datasets, models applied, and their assumptions	63
Table 5: The lipid biomarkers and their sources used in this study	64
Table 6: Sediment parameters used for modeling lipid biomarker distributions. Biodiffusion rate coefficient D_B , non-steady state model of the distribution of ^{210}Pb activity; determined by R. Taylor (NCSU), sediment burial velocity ω , organic ^{14}C analysis at 20-35 cm depth; determined by R Taylor (NCSU); time since ice-shelf collapse (Ferrigno, 2006), and thickness of sediment layer accumulate after ice shelf collapse that was calculated from sediment burial velocity and time since ice shelf collapse.	65
Table 7: The combinations of biodiffusion rate coefficients used to calculate three scenarios of lipid flux responses	76
Table 8: Flux and degradation rate constant of lipid biomarkers in post-ice-shelf collapse sediments (top 8 cm for station G, top 10 cm for stations H – J, and whole 20 cm for the reference station K) determined using the diffusion-(advection)-reaction model	89
Table 9: Flux and degradation rate constant of lipid biomarkers in pre-ice-shelf collapse sediments (8-20 cm for station G and 10-20 cm for station H – J) determined using the degradation model.....	90
Table 10: Biodiffusion rate coefficients (D_b) and tracer methodology in coastal, pelagic/deep-sea, and Antarctic continental shelves sediments	93

Table 11: POC fluxes in previous studies and the conversion to lipid flux. * POC/POM= 0.5 using elemental ratio (Martiny et al., 2013), contribution of lipids in POM is 1% (Burdige, 2006). Net community production (NCP) and net primary production (NPP) based carbon exports were calculated using adjusted Martin's curve (Grebmeier and Barry, 2007; Martin et al., 1987)..... 96

Table 12: Lipid biomarker compound groups that used for RDA and their sources..... 125

List of Figures

Figure 1: The study site, Larsen A embayment map with ice shelf front changes (Ferrigno et al. 2006) and five cross-shelf sampling stations. Numbers in boxes represent the year of ice shelf front.....	15
Figure 2: Downcore profiles of total organic carbon (TOC) concentrations and total lipid concentrations at cross-shelf transect stations (G-K). bsf: below sea floor	23
Figure 3: Relative abundances of fatty acids in 11 depths of sediment cores from each sampling station.....	27
Figure 4: Distribution of C ₂₇ , C ₂₈ , and C ₂₉ sterols in the sediments (0-20 cm) in Station G – K, and in previously studied Antarctic sites.	31
Figure 5: Mass spectra of highly branched isoprenoids (HBIs), (a) C _{25:2} , (b) C _{25:3} , (c) C _{30:5} I, and (d) C _{30:5} II	34
Figure 6: <i>n</i> -alkanes relative abundances in sediment downcore and across the embayment ACL: average chain length of C ₁₇ to C ₃₆ <i>n</i> -alkanes	36
Figure 7: Downcore profiles of carbon preference index (CPI) for <i>n</i> -alkane carbon number ranges C ₂₄ -C ₃₄ , C ₂₆ -C ₃₆ , and C ₂₀ -C ₂₆	37
Figure 8: Downcore profiles of branched isoprenoid tetraether (BIT) index	42
Figure 9: Bar plots with a standard deviation of average branched GDGT distribution in the five sampling stations (n = 11 for each station). Roman numerals refer to the structures; I, II and III are branched GDGTs without cyclopentane; Ib, IIb, and IIIb are branched GDGTs with one cyclopentane; Ic, IIc, and IIIc are branched GDGTs with two cyclopentane.	43
Figure 10: Inventories of TOC and lipids in 20-cm sediment cores across the sampling stations; a) TOC and total lipids inventories; b) phytoplankton, bacterial and archaeal biomarkers inventories. Biomarker assignments are on Table 3.....	45
Figure 11: Sediment lipid biomarker variable loadings and sample scores for the first two principal components identified by a PCA model based on relative abundance of fatty acids, sterols, hydrocarbons, ketones and core GDGTs (see material and method for details). (A) Biomarker variable loadings (see Table 3 for abbreviations). Different colors	

indicate different sources. (B) Sediment sample scores; numbers indicate sediment depths (cm), color indicate sampling stations (see legend) and down core path is indicated by line.....	53
Figure 12: Schematic explanation of the models to estimate initial lipid concentrations for biodiffusion zone sediments and pre- collapse sediments in Station G - J. $C_{0,pre}$: extrapolated initial lipid concentration during the pre-ice-shelf collapse period, $C_{0,post}$; estimated initial lipid concentrations during post-ice-shelf collapse period.	75
Figure 13: Downcore distribution of lipid biomarkers at the reference station (K). The lipid biomarkers concentrations decrease logarithmically ($R^2 > 0.59$, $p < 0.01$).	77
Figure 14: Comparison of estimated total pelagic lipid fluxes applying different models, the steady-state and the non-steady-state biodiffusion-reaction models for biodiffusion zone sediments of Station G, H and I. Values on the bar plots represent the goodness of model fit (R^2).	79
Figure 15: Post-ice-shelf-collapse fluxes of lipid biomarkers across the embayment. a) estimated fluxes of total pelagic lipids; b) estimated fluxes of individual biomarkers; the fluxes for Station G estimated using the non-steady-state biodiffusion-reaction model, for Station H and I using the steady-state biodiffusion reaction model, and for Station J and K using the biodiffusion-advection-reaction model. Only the estimations made from the significant model fitting ($p < 0.1$) were shown here.	81
Figure 16: Pre-ice-shelf-collapse fluxes of lipid biomarkers across the embayment. a) fluxes of total pelagic lipids estimated without biodiffusion; d) fluxes of individual lipid biomarkers before the ice shelf collapse; c) fluxes of total pelagic lipids estimated with biodiffusion. Only the estimations made from the significant model fitting ($p < 0.1$) are shown here.	82
Figure 17: Box plots of estimated lipid degradation rate constants across the sampling stations. a) post-ice-shelf-collapse degradation rate constants. Significance levels; * represents $p < 0.05$; n.s. represents not significant. b) pre-ice-shelf-collapse degradation rate constants estimated without biodiffusion. c) pre-ice-shelf-collapse degradation rate constants estimated with biodiffusion.	83
Figure 18: Sensitivity analyses. a and b) The effect of varying the magnitudes of biodiffusion rate coefficient (D_b) and sediment burial velocity (ω) in biodiffusion-advection-reaction model for Condition 1 datasets. c) The effect of varying the magnitudes of D_b in biodiffusion-reaction model for Condition 2 datasets (Station G;	

non-steady state model and Stations H, and I; steady state model). d) The effect of varying the magnitudes of D_b in first-order reaction model ($D_b = 0$) and in bioturbation-advection-reaction model ($D_b > 0$) for Condition 3 datasets.	85
Figure 19: Changes in total pelagic lipid flux following ice shelf collapse in Stations G to J. Potential changes in flux at the reference station (K) was 0.6.	88
Figure 20: Downcore oxygen concentrations in each sampling stations from G to K	99
Figure 21: Downcore distribution of total organic carbon across the embayment.....	103
Figure 22. Downcore geochemistry profiles. Colors represent sampling stations. Error bars represent standard deviation (n=3 for O ₂ , pH, and surface samples of TOC, $\delta^{13}C_{TOC}$, and lipids; n=2 for Chl-a, Phao, Fe(II), silicate, phosphate, nitrate, nitrite, and Ammonium concentrations).....	118
Figure 23: Downcore profiles of the relative abundance of microbial taxonomic groups across the embayment. Top 10 abundant taxa are color coded with the label: o, order; f, family; g, genus	120
Figure 24: Non-metric multidimensional scaling (NMDS) plot of microbial communities based on Bray-Curtis dissimilarity for 16S rRNA gene libraries. The community profiles from each sample; a) color represents sampling stations. Ellipses represent 95% intervals around centroids for each sampling station. b) color represents sediment depth.	121
Figure 25: Canonical correspondence analysis (CCA) ordination diagram of axes one and two of the bacterial and archaeal community. CCA was conducted with selected environmental variables (lipid: lipid concentrations, TOC: total organic carbon, pH, phosphate, ammonium, $\delta^{13}C_{TOC}$, NO ₂ ⁻ : nitrite, NO ₃ ⁻ : nitrate). The percent of the variation in the community explained by each axis is in parenthesis. All the environmental variables were determined to be statistically significant using the marginal effect of the terms ($P < 0.002$). The variables are indicated as vectors. The community profiles from each sample are represented as circles; a) color represents sediment depth, b) color represents sampling stations.	123
Figure 26: Redundancy analysis (RDA) ordination diagram of axes one and two of the bacterial and archaeal community in samples from five cross-shelf Stations G – K. The percent of the variation in the community explained by each axis is in parenthesis. The variables (<i>n</i> -alkane, $\Delta^{5,22}$ sterols, C ₃₀ HBIs: highly branched isoprenoids, PAH: polyaromatic hydrocarbons, stenones, even-carbon MUFAs: mono-unsaturated fatty	

acids, sterol $C_{28}\Delta^5, 24(28)$:24-methylenecholesterol) are indicated as vectors. All of the lipid groups were determined to be statistically significant using the marginal effect of the terms ($P < 0.014$). The community profiles from each sample are represented as circles; a) color represents sediment depth, b) color represents sampling stations. Carbon sources of microbes 126

Figure 27: Pearson's correlation coefficients heat maps showing the association between environmental variables and the relative abundance of bacterial and archaeal clusters. a) The top dendrogram defines clusters of environmental variables and relative abundances of lipid biomarkers that best explain the microbial community (based on CCA and RDA). The left dendrogram defines clusters of taxonomic groups sharing similar correlations with environmental and lipid biomarker parameters. b) The bar plot shows DNA-weighted abundance of each taxonomic group. The side color maps show c) average relative abundances downcore (surface to bottom) and d) across the embayment (Station G to K). 128

Figure 28: The summary of the horizontal and vertical variability of microbial community characteristics. 136

Figure 29: Euclidian distance clustering that clusters of taxonomic groups sharing similar correlations with environmental and lipid biomarker parameters. Numbers on the nodes represent approximately unbiased P values were computed multiscale bootstrap resampling (10,000 iterations). Taxa labels, k, kingdom; p, phylum; c, class; o, order; f, family; g, genus. 138

Figure 30: Comparison of the mean relative abundance of KEGG orthologs (KOs) function groups between the top (0-10 cm) and bottom (10-20 cm) of sediment samples. All the relative abundances of KO groups were significantly different between top and bottom ($p < 0.006$). 141

Figure 31: Comparison of the mean relative abundance of KEGG orthologs (KOs) function groups among five sampling stations (G-K). All the relative abundances of KO groups at Station H and I were significantly different from Station G, J and K ($p < 0.05$). 143

Acknowledgements

This dissertation research was funded by the National Science Foundation Office of Polar Programs (ATN0732405 to CLVD), the Deutsche Forschungsgemeinschaft, Gottfried Wilhelm Leibniz Award (to K-UH). MSS was supported by the Japan Student Service Organization, Duke University, the Center for Dark Energy Biosphere Investigation (C-DEBI) and the European Association of Organic Geochemistry.

The completion of this dissertation would not have been possible without the contributions of many collaborators and the support of friends, and family members.

I would like to express the deepest appreciation to my committee chair, Dr. Cindy Van Dover, for her excellent guidance, caring, and patience. Since the day I picked up her book "The Octopus's Garden" in the college library back in Tokyo, she continually and convincingly conveyed a spirit of adventure regarding research and scholarship. Without her guidance and persistent help, this dissertation would not have been possible.

I would like to thank Dr. Kai-Uwe Hinrichs, who let me visit his lab at the University of Bremen. Visiting his lab was a great opportunity for me to learn lipid analysis techniques. I thank him for his support and his insightful comments and encouragement as well. I would also like to thank, Dr. Dana Hunt and Dr. Nicolas Cassar, who have generously given their time and expertise to guide my research for the

past several years and helping me to develop my background in microbiology and biogeochemistry. I thank them for their contribution and encouragement, but also for the hard questions, which incited me to widen my research from various perspectives.

My sincere thanks also go to LARISSA collaborators. Dr. Mike McCormick, who helped me from the beginning of the cruise sampling planning, throughout the cruise, and for four years after that. He continuously helped me to develop ideas to connect lipids and microbes in the sediments for the third chapter. Dr. David DeMaster and Rich Taylor shared sediment bioturbation coefficients and sediment age. Their help on the sediment diagenetic modeling was essential to develop my second chapter. Drs. Maria Vernet, Mattias Cape, Craig Smith, Pavica Sersen, Amy Leventer, and Eugene Domack, Bruce Huber, helped me to deepen my knowledge on the Larsen A Embayment.

I must acknowledge the colleagues and friends in Hinrichs Lab at MARUM and University of Bremen, for technical and intellectual support to my research over the years. Especially, I need to express my gratitude to Dr. Marcos Yoshinaga for training me all about lipids and for critiques on my work. Thanks to Dr. Marcus Elvert for sharing knowledge in identifying lipid biomarkers and assisting interpreting compound specific isotope analysis data, and raised my basic German speaking skill. Jenny Wendt and Xavier Prieto are acknowledged for their support of TOC and IRMS analyses. Many friends made Bremen my third home, Nadine Broda, Travis and Sanne Meador, Miriam

Scollich for sharing their home with me and took care of me living in Bremen. Nadine, Travis, Miriam, Julius, Lars, Kevin, and Felix also taught me many things in the lab and made great critiques to my work. My research would not have been possible without their assistance and hospitality.

Special thanks to Van Dover lab members and alumnus, Andrew, Sophie, David, Bernie, Jamie, and Phil. Many thanks to DUMML community; Rachel, Janil, Patty, Tom and Jerry for your support, and DUMML alumnus and friends; Abby, Yajuan, Chris, Charmaine, Yasmin, Mickey, Kersey, Maria, and Thais.

I would like to thank my parents, Yoshio and Kazumi Shimizu and my sister, Nozomi for supporting me and making sure that I am doing fine in the foreign country. I also would like to express gratitude to the Sutherland family, who made North Carolina a real home for me.

Finally, I would like to thank my husband, Jordan. He was always next to me, cheering me up or calming me down throughout this journey.

1. General Introduction

1.1 *Global warming in polar environments and ice retreat*

Recent global warming of Earth's atmosphere has increased sea surface temperature by a global average of 0.6 °C over the past century (Pachauri, 2008). The increased sea surface temperature has and continues to substantially reduce glaciers, ice sheets, and sea ice (Bintanja et al., 2013; Hoegh-Guldberg and Bruno, 2010). Polar environments have been the most affected by the air temperature increase (Hoegh-Guldberg and Bruno, 2010). Physical changes, such as sea surface temperature increase, stratification increase, and ice loss cause biological responses at multiple levels: physiology of individual organisms, population-level responses, and ecosystem structure and function (Doney et al., 2012). One of the most well-known changes in polar environments is that decreased in sea ice extent results in a decline of marine mammals and birds populations (Ducklow et al., 2013; Hoegh-Guldberg and Bruno, 2010). Sea ice plays a critical role for sea birds and mammals as habitat platforms. The population size of ice-dependent organisms such as polar bears (*Ursus maritimus*) in the Arctic, and Adélie penguins (*Pygoscelis adeliae*) and seals in Antarctica are decreasing in response to habitat loss, and these organisms are replaced with ice-tolerant species such as Chinstrap (*P. Antarctica*) and Gentoo (*P. papua*) penguins (Hoegh-Guldberg and Bruno, 2010; Schofield et al., 2010). Sea ice also supports particular food webs that are

dependent on sea-ice algae. The sea ice loss in the Southern Ocean explains declining krill populations (Atkinson et al., 2004). Yet the impacts of ice shelf collapse on ecosystems, including pelagic and benthic ecosystems, are not well explored.

The Antarctic Peninsula (AP) is greatly affected by global warming; locally the temperatures increase at a rate of 3.7 ± 1.6 °C (century)⁻¹, six times faster than the global average (Pachauri, 2008; Vaughan et al., 2003). Due to the regional warming, during the last 30 years, ice shelves along the Antarctic Peninsula have experienced more than 16000 km² of disintegration; the area is almost equivalent to the state of Georgia. For instance, 400 km² of the Wilkins Ice Shelf in the West Antarctic Peninsula disintegrated in 2008 (Scambos et al., 2009), and in the East Antarctic Peninsula, the Larsen B Ice Shelf has lost 3250 km² in 2004 (Scambos et al., 2004). North of the Larsen B, the Larsen A Ice Shelf had been retreating progressively since the 19th century, and a massive disintegration (1500 km²) occurred in 1995 (Rott et al., 1996; Schofield et al., 2010). It completely disappeared in 2000 (Ferrigno, 2006; Rott et al., 1996).

1.2 Ecological impacts of ice shelf melt

Ice shelves are thick floating ice extending from glaciers. Their thickness can be between 50 and 600 meters (National Snow and Ice Data Center, 2010), which does not allow sunlight to reach the water column beneath. Melting of ice shelves has direct impacts on the physical characteristics of the ocean: opening up the sea surface and

introducing sunlight to the ocean surface and changing ocean circulation patterns. These physical modifications could directly affect ecosystems (Doney et al., 2012).

Pelagic biota abundances increased after ice shelf collapse in the Larsen A Embayment. Phytoplankton can grow, and other fauna can expand their habitat into the opened sea surface. The Larsen A area is now a productive environment with nutrient-rich and high chlorophyll-a containing seawater (Bertolin and Schloss, 2009; Sañé et al., 2011b). The extent of primary productivity and the availability of organic matter influence the structure and abundances of heterotrophic communities including both macrofauna (Levin and Gage, 1998) and microorganisms (Horner-Devine et al., 2003). Phytoplankton blooms in the euphotic zone of the oceans serve as a food source for zooplankton (Löder et al., 2011) and other organisms. In the Larsen A embayment, typical Antarctic fish have become established, although abundances were ten times less than the eastern Weddell Sea at the time of an expedition in 2007 (Gutt et al., 2011). Minke whales (*Balaenoptera bonaerensis*) and seals were found in the Larsen A in a 2007 expedition (Gutt et al., 2011). Compared to the apparent increases of pelagic biota, the influence of ice shelf collapse on benthic fauna is elusive. In 2007, post-ice shelf collapse Larsen A macro- and meiobenthic fauna compositions were similar to those in northern Antarctic Peninsula area where have been open ocean at least 10,000 years. The species richness and density of these organisms were still an order of magnitude smaller than in

the northern AP (Gutt et al., 2011). Although most of the bloom biomass is remineralized in the food web of the euphotic zone, some of the organic matter escape degradation in the surface waters and is exported to the meso- and bathypelagic. Estimates on the amount of exported biomass range from around 2% (Fischer et al., 2000) to up to 50% (Smetacek et al., 2012). Settled particulate organic carbon (POC) is taken up by meio- and macrofaunal benthic communities as well as further utilized by microorganisms (Moodley et al., 2002; Witte et al., 2003). Benthic fauna survived under ice shelves with advected organic matter (Riddle et al., 2007). Therefore, the benthic fauna found in Larsen A could have been there even before the ice shelf collapse. Benthic community compositions, however, may be more dynamic than had been previously thought. Using a photo survey approach, Gutt (2013) found a dramatic decrease in benthic ascidians (*Molgula pedunculata*) and increases in deposit feeding ophiuroids in the Larsen A Embayment between 2007 and 2011. Although they could not elucidate environmental causes (e.g., ice shelf collapse, sea ice coverage, temperature, and salinity), this study showed that benthic community compositions and abundances could be dynamic in the intermediate to long term (Gutt et al., 2013).

Due to permanent darkness, most of the life in the abyssal seafloor is dependent on this input of photosynthesis- derived particulate organic carbon (POC) from the ocean surface (Jørgensen and Boetius, 2007; Sevastou et al., 2013). Sediment

geochemistry and microbial communities can undergo dramatic changes following ice shelf collapse. The organic inputs including vertical and lateral transport to the seafloor were minuscule before ice shelf collapse (Sañé et al., 2011b). A complete trophic regime shift from no production all year round to seasonal production in the sea surface could result in increased organic matter input as particulate organic matter to sediments. Increases in organic matter input to sediments affect the geochemical characteristics in sediment porewater. Enhanced microbial activities quickly consume oxygen in the surface sediments. The inputs of organic detritus also increase nitrogen species such as ammonium and nitrate. These changes in the geochemical setting could affect microbial community compositions. For example, increases in ammonium and nitrate in sediments can increase relative abundances of ammonium-oxidizing bacteria and archaea and nitrate reducers. The increase in organic matter input and changes in the carbon and the nitrogen cycles in Larsen A sediments are expected, but microbial composition and impacts of ice shelf collapse to microbial community in Larsen A embayment, however, have not yet been explored.

Although research expeditions can provide the data to monitor the post-ice-shelf-collapse ecosystem in the Larsen A Embayment, the dataset is limited to explain changes in ecosystems and organic matter flux to the seafloor before and after ice shelf collapse.

Lipid biomarkers accumulated in sediments could provide an opportunity to investigate the history of ecosystem changes affected by global warming.

1.3 Lipid biomarkers in marine sediments

Lipids are the major component of cell membranes of all living organisms.

Lipids are one of the most important biomolecules in organisms not only for building cell membranes but also for storing energy and maintaining membrane flexibility and transport. The lipid biomarkers are useful for two characteristics; 1) molecular structural diversity and 2) stable carbon isotope. The molecular structure is useful to trace certain organisms. Thus, the lipids in marine sediments can serve as biomarkers of organisms in the water column above the seafloor and sediments, beneath the seafloor. Carbon stable isotopes can elucidate carbon sources and/or carbon fixation pathways. Lipids also can serve as proxies to infer sea surface temperature (Schouten et al., 2002; Wuchter et al., 2004), the relative importance of terrestrial and marine organic matter input on the seafloor (Weijers et al., 2006a) and sea ice coverage (Belt et al., 2008; Massé et al., 2011). Lipid biomarkers are thus useful tools for understanding environmental changes in seawater and sediments on centennial or millennial timescales.

The structures of lipids are fundamentally different among the three domains (Archaea, Bacteria, and Eukarya). Archaeal lipids constituents are isoprenoidal chains attached to glycerol backbones through ether linkages as diether lipids (archaeol) or

tetraether lipids (glycerol dialkyl glycerol tetraether (GDGT) (Figure 1) (S.-V. Albers and Meyer, 2011; Koga et al., 1993). Bacterial and eukaryotic lipids contain two fatty acid chains attached to the backbones through ester linkages (Gurr et al., 2002). These fatty acids can be distinguished by the number of carbon atoms and the number of unsaturation.

The lipids in sediments stay as fossil biomarkers and degrade over time. Degradation and preservation of lipid biomarkers are controlled by lipid biomarker characteristics and environmental factors. For example, chemical structures of lipids determine reactivity and association with minerals that increase preservation (i.e., saturated fatty acids are more recalcitrant than poly-unsaturated fatty acids) (Wakeham and Canuel, 2006). Environmental factors such as temperature, dissolved oxygen availability, and concentrations of electron acceptors play important roles in degradation processes (Canuel and Martens, 1996). Thus, degradation rates vary among lipid biomarkers and locations. Lipids are some of the most recalcitrant biomolecules compared to, for example, proteins and DNA (Baldock et al., 2004; Sañé et al., 2011b). Although extracellular DNA that was released from cells after cell death exists in sediments, the amplifiable extracellular DNA is two orders of magnitude less than the amplifiable intracellular DNA (Corinaldesi et al., 2008). The turnover time of DNA is 12 to 93 days in shallow marine sediments (Dell'Anno and Corinaldesi, 2004; Lorenz and

Wackernagel, 1994), and relatively much shorter than lipids that could take more than 100 years to degrade (Burdige, 2006). Recalcitrant lipids in marine sediments originate from both the water column and the *in situ* microbial community. Lipids are useful to track organic matter sources and degradation in sediments.

Stable carbon isotope analysis helps to determine carbon sources and carbon cycle (Pancost and Sinninghe Damsté, 2003; Schubotz et al., 2011). Stable carbon isotopic values of lipids are determined by carbon sources and isotope fractionation during biological processes. The fractionation depends on the carbon fixation pathways that organisms use and CO₂ concentrations in the environment (Hayes, 2001). For example, the sea ice phytoplankton usually contains ¹³C-enriched lipids, because CO₂ availability in sea ice is limited (Rau et al., 1991). The combination of lipid analysis and the compound-specific stable carbon isotope data provide the insights of carbon sources and carbon cycles.

1.4 Research Objectives

This dissertation research aimed to understand the source, quality, and fate of organic matter in sediments in the Larsen A Embayment, including the changes in organic matter flux and microbial community after the ice shelf collapse. In the first chapter, lipid biomarker contents and their sources were explored. In the second chapter, changes in pelagic organic matter flux were quantified using vertical

distributions of lipid biomarkers in sediments through degradation, biodiffusion, and advection models. In the third chapter, the impacts of organic matter input and geochemical variables to the seafloor microorganisms were studied.

2. Distributions and Sources of Lipid Biomarkers Across the Larsen A Embayment, Weddell Sea

Megumi S Shimizu ^a, Marcos Y Yoshinaga ^b, Marcus Elvert ^b, Kai-Uwe Hinrichs ^b, Cindy Lee Van Dover ^a

^a Duke Marine Laboratory, Nicholas School of the Environment, Duke University, 135 Duke Marine Lab Road, Beaufort NC, USA

^b MARUM Center for Marine Environmental Sciences and Department of Geosciences, University of Bremen, Leobener Strasse 8, MARUM, 28359 Bremen, Germany

2.1 Introduction

Organic matter in marine sediments of the Southern Ocean is dominated by marine biogenic input because the area is largely free of anthropogenic activities and terrestrial vegetation. Evidence of this has been provided, for example, by a dominance of phytoplankton-derived lipid biomarkers such as C₁₆ fatty acids and dinosterol in surface sediments of McMurdo Sound (Eastern Antarctica) and the Bransfield Strait (Western Antarctic Peninsula) (Venkatesan, 1988; Venkatesan and Kaplan, 1987). Other sources of organic matter in the Antarctic shelf sediments include bacteria, archaea (Carr et al., 2013), zooplankton (Falk-Petersen et al., 1999; Kattner and Hagen, 1995) and marine mammals (Venkatesan et al., 1986; Venkatesan and Santiago, 1989). Particulate organic matter reaching the seafloor is available to the benthic fauna and

microorganisms. While benthic fauna usually consume fresh, labile organic matter (Smith et al., 1993), refractory organic matter can be degraded by microorganisms in sediments (Wakeham and Canuel, 2006). In cases of the Antarctic continental shelf, the labile organic matter could be well preserved in sediments because microbial respiration is limited by low temperatures and relatively lower substrate concentrations compared to shelf environments in warmer environments (Mincks et al., 2005).

Our study site, the Larsen A Embayment of the Eastern Antarctic Peninsula, has undergone a rapid transition from an ice-shelf-covered to a seasonal sea-ice-covered condition. Following the ice-shelf collapse, the Larsen A Embayment has become as productive as other non-ice-shelf-covered Antarctic Peninsula (AP) areas, with an annual net primary productivity (NPP) rate that reaches $200 \text{ g C m}^{-2} \text{ year}^{-1}$ (Cape et al., 2014). Abundances of pelagic biota have increased, including phytoplankton (Bertolin and Schloss, 2009; Sañé et al., 2011a), fish [e.g., Antarctic silverfish (Gutt et al., 2011)], and marine mammals [e.g., Antarctic Minke whales and seals (Gutt et al., 2011)]. These studies indicate a trophic regime shift from year-round no production to seasonal production in overlying surface waters of the Larsen A Embayment after the ice-shelf collapse. Moreover, enhanced planktonic production might result in increased particulate organic matter flux, which would be reflected in enhanced bulk carbohydrate, protein and lipid accumulation in sediments (Sañé et al., 2012). Although the Larsen A Embayment is free of the ice shelf, the embayment is covered by sea ice

most of the time. The annual duration of open water conditions ranges between 0-140 days (Cape et al., 2014). The duration is usually less than half that of the Western Antarctic Peninsula, where the sea-ice-free period usually lasts more than 160 days per year.

We explore the types and sources of lipid biomarkers and their distributions in sediments under current conditions of extensive sea-ice cover across the Larsen A Embayment. Total Organic Carbon (TOC), $\delta^{13}\text{C}_{\text{TOC}}$, and various lipid biomarker groups were examined in sediments collected across the embayment (Figure 1). Because lipids are relatively recalcitrant compared to other biomolecules such as DNA and proteins (Hedges, 1995; Wakeham and Canuel, 2006), they may serve as molecular records of sources of organic matter. Because certain types of lipids are synthesized by particular groups of organisms, they are often used to trace the presence and distribution of these organisms (Cranwell, 1982; Volkman et al., 1998). Lipid biomarker techniques thus have the potential to document past environmental and ecological changes and may be especially useful for understanding remote areas like polar regions that are difficult to access year-round.

2.2 Materials and Methods

2.1.1 Sampling

Sample collection at the Larsen A Embayment site was part of the multidisciplinary project “Larsen Ice Shelf System, Antarctica” (LARISSA). Sampling was conducted from 7 March to 17 April 2012, onboard the Research Vessel Ice Breaker (RVIB) *Nathaniel B Palmer* (NBP12-03) off the coast of the East Antarctic Peninsula, Weddell Sea (Maria Vernet, Chief Scientist). Sediments were collected using a multicorer (twelve 15-cm diameter cores per deployment, with each core spaced 10 cm to 100 cm apart) at five cross-shelf stations (Table1). The transect across the embayment represents a time window that covers ice-shelf-collapse from 1843 to 2000 (Figure 1). Due to the low sedimentation rate in the Larsen Embayment [Larsen A: $< 20 \text{ cm kyr}^{-1}$, R. Tayler and D. DeMaster, personal communication; Larsen B: $< 40 \text{ cm kyr}^{-1}$, (Sañé et al., 2011a)] the sediment layer that accumulated after ice-shelf collapse is limited to a maximum of a few centimeters. Bioturbation following ice-shelf collapse mixes newly deposited organic matter to depths of less than 10 cm in the sediment (Sañé et al., 2011a). Each sampling site (Station G to J) has a different historical record with respect to exposure to open waters and ice shelf-covered condition (Ferrigno, 2006). Station K (148 km offshore) serves as a reference station with no ice-shelf coverage since 10 ka BP (Davies et al., 2012) (Figure 1). Each core was sectioned on board immediately after sample recovery at 0.5-cm intervals to 2 cm, 1-cm intervals to 10 cm, and 2-cm intervals

from 10 cm to 20 cm. After sample processing, the sediment samples for lipid analysis were stored at -80 °C.

Table 1: Sampling station positions and water depths

Stations	Latitude/ Longitude	Ice shelf collapse (years)	Distances from the shore (km)	Water depths (m)
G	64°44.20'S / 60°35.32'W	1995 - 1997	11	688
H	64°48.20'S / 60°13.61'W	1989 - 1995	32	601
I	64°42.38'S / 59°35.83'W	1986 - 1989	56	601
J	64°39.59'S / 58°20.28'W	1843 - 1945	117	596
K (reference)	64°59.61'S / 57°45.30'W	-	148	424

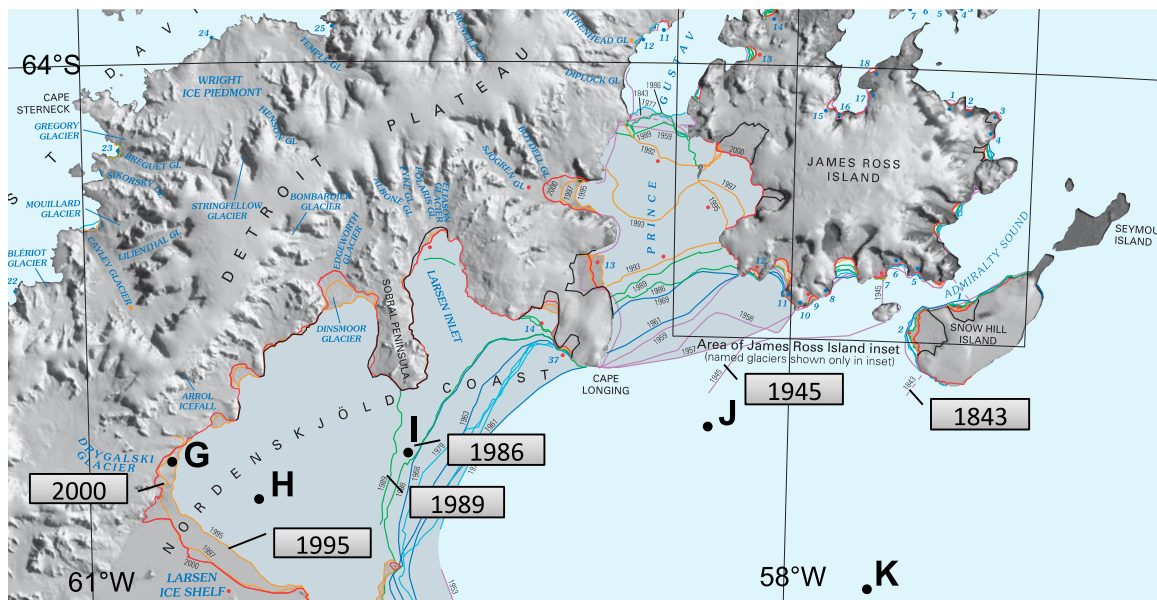


Figure 1: The study site, Larsen A embayment map with ice shelf front changes (Ferrigno et al. 2006) and five cross-shelf sampling stations. Numbers in boxes represent the year of ice shelf front.

2.1.2 Lipid Analysis

Lipids were ultrasonically extracted from 5 to 20 g of wet sediment with a solvent mixture of dichloromethane (DCM) and methanol (MeOH) (9:1, v:v) (3 × 15 min). The extracts were combined and water was added to separate phases. After recovery of the DCM phase, the remaining MeOH-water phase was washed three times with DCM and all organic phases were combined and dried using nitrogen blow down to yield a total lipid extract (TLE). Before extraction, each sample was spiked with internal standards (2-methyloctadecanoic acid for fatty acids, 1-nonadecanol for alcohols, and 5 α -cholestane for hydrocarbons). Using an amino-propyl column (SUPELCO), total lipid extracts (TLEs) were separated into four fractions: hydrocarbons,

ketones, alcohols, and fatty acids (Hinrichs et al., 2000). Hydrocarbons were eluted with hexane, ketones with hexane and DCM (3:1, v:v), alcohols with DCM and acetone (9:1, v:v), and fatty acids with 8% formic acid in DCM. Prior to analysis, alcohols and fatty acid fractions were derivatized with bis(trimethylsilyl)trifluoroacetamide (BSTFA) and pyridine at 70 °C for 1.5 h to yield trimethylsilyl ether and esters, respectively.

Hydrocarbons, ketone, fatty acids and alcohol fractions in hexane were analyzed by coupled gas chromatography-mass spectrometry (GC-MS, with an Agilent 7890A GC, coupled to an Agilent 5975c VL mass selective detector) for identification and gas chromatography-flame ionization detector (GC-FID) for quantification of lipid compounds. The mass spectrometer was operated in electron impact mode at 70 eV with a full scan mass range of m/z 50–800. Analyte separation was achieved on an Optima 5 MS Accent capillary column (30 m \times 250 μm \times 0.25 μm , Macherey-Nagel, Düren, Germany) using an oven temperature program of 60 °C (held 1 min) to 150 °C at 10 °C min^{-1} and then to 320 °C (held 30 min) at 4 °C min^{-1} . Compounds in the hydrocarbon, fatty acid, and alcohol fractions were quantified using the internal standards. Compounds in the ketone fraction were quantified using an injection standard (squalane).

Glycerol dialkyl glycerol tetraethers (GDGTs) and archaeols (ARs) in TLEs were analyzed by a Dionex Ultimate 3000 high performance liquid chromatography (HPLC) system connected to a Bruker maXis Ultra-High Resolution quadrupole time-of-flight

tandem mass spectrometer (qTOF-MS) equipped with an atmospheric pressure chemical ionization (APCI-II) ion source operating in positive mode (Bruker Daltonik, Bremen, Germany). The mass spectrometer was set to a resolving power of 27,000 at m/z 1222 and every analysis was mass-calibrated by loop injections of a calibration standard and correction by lock mass, leading to a mass accuracy of better than 1–3 ppm under different chromatographic conditions using normal phase (NP) HPLC (Becker et al., 2013). Identification and quantification were conducted using Bruker Data Analysis software. Core GDGTs and archaeols concentrations were calculated using C_{46} GTGT injection standard (Huguet et al., 2006) and were corrected for response factors determined by injections of purified acyclic GDGT (GDGT-0) and core archaeol standards (0.1, 1, and 10 ng).

2.2.3 Total organic carbon contents and stable carbon isotope values

Total organic carbon (TOC) contents were analyzed from freeze-dried, homogenized sediments. Aliquots of dry sediments (2 mg) were subjected to hydrochloric acid overnight to remove the inorganic carbon. Samples for TOC concentration and $\delta^{13}C$ were measured in duplicate using a ThermoFinnigan Flash Elemental Analyzer 2000 coupled to a ThermoFinnigan Delta Plus isotope ratio mass spectrometer via a ConFlow II interface. Average values are reported after correction with an in-house (Wadden Sea) sediment standard. Reported values are within a measurement error of $\pm 0.1\%$.

2.2.4 Compound-specific stable carbon isotope measurement of HBIs

Compound-specific stable carbon values ($\delta^{13}\text{C}$) of highly branched isoprenoids (HBIs) were determined using GC-irMS. The hydrocarbon fractions separated by column chromatography were injected onto a Trace GC Ultra (ThermoFinnigan) equipped with a Restek Rxi-5ms column (30 m \times 250 μm \times 0.25 μm , Restek, Bad Homburg, Germany) and coupled a Delta V Plus IRMS via GC-IsoLink connected to a ConFlow IV interface (Thermo Fisher Scientific GmbH, Bremen, Germany). The oven temperature conditions were identical to those applied for GC-FID. The instrument background and isotope standards were run daily to monitor instrument performance. The $\delta^{13}\text{C}$ values were reported relative to the standard Vienna- PeeDee Belemnite and defined by the equation $\delta^{13}\text{C} (\text{‰}) = (R_{\text{sample}}/R_{\text{standard}} - 1) \times 1000$ with $R = {}^{13}\text{C}/{}^{12}\text{C}$ and $R_{\text{standard}} = 0.0112372$.

2.2.5 Trapezoidal numerical integration

The TOC and lipid biomarker inventories were calculated by depth-integration using the trapezoidal numerical integration over 20 cm downcore (11 depths: 0.25, 1.5, 2.5, 4.5, 6.5, 8.5, 11, 13, 15, 17, 19 cm below seafloor). The R package 'pracma' was used to calculate depth-integrated concentrations (Borchers, 2015).

2.2.6 BIT Index

The BIT (Branched and Isoprenoid Tetraether) index is a proxy for soil organic matter input. Values of BIT index were calculated based on the relative abundance of

branched GDGTs derived from bacteria living in terrestrial environments (Weijers et al., 2006b) versus a structurally related isoprenoidal GDGT, crenarchaeol produced mainly by marine Thaumarchaeota (Hopmans et al., 2004).

$$\text{BIT} = \frac{[\text{brGDGT I}] + [\text{brGDGT II}] + [\text{brGDGT II}]}{[\text{brGDGT I}] + [\text{brGDGT II}] + [\text{brGDGT II}] + [\text{crenarchaeol}]}$$

2.2.7 Statistical Analysis

Analysis of variance (ANOVA) was conducted to compare mean concentrations or stable isotope values across the sampling stations. If significant variations were evident as a result of the ANOVA, then Tukey–Kramer HSD tests were performed to compare the mean values among sampling stations. For all ANOVA and Tukey–Kramer HSD test results, an alpha level of 0.05 was used as the criterion for statistical significance unless stated otherwise.

2.2.8 Principal component analysis

Principal component analysis (PCA) was performed to interpret the differences in lipid biomarker composition and similarities among samples (Yoshinaga et al., 2008; Yunker et al., 2005). Fatty acids, sterols, hydrocarbons, ketones, and core GDGTs and ARs were used in the analysis. Absolute concentrations of FAs (fatty acids), sterols, and hydrocarbons were normalized to TOC concentrations to remove artifacts related to the large concentration differences. Before PCA, gaps in the dataset were filled in as follows. When gas chromatography peaks were undetectable, biomarker concentrations were estimated for the core samples using linear interpolation of log concentration for a

portion of the core or linear regression down the core. PCA was performed using the vegan package in R (Oksanen et al., 2008).

2.3 Results and Discussion

2.3.1 General description of total organic carbon characteristics and lipid biomarkers

2.3.1.1 TOC (concentration and stable isotopic composition)

Total organic carbon (TOC) concentrations in surface sediments (top 1 cm) ranged between 0.12 – 0.83 wt%, with minimum TOC at Station G (nearshore) and maximum TOC at Stations J and K (furthest offshore and reference stations, respectively; Figure 2, Table 1). TOC concentrations in surface sediments were similar to those found in sediments from highly oligotrophic areas such as the South Pacific Gyre (0.3 to 0.5 wt%) (D'Hondt et al., 2009) and were consistent with previously published values for the Weddell Sea (Ishman and Szymcek, 2003; Pudsey and J. Evans, 2001). The concentrations are lower than in other parts of the Southern Ocean, such as the Bransfield Strait (~ 1.0 wt %) (Venkatesan, 1988; H. Yoon et al., 2003), the McMurdo Sound (0.4 ~ 1.5 wt %) (Venkatesan, 1988) and the northern Antarctic Peninsula (1.2 wt%) (Lu et al., 2012). Within the Larsen A Embayment, TOC concentrations decreased downcore. Such decreases in TOC concentrations downcore are attributed to degradation of organic matter (Wakeham and Canuel, 2006). TOC concentration was lowest in nearshore sediments and increased offshore (Figure 2); TOC concentrations at nearshore Station G were significantly lower ($p < 0.01$) than other stations, and the concentrations at offshore

J and K were significantly higher ($p < 0.01$) than other stations. This nearshore-offshore gradient of increasing TOC concentrations in surface sediments is consistent with the distribution of surface primary production as observed by satellite images of the area taken between 1997 and 2011 (Cape et al., 2014).

Stable carbon isotopes of TOC have been used as a basic metric for identifying major sources of organic matter in marine sediments (Degens, 1969; Fry and Sherr, 1989; Meyers, 1994). Stable carbon isotope values of TOC were similar across the embayment at the surface of the cores (0-1 cm; $\delta^{13}\text{C} = -23.0 \pm 0.2\text{‰}$; $p > 0.1$; Table 2). The mean $\delta^{13}\text{C}$ value of TOC ($\delta^{13}\text{C} = -23.2 \pm 0.5\text{‰}$) was similar to previously reported values for sediments of the Antarctic Continental Shelf (Carr et al., 2013; Sackett, 1986; Venkatesan, 1988; Venkatesan and Kaplan, 1987). In general, organic carbon stable isotope ratios in polar regions are relatively lower ($\delta^{13}\text{C} = -28$ to -26‰) compared to tropical and temperate regions ($\delta^{13}\text{C} = -22$ to -18‰). Rau (1982) explained that both lower temperature (high CO_2 solubility and concentrations) and lower growth rate of phytoplankton in polar regions than in warmer regions induce the relatively ^{13}C -depleted organic carbon synthesized by phytoplankton. Although high input of terrestrial organic matter tends to shift the carbon stable isotope ratios towards lower values (Fry and Sherr, 1989; Lamb et al., 2006), we expect the majority of contemporary particulate organic carbon to be phytoplankton-derived in our study site. The terrestrial organic matter input is negligible on the Antarctic continental shelf (Venkatesan and

Kaplan, 1987) unlike in the Arctic continental shelf, where terrestrial organic matter input is increasing due to permafrost melting (Guo et al., 2004; Magen et al., 2010).

There was no apparent cross-embayment pattern in the $\delta^{13}\text{C}$ values of TOC; this is likely because the major organic matter source is shared across the embayment. The only significant difference was noticed at Station G, where TOC was ^{13}C -enriched compared to the other stations ($p < 0.05$, Table 2). In general, heterotrophic processes enrich the ^{13}C of organic carbon (Fry, 1988; Hayes, 1993). As a consequence, in sediments, the TOC is enriched in ^{13}C relative to its primary precursor (organic matter produced by photosynthesis) (Hayes et al., 1989). The relatively enriched ^{13}C TOC in Station G may thus be due to intense heterotrophic degradation. An alternative explanation is that Station G may be receiving organic matter from phytoplankton grown in different conditions; $\delta^{13}\text{C}$ of organic carbon could vary by growth condition of source organisms (e.g. growth in sea ice, spring bloom) (Mincks et al., 2008; Popp et al., 1999; Rau et al., 1991).

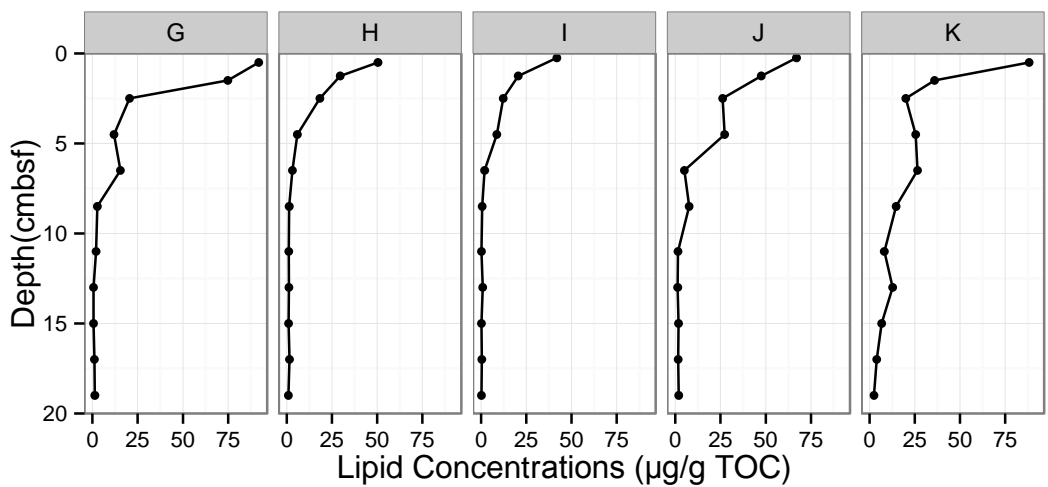
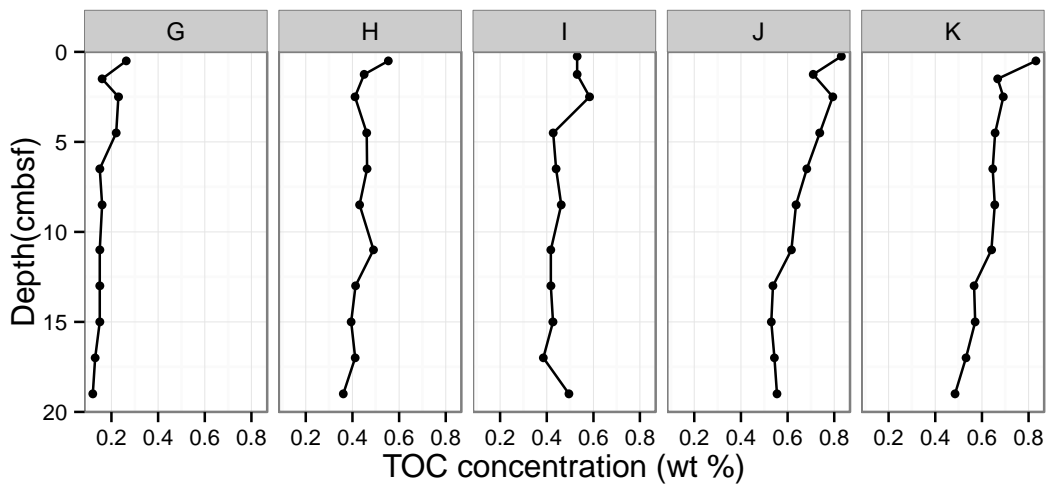


Figure 2: Downcore profiles of total organic carbon (TOC) concentrations and total lipid concentrations at cross-shelf transect stations (G-K). bsf: below sea floor

Table 2: TOC contents and $\delta^{13}\text{C}$, lipid concentrations, and relative abundance within fatty acids, sterols, hydrocarbons, ketones, and core GDGTs and ARs in surface (0-1 cm) (n = 3 replicate samples per analysis) and bottom (18-20cm) sediments (n=1 sample per analysis) at five sampling stations (G-K). \pm Standard deviation for %TOC, $\delta^{13}\text{C}$ TOC, and total concentrations. n.a.: not available

	Surface (0-1cm)					Bottom (18-20cm)				
	G	H	I	J	K	G	H	I	J	K
%TOC	0.3 \pm 0.1	0.6 \pm 0	0.5 \pm 0	0.8 \pm 0.1	0.8 \pm 0.1	0.1	0.4	0.5	0.5	0.5
$\delta^{13}\text{C}$ TOC (‰)	-22.8 \pm 0.2	-23.3 \pm 0	-23.2 \pm 0.4	-22.9 \pm 0.7	-22.9 \pm 0.5	-22.6	-23.7	-23.8	-23.0	-24.0
Total Lipids ($\mu\text{g/g}$ dry sediments)	22.3	27.9	22.5	55.4	70.7	0.2	0.3	0.1	1.1	1.2
<i>fatty acids</i>										
Total ($\mu\text{g/g}$ dry sediments)	11.9 \pm 6.7	17.5 \pm 5.1	12 \pm 7.6	22.7 \pm 4	17.8 \pm 4.4	0.1	0.3	0.1	1.0	0.7
Total ($\mu\text{g/g}$ TOC)	42.3 \pm 22.7	17.7 \pm 1.4	17.7 \pm 2.2	34.6 \pm 10.3	62.4 \pm 35.9	1.1	0.8	0.1	1.8	1.5
%SCFAs	41.7	31.1	28.1	58.0	23.9	40.0	65.8	56.5	30.7	28.8
%MUFAs	36.6	41.8	41.8	20.8	50.5	49.3	7.0	25.1	21.8	38.4
%LCFAs	3.9	5.9	4.4	1.4	2.8	0.2	6.7	0.0	0.4	11.8
%BRANCH	13.3	13.7	18.1	13.7	7.2	8.9	20.0	18.2	46.9	18.7
%PUFAs	4.5	3.3	7.5	6.1	15.6	1.6	0.6	0.1	0.2	2.2
<i>Sterols</i>										
Total ($\mu\text{g/g}$ dry sediments)	10 \pm 2.5	9.9 \pm 0	10.1 \pm 2.1	32.3 \pm 7.6	51.5 \pm 28.1	0.0	0.0	0.0	0.0	0.2
Total ($\mu\text{g/g}$ TOC)	46.2 \pm 22	34.8 \pm 7.2	22 \pm 12.6	27.3 \pm 2.5	22.2 \pm 2.4	0.1	0.1	0.0	0.0	0.4
%C26	2.7	2.6	2.2	2.8	3.2	8.1	3.2	11.9	3.3	2.2
%C27	45.1	40.8	44.7	33.9	48.5	43.8	25.7	42.9	38.2	33.5
%C28	31.2	27.1	28.6	31.7	23.4	20.6	10.7	15.1	17.7	18.1
%C29	9.7	13.0	9.8	9.9	14.5	8.5	19.2	16.0	19.3	26.2
%C30	2.7	2.9	2.9	2.5	2.1	2.9	12.4	7.3	5.4	8.7

Table 2 (cont.)

	Surface (0-1cm)					Bottom (18-20cm)				
	G	H	I	J	K	G	H	I	J	K
<i>Hydrocarbons</i>										
Total ($\mu\text{g/g}$ dry sediments)	0.3 \pm 0.1	0.1 \pm 0	0.2 \pm 0.1	0.2 \pm 0	0.6 \pm 0.2	0.0	0.0	0.0	0.0	0.2
Total ($\mu\text{g/g}$ TOC)	1.5 \pm 0.4	0.3 \pm 0	0.3 \pm 0.1	0.2 \pm 0.1	0.7 \pm 0.2	0.1	0.0	0.0	0.0	0.3
%HBIs	88.2	90.3	38.1	39.6	62.2	0.1	3.6	1.4	3.4	7.1
%odd <i>n</i> -alkane	6.4	4.5	33.2	33.5	21.5	54.9	59.5	53.7	44.9	53.1
%even <i>n</i> -alkane	5.4	5.1	28.7	26.9	16.3	44.9	36.9	44.9	44.8	39.8
$\delta^{13}\text{C}$ HBI C _{25:2} (‰)	-14.1	-12.5	-13.0	-11.9	-13.1	n.a.	n.a.	n.a.	n.a.	-15.7
$\delta^{13}\text{C}$ HBI C _{30:5} (I) (‰)	n.a.	n.a.	n.a.	n.a.	-43.3	n.a.	n.a.	n.a.	n.a.	n.a.
<i>Ketones</i>										
Total (mg/g TLE)	0.4 \pm 0.3	0.2 \pm 0	0.4 \pm 0.2	0.1 \pm 0	1 \pm 0.4	0.1	0.1	0.0	0.1	0.2
Total ($\mu\text{g/g}$ TOC)	0.4 \pm 0.3	0.1 \pm 0	0.1 \pm 0	0.1 \pm 0.1	0.7 \pm 0.4	0.0	0.0	0.0	0.0	0.0
%PAHs	7.4	0.1	0.1	0.1	0.1	0.0	0.2	0.0	0.3	0.3
%Stenones	56.4	47.1	49.7	47.3	42.1	20.4	52.7	49.4	42.0	26.4
%Hopanones	9.7	10.3	8.9	7.5	7.3	79.6	13.8	28.8	22.5	25.3
%Waxesters	26.5	33.7	35.3	35.3	43.4	0.0	14.4	18.0	7.1	21.3
<i>core GDGTs and ARs</i>										
Total (mg/g TLE)	0.9 \pm 0.3	1.1 \pm 0.3	0.8 \pm 0.3	0.3 \pm 0.1	1.2 \pm 1	0.1	0.1	0.1	0.0	0.7
Total ($\mu\text{g/g}$ TOC)	0.8 \pm 0.8	0.6 \pm 0.2	0.3 \pm 0.1	0.3 \pm 0.2	0.6 \pm 0.4	0.0	0.0	0.0	0.0	0.7
%AR	3.8	2.6	5.3	5.7	4.4	3.1	3.1	0.0	0.0	7.4
%isoprenoidal GDGTs	92.6	93.9	90.0	88.2	87.7	80.2	80.2	93.4	70.7	74.0
%branched GDGTs	0.3	0.4	0.7	1.3	3.5	6.4	6.4	6.3	12.1	13.6
%GDDs	3.3	3.2	4.0	4.8	4.4	10.3	10.3	0.3	17.2	5.0

2.3.1.2 Total lipid classes

We identified and quantified 27 fatty acids (FAs), 19 sterols, 23 hydrocarbons, 11 ketones, 2 archaeols (ARs) and 23 glycerol dialkyl glycerol tetraethers (GDGTs) in the sediment cores (Table 3). In surface sediments (0-1 cm), TOC-normalized mean concentrations were 35.0 $\mu\text{g/g}$ for FA, 30.5 $\mu\text{g/g}$ for sterols, 0.4 $\mu\text{g/g}$ for hydrocarbons, 0.3 $\mu\text{g/g}$ for ketones, and 0.5 $\mu\text{g/g}$ for GDGTs and archaeols (Table 2). In the bottom (18-20 cm) sediments, these lipid biomarker concentrations decreased by 70 to 99% relative to the surface values (Table 2).

2.3.1.3 Fatty Acids

Fatty acids were the major lipid components in all samples (25-96% of total lipids), with a dominant C_{16} maximum (16:0 and/or 16:1 ω 7) and a secondary C_{18} (18:0 and/or 18:1 ω 7) or C_{20} (20:5) maximum (Figure 3). A secondary maximum of C_{18} fatty acids was found at Stations G, H, and J, and of C_{20} at Station K (reference station). Station J exhibited a secondary maximum of C_{14} transitioning to C_{15} towards the deeper sediments. Little or no fatty acids beyond C_{27} were detected. Branched chain iso and anteiso C_{15} fatty acids relative abundance increased downcore at Stations J and K.



Figure 3: Relative abundances of fatty acids in 11 depths of sediment cores from each sampling station

The predominance of C₁₆ fatty acids and the high short-chain (C₁₄₋₁₈) to long-chain (C₂₀₋₂₆) ratios (3 to 189) document the importance of the marine-derived organic matter because the latter components are derived from terrestrial input. A higher percentage of C₁₆ among fatty acids was also observed in sediments of Bransfield Strait, which are rich in diatoms (Venkatesan and Kaplan, 1987), and McMurdo Sound sediments (Venkatesan, 1988). The difference of FA distribution in these Antarctic sediments to our samples is the secondary maximum of C₂₄ or C₂₆ compared to C₁₈ or C₂₀ observed in this study. A secondary peak at C₂₀ was found in Antarctic and Arctic sea-ice diatom communities (Fahl and Kattner, 1993; Falk-Petersen et al., 1998; D. S. Nichols et al., 1993) and sea water (Skerratt et al., 1995), where the main FA compositions were 16:0, 16:1 ω 7, and 20:5. FAs at Station K thus appear to be highly influenced by input from diatom communities. A secondary maximum of C₁₈ FA was found in the sediments under the Ross Ice Shelf (Carr et al., 2013), where the dominant FAs were 16:0, 16:1 ω 7, and 18:1 ω 7. Although the authors suggested that two of the dominant monounsaturated FAs (16:1 ω 7 and 18:1 ω 7) were derived from *in situ* bacterial communities, these could also be derived from phytoplankton (Viso and Marty, 1993; Volkman et al., 1989; Wakeham, 1995). The increasing relative abundance of branched C₁₅ FAs downcore suggests that the contribution of an *in situ* bacterial community at Stations J and K increases downcore (Kaneda, 1991).

2.3.1.4 Sterols

We identified 19 sterols in the C₂₆ to C₃₀ carbon number range. With an average of 42.6% of the total sterols, the C₂₇ sterols were dominant in surface sediments, followed by C₂₉ and C₂₈ sterols (Table 2, Figure 4). The sterol fraction of our samples were dominated by cholest-5-en-3 β -ol (cholesterol), 5,22E-dien-3 β -ol (dehydrocholesterol), 24-methylcholesta-5,24(28)-dien-3 β -ol (24-methylenecholesterol), and 24-ethylcholest-5-en-3 β -ol (sitosterol). This sterol distribution is different from that reported in sediments from the Bransfield Strait where dinosterol accounted for over 96% of total sterols (Venkatesan et al., 1986; Venkatesan and Kaplan, 1987), but similar to that found in sediments from McMurdo Sound (Venkatesan, 1988).

The C₂₇: C₂₈: C₂₉ sterols ratios showed great variability among the samples. The proportions of C₂₈ were within 10-40%, and C₂₇ and C₂₉ ranged between 20-70% (Figure 4). Although there was no trend among sampling stations, the proportion of C₂₈ decreased in deeper sediments. When plotted in a ternary diagram according to Huang and Meinschein (1979), the ratios in our samples plot in an area where open ocean, coastal sediments, and terrestrial organic matter overlap, and are similar to McMurdo Sound sediments (Venkatesan, 1988) and Antarctic lake sediments (Matsumoto et al., 1982) (Figure 4).

Some of our samples contained higher fractions of C₂₉ sterols than typical marine sediments and were more similar to terrestrial organic matter. Although C₂₉ sterols such

as sitosterol and 24-methylenecholesterol are usually considered biomarkers for higher plants (Volkman, 2003), these could also be found in significant proportions in algae and diatoms. For example, sitosterol, a typical terrestrial higher plant biomarker (Huang and Meinschein, 1979), can also be sourced by green algae (Kohlhase and Pohl, 1988) and was found as a dominant sterol in Antarctic lakes and lake sediments (Matsumoto et al., 1982; Orcutt et al., 1986). 24-methylenecholesterol was found as a major sterol of green algae (Volkman, 1986). It was also found in sea ice diatom communities but not in open-ocean diatom communities; Nichols (1989, 1993) suggested that this sterol could be produced under the extreme physiological condition of diatoms growing in sea ice. Finally, the four major sterols found in our samples (cholesterol, 22-dehydrocholesterol, 24-methylenecholesterol, and sitosterol) are similar to major sterols found in Arctic sea ice (Belt et al., 2013). The C_{27} : C_{28} : C_{29} sterols ratios of sea ice diatom communities have relatively low C_{27} sterols oppose to that typical marine plankton contain C_{27} and C_{28} as dominant sterols. Sea ice diatom communities exhibit a broad range of ratios of C_{28} and C_{29} sterols (Figure 4), and this variation is likely driven by diatom community compositions (P. D. Nichols et al., 1989). The sterol distribution in our sediment samples is highly influenced by, and likely reflects the contribution from sea ice diatoms. Moreover, the wide range of C_{27} : C_{28} : C_{29} sterols ratios may indicate a diverse community of sea-ice diatoms.

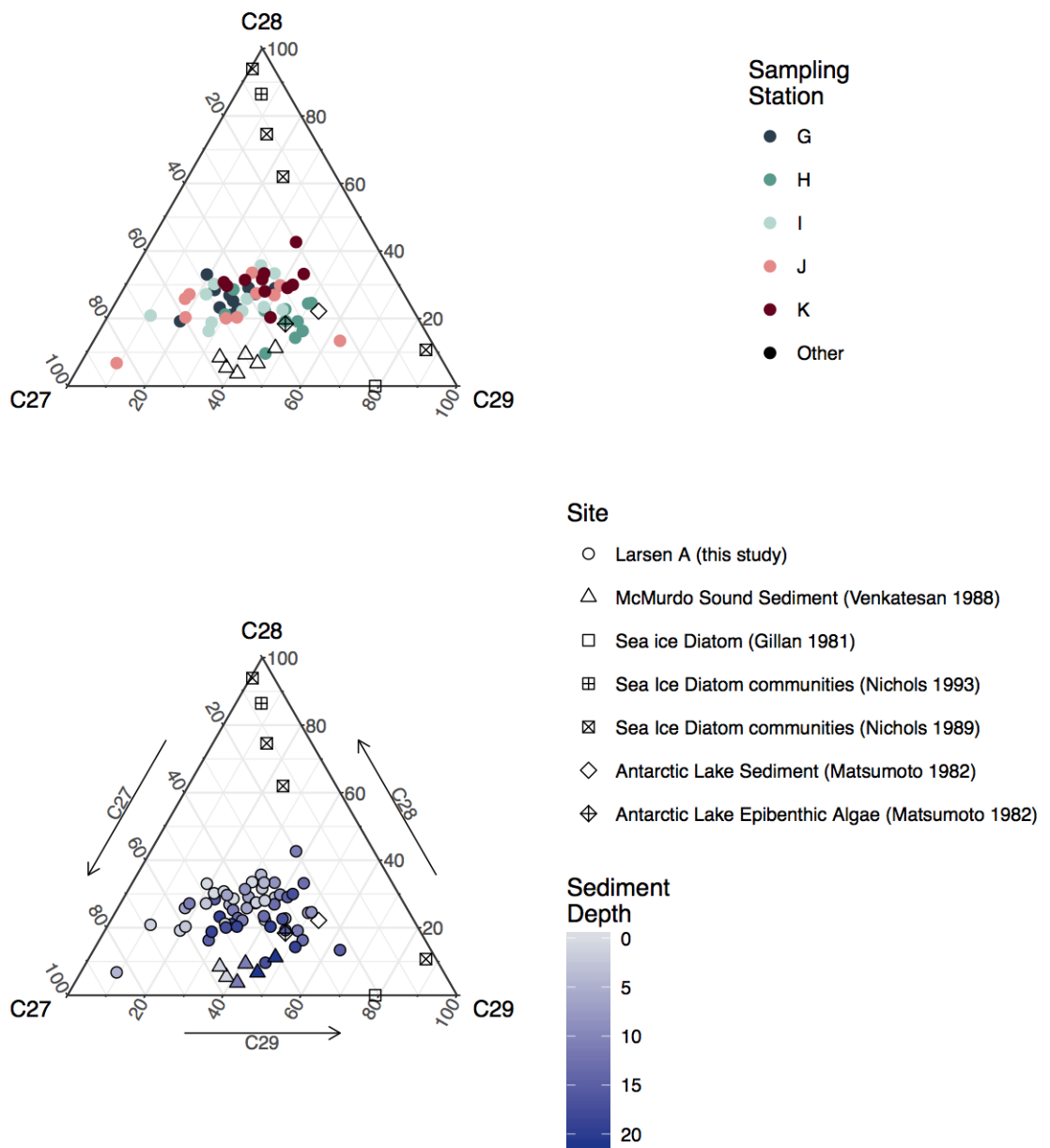


Figure 4: Distribution of C_{27} , C_{28} , and C_{29} sterols in the sediments (0-20 cm) in Station G – K, and in previously studied Antarctic sites.

2.3.1.5 Hydrocarbons – Highly branched isoprenoids

Total hydrocarbons were 75 to 88 times lower in concentration than total fatty acids and total sterols (Table 2). In average, 56.4% of the hydrocarbon fractions in surface sediments consisted of highly branched isoprenoids (HBIs) (Table 2). Four basic structures of HBIs were identified in our samples; $C_{25:2}$, $C_{25:3}$, $C_{30:5}$ (I), $C_{30:5}$ (II) (Figure 5). Among HBIs, $C_{25:2}$ was most abundant with an average of 22.2% of total hydrocarbons. Among HBIs, $C_{25:2}$ was exceptionally abundant with an average of 22.2% of total hydrocarbons. We found that relative abundances of HBIs were higher in nearshore sediments at Stations G and H than in offshore Stations I and J ($p < 0.05$) and decreased downcore.

HBIs are considered as biomarkers for diatoms (Fahl and Stein, 2012; Johns et al., 1999; Volkman et al., 1994) and $C_{25:2}$ has been specifically proposed as a sea ice diatom biomarker in Antarctic environments (Massé et al., 2011). To further confirm the source of HBIs (sea ice vs. open ocean diatoms), we measured the compound-specific stable carbon isotope composition of HBIs. This is based on that sea-ice diatom biomass is known to be ^{13}C -enriched relative to open-ocean diatom biomass (Rau et al., 1991). The $\delta^{13}\text{C}$ value of $C_{25:2}$ ($-12.9 \pm 0.8\text{‰}$) was significantly more positive than that of TOC ($\delta^{13}\text{C} = -23.2 \pm 0.5\text{‰}$) ($p < 0.001$) in surface sediments across the embayment (Table 2). Our results are consistent with previous studies of HBI $C_{25:2}$ in Antarctic sediment and sea ice diatoms, where $\delta^{13}\text{C}$ values ranging from -8.5 to -17.5‰ have been determined (Massé et

al., 2011; Sinninghe Damsté et al., 2007). HBI C_{30:5} (I) at offshore station K, on the other hand, was significantly ¹³C-depleted ($\delta^{13}\text{C} = -43.3\text{‰}$) relative to TOC ($\delta^{13}\text{C} = -23.2\pm 0.5\text{‰}$). We could not measure the isotopic compositions of the other two HBIs because of their low concentrations in samples.

The HBIs and their stable carbon isotope ratios revealed three possible sources of different species or different growth condition of diatoms. The first is an Antarctic sea ice diatom biomarker, the HBI C_{25:2} (Johns et al., 1999; Massé et al., 2011). These authors identified HBI C_{25:2} as sea ice diatom biomarker among other HBIs based on the ¹³C-enrichments in Antarctic water columns, sea ice, and sediments. This ¹³C-enrichment in sea-ice diatoms is probably caused by growth under CO₂ limitation; sea-ice algae in the Southern Ocean produce relatively ¹³C-enriched organic compounds (Gibson et al., 1999). The second potential diatom biomarker is the HBI C_{30:5} (I), representing spring bloom diatoms based on its strong ¹³C-depletion which is typical for the phytoplankton blooms in Antarctic open waters (Mincks et al., 2008; Popp et al., 1999) due to low sea surface temperature and high concentration of dissolved CO₂ (Rau et al., 1992; Sackett et al., 1965). The third potential diatom biomarker represents HBI C_{25:3}, suggested to be sourced by diatoms growing during the intense phytoplankton bloom associated with the marginal ice zone (2013) (2013). These authors found that the concentrations of HBI C_{25:3} positively correlated with those of HBI C_{25:2}, but with the triene displaying more negative $\delta^{13}\text{C}$ values than the diene (Massé et al., 2011). While we also found a positive

correlation between the concentrations of two C₂₅ HBIs ($r^2= 0.97, p<0.01$), the stable carbon isotope values for the triene could not be determined due to its low concentrations.

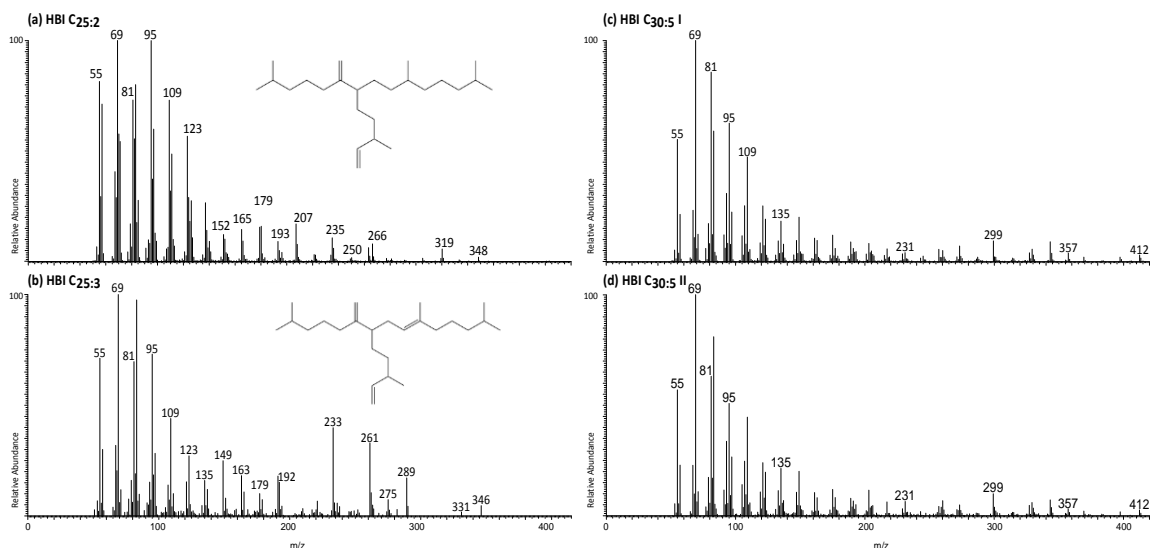


Figure 5: Mass spectra of highly branched isoprenoids (HBIs), (a) C_{25:2}, (b) C_{25:3}, (c) C_{30:5} I, and (d) C_{30:5} II

2.3.1.6 Hydrocarbons – *n*-alkanes

The major *n*-alkanes identified in this study ranged from C₁₇ to C₃₆. The *n*-alkanes C₁₇, C₁₈, and C₃₆ were only found at the offshore reference station (K). The distribution patterns of the *n*-alkanes showed variation between the sites sampled. The profiles for most of the samples showed C₂₇ or C₂₉ as major *n*-alkanes (Figure 6), with an average chain length of C₁₇ to C₃₆ *n*-alkanes ranging from 22.5 to 28.6. The C₂₄ to C₃₄ *n*-alkanes were dominated by odd-numbered compounds with a mean carbon preference index

(CPI) (E. E. Bray and E. D. Evans, 1961) of 1.4 (Figure 7). This supports a partial biological source for the *n*-alkanes in addition to non-specific sources, including possibly petrogenic sources, especially for the shorter chain (C₂₀₋₂₆) *n*-alkanes, which display a CPI of close to 1 (Figure 7). Such distributions are similar to those in a petroleum dominated environment (Mackie et al., 1978; Platt and Mackie, 1980) or at sites of thermogenic hydrocarbon production (Konn et al., 2009). The lack of hopanes, steranes, and unresolved complex mixtures, however, suggest that *n*-alkanes in our samples did not originate from petrogenic inputs (Zegouagh et al., 1998) microbially degraded products (Venkatesan and Kaplan, 1982).

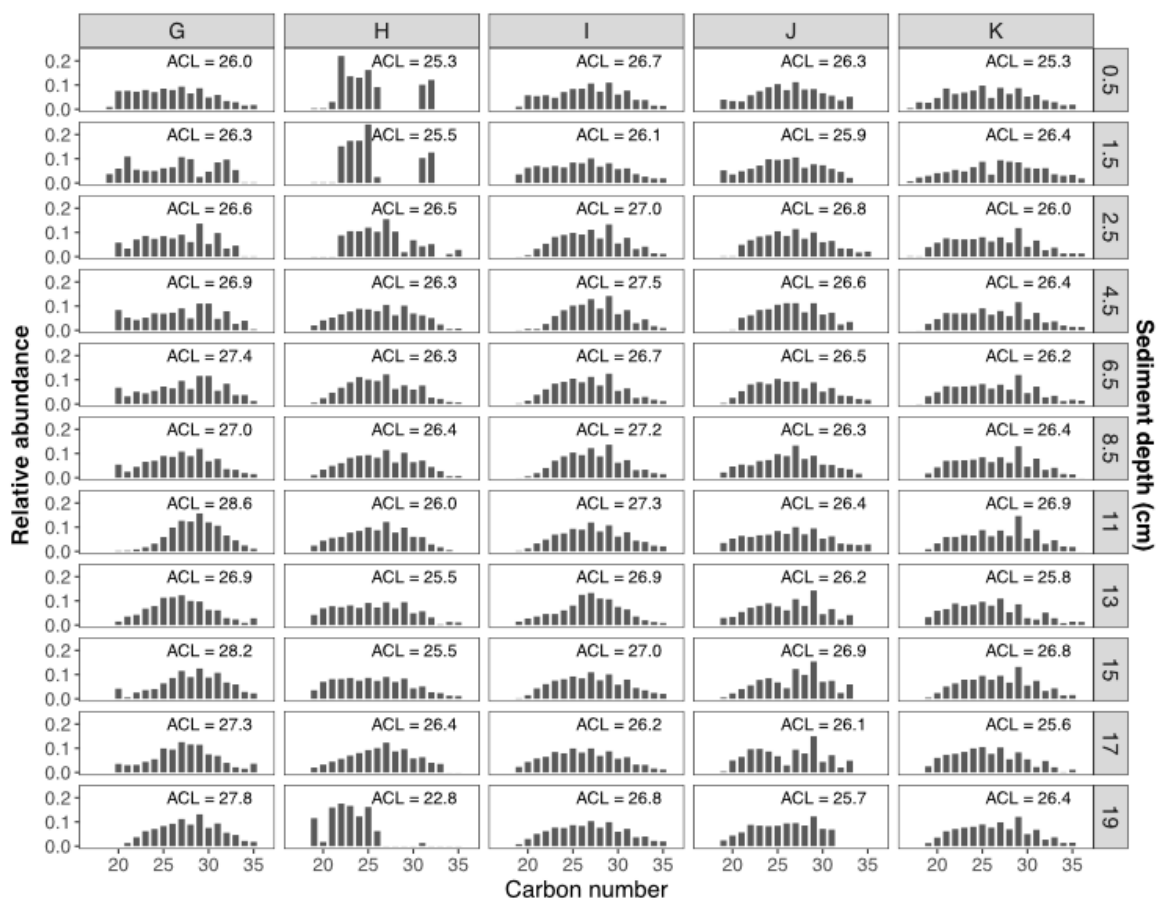


Figure 6: *n*-alkanes relative abundances in sediment downcore and across the embayment ACL: average chain length of C₁₇ to C₃₆ *n*-alkanes

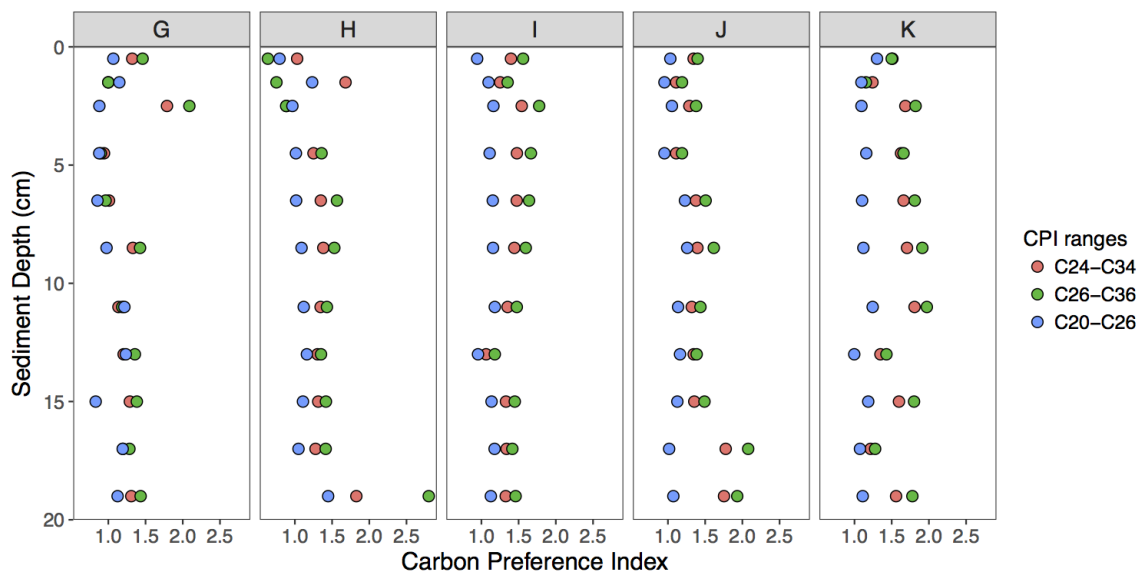


Figure 7: Downcore profiles of carbon preference index (CPI) for *n*-alkane carbon number ranges C₂₄-C₃₄, C₂₆-C₃₆, and C₂₀-C₂₆.

Are the biological source of *n*-alkane marine or terrestrial? Usually, long chain odd-carbon *n*-alkanes are major components of leaf waxes and thus attributed to terrestrial vascular plants input (Eglinton and Hamilton, 1967). The stronger odd-carbon preference in longer chain *n*-alkanes (Figure 7) and the predominance of the C₂₉ *n*-alkane also support a terrestrial origin for these compounds. There are at least two possible explanations for input of vascular-plant-derived *n*-alkanes to Antarctic sediments: aeolian transport or ancient plant material deposited during the pre-Quaternary period when vascular plants were present on the Antarctic continent (Kvenvolden et al., 1987). Neither of the sources can explain the *n*-alkane distribution of our samples; aeolian transport is likely negligible in Antarctica (Venkatesan, 1988; Venkatesan and Kaplan, 1987), and our 20-cm sediment cores would not reach pre-Quaternary sediments (with

the sediment age of >1000 years at the 20 cm depth of the cores; unpublished data R. Taylor). Furthermore, relatively low contribution (2.7%) of long-chain fatty acids (LCFAs) also indicate little or no higher plants input in the Larsen A sediments.

Microalgal species typically produce odd-numbered, short-chain *n*-alkanes such as C₁₅ and C₁₇. Previous studies, however, showed that many Antarctic sea ice algae (Cripps, 1995; P. D. Nichols et al., 1989; 1988), krill, salps (Cripps, 1990), and sediments (Venkatesan, 1988; Venkatesan and Kaplan, 1987) exhibited *n*-alkane compositions similar to those of higher plants (long-chain *n*-alkanes with maximum at C₂₇, C₂₉, or C₃₁ and the CPI ranging between 0.8 and 2.1). Therefore *n*-alkane distributions in our samples could be explained by inputs from marine organisms including sea ice algae and other zooplankton as previously reported in Arctic surface sediments (Zegouagh et al., 1998) and Southeast Atlantic Ocean sediments (Hinrichs et al., 1999).

2.3.1.7 Ketones

Stenones, hopanones, and wax esters were detected, and among them, stenones were the most abundant (average 48.5% in total ketone), followed by wax esters (34.9%), and hopanones (8.8%) (Table 2). In general, the highest relative abundance of stenones was found at nearshore stations and highest content of wax esters in sediments at offshore stations. Whereas the relative abundances of stenones within the ketone fraction were similar throughout the core, the contribution of wax esters decreased downcore, and the relative abundance of hopanones increased downcore.

2.3.1.7 GDGTs and ARs

Archaeal isoprenoidal GDGTs (iGDGTs), hydroxyl-GDGTs, GDDs, and hydroxyl-GDDs, archaeol (AR), and methoxy archaeol (MeO-AR) were detected. iGDGTs were most abundant and represented more than 70% of total GDGTs and ARs. Among the iGDGTs, pentacyclic iGDGT-5 (crenarchaeol) was the most abundant, followed by iGDGT-0. We did not find a consistent downcore pattern in the relative abundances of isoprenoidal GDGTs and ARs.

The iGDGTs, hydroxyl GDGTs, and archaeol are widespread in environmental samples and cultured archaeal samples (Elling et al., 2014; Koga et al., 1993; Liu et al., 2012; Pearson and Ingalls, 2013). These archaeal lipids could be derived from the archaeal community in the water column (Sinninghe Damsté et al., 2002a) and in sediments (Liu et al., 2011; Takano et al., 2010). The most abundant archaeal lipid in our samples, crenarchaeol (iGDGT-5), is frequently used as a lipid biomarker for Thaumarchaeota (Buckles et al., 2013; Sinninghe Damsté et al., 2002b), although this lipid could also be contained in some planktonic Marine Group II, Euryarchaea (Lincoln et al., 2014). Given the predominance of crenarchaeol (iGDGT-5) and iGDGT-0 among iGDGTs, we assume that the archaeal lipids are mostly derived from Thaumarchaea. In fact, we detected the recently discovered lipid biomarker methoxy archaeol (MeO-AR) that was identified from a pure culture of Thaumarchaea, *Nitrosopumilus maritimus* (Elling et al., 2014).

2.3.1.8 Branched GDGTs

We identified bacterial-derived branched-GDGTs (brGDGTs) with increasing trends of relative abundances from nearshore to offshore stations, and from the surface to deeper sediments ($p < 0.01$). brGDGTs are typically considered to be produced by soil bacteria (Weijers et al., 2009). The branched isoprenoid tetraether (BIT) index (the measure of soil organic matter input) (Hopmans et al., 2004) ranged between 0.006 and 0.3 (Figure 8). The upper values are higher than other marine sediments; BIT values for marine sediments are usually < 0.1 (Schouten et al., 2013). We considered three potential sources of branched GDGTs: soil (terrestrial input), water column, and sediment (*in situ* production). Soil organic matter could be delivered by ice shelf basal melt (Gilbert and Domack, 2003) and ice rafting (Schouten et al., 2007a). The stable ice shelf could irregularly release basal glacial sediment that carried from the Antarctic continent (Gilbert and Domack, 2003). The increasing BIT index downcore (Figure 8) supports the soil organic matter input due to the Larsen A Ice Shelf basal melt. Icebergs could travel through the Weddell Gyre to the offshore of the Larsen A Embayment (Diekmann and Kuhn, 1999). The increasing trend of BIT index towards offshore (Figure 7) supports soil organic matter input by ice rafting. The second potential source, bacteria inhabiting anoxic waters were recently suggested as additional sources of branched GDGTs (Liu et al., 2014). Given the well-oxygenated waters of the Larson continental shelf (Caspel et al., 2015), the water column bacterial community is unlikely the source of branched

GDGTs. The third potential source, sediment bacteria, was suggested by Fietz (2012) and Peterse (2009). Interestingly, Peterse (2009) found that same increasing pattern of BIT index towards offshore in Arctic sediments as we found in our samples (Figure 8). In addition, the branched GDGTs in our samples contained higher relative abundances of branched GDGTs with a cyclopentane moiety (up to 30% of total branched GDGTs) compared to typical soil samples (less than 10%) (Peterse et al. 2009) (Figure 9), supporting the input from sediment bacteria. Notably, BIT values increased with depth in four of the five sites (Figure 8), consistent an accumulation of branched GDGTs by in situ production. In summary, our results suggest that at least a part of branched GDGTs could be produced *in situ* by sediment bacteria, in addition to soil organic matter potentially transported by the ice shelf and icebergs.

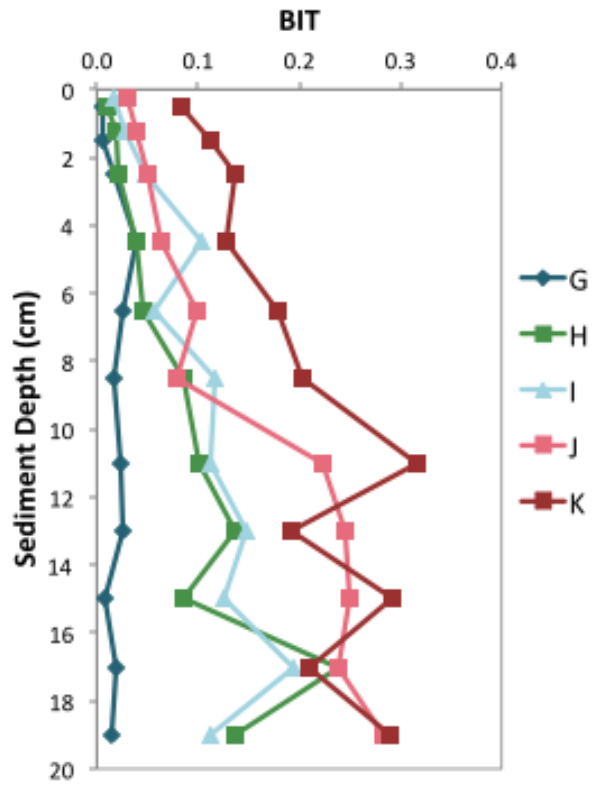


Figure 8: Downcore profiles of branched isoprenoid tetraether (BIT) index

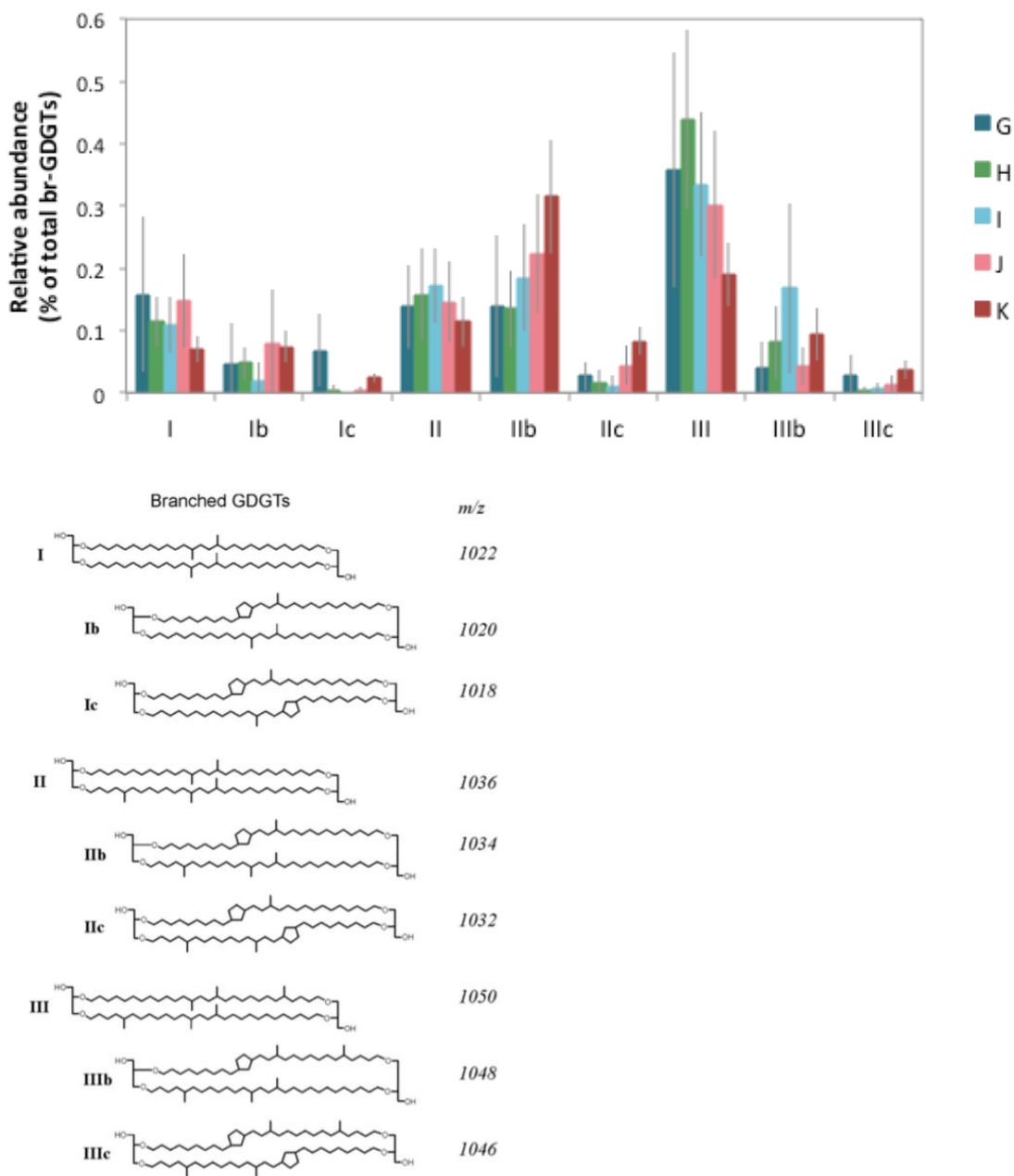


Figure 9: Bar plots with a standard deviation of average branched GDGT distribution in the five sampling stations ($n = 11$ for each station). Roman numerals refer to the structures; I, II and III are branched GDGTs without cyclopentane; Ib, IIb, and IIIb are branched GDGTs with one cyclopentane; Ic, IIc, and IIIc are branched GDGTs with two cyclopentane.

2.3.2 TOC and lipid biomarker inventories across the transect

The TOC and lipid biomarker inventories (depth-integrated concentrations) throughout the sediment cores allowed us to compare the lipid biomarker concentrations among cores and to investigate the pattern across the sampling sites. Lipids were grouped into phytoplankton, bacterial and archaeal biomarkers according to previous studies (Table 3). TOC inventories increased towards offshore (Figure 10) and positively correlate with primary productivity gradients across the embayment (Cape et al., 2014) ($r^2 = 0.95$, $p = 0.01$). Total lipid inventories at nearshore stations G and H were 50 to 75% smaller compared to those at offshore stations J and K (Figure 10). Total lipid inventories were positively correlated with time since ice-shelf disintegration ($r^2 = 0.96$, $p = 0.04$), indicating that the longer a site is exposed to open ocean conditions, the more lipids accumulated. Specifically, the bacterial biomarker inventory exceeded the phytoplankton inventory at Station J (Figure 10) and bacterial and archaeal inventories do not follow primary productivity gradients across the embayment or the time passed since the ice shelf collapse. These indicate localized bacterial and archaeal production in the water column and/or sediments.

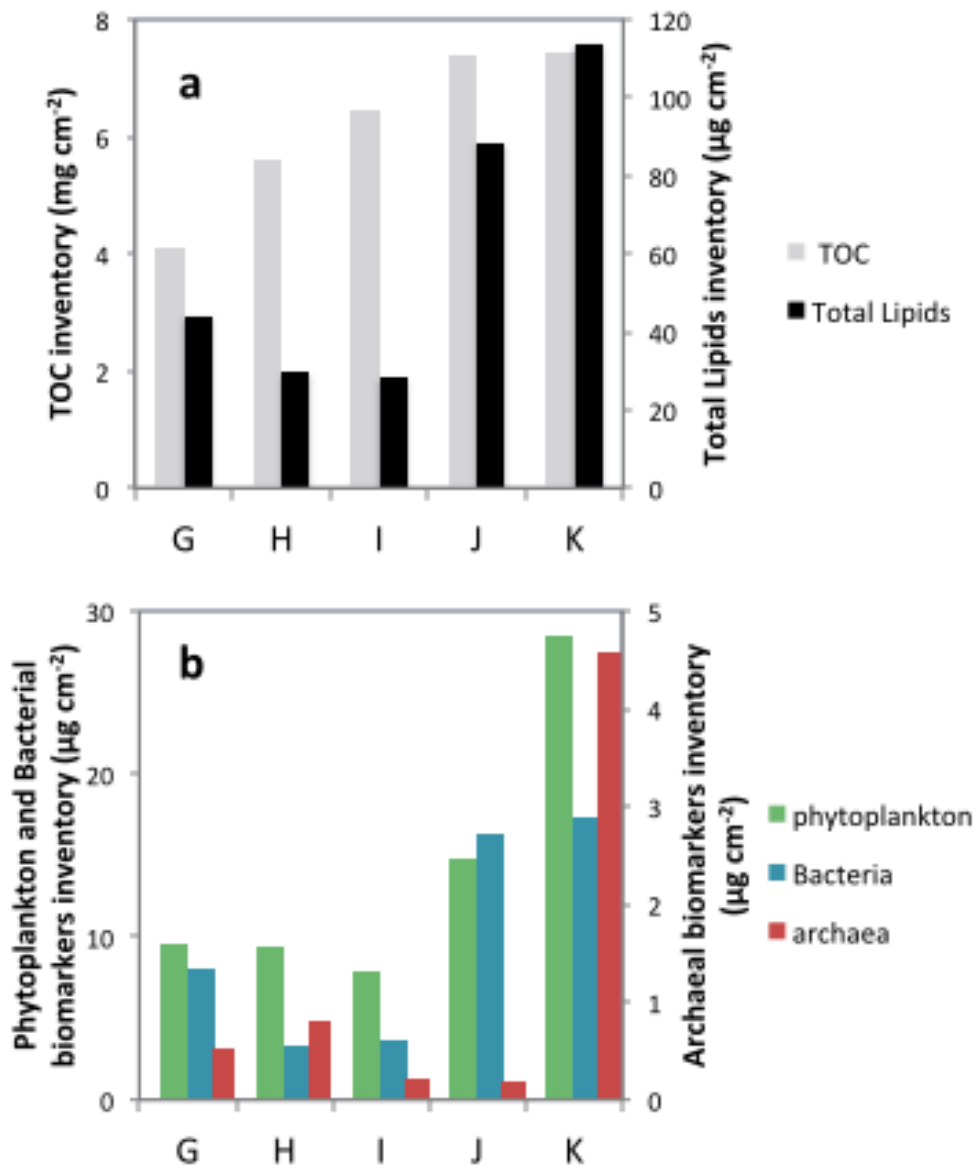


Figure 10: Inventories of TOC and lipids in 20-cm sediment cores across the sampling stations; a) TOC and total lipids inventories; b) phytoplankton, bacterial and archaeal biomarkers inventories. Biomarker assignments are on Table 3.

Table 3: List of lipid biomarker compounds and groups identified and their major sources

Compound or group	Major source	References
<i>Fatty acids</i>		
14:0, 15:0, 16:0, 18:0	Unspecific marine	(Cranwell, 1982)
15:0a/i, 17:0a/i	Bacteria	(Kelly and Scheibling, 2012; Parkes and Taylor, 1983; Smith et al., 2006; Viso and Marty, 1993)
16:1 ω 5	Bacteria	(Dowling et al., 1986; Elvert et al., 2003; Taylor and Parkes, 1983)
16:1 ω 7	Marine phytoplankton and cyanobacteria Bacteria	(Viso:1993bv Volkman et al., 1989; Wakeham, 1995) (Londry et al., 2004; McCaffrey et al., 1989)
16:1 ω 9	Phytoplankton	(Viso and Marty, 1993)
17:0	Bacteria	(Dalsgaard et al., 2003)
18:1 ω 5	Phytoplankton	(Parrish et al., 2005)
18:1 ω 7	Bacteria	(Cranwell, 1982; McCaffrey et al., 1989)
	Marine phytoplankton, zooplankton, and cyanobacteria	(C. S. Albers et al., 1996; Wakeham, 1995)
18:1 ω 9	Bacteria Marine phytoplankton Marine zooplankton	(Londry et al., 2004) (Wakeham, 1995) (C. S. Albers et al., 1996)
20:1	Zooplankton	(Falk-Petersen et al., 1999; Kattner and Hagen, 1995)
20:5 ω 3, 20:4 ω 6	Diatoms	(Dunstan et al., 1994; Shaw et al., 1989)
22:1	Zooplankton	(Falk-Petersen et al., 1999)
22:6 ω 3	Dinoflagellate	(Mansour et al., 1999a)
24:6 ω 3	Brittle stars (<i>Ophiuroidea</i>)	(Drazen et al., 2008)
LCFAs (20:0,	Vascular plants	(Eglinton and Hamilton,

22:0, 24:0, 26:0)	Microalgae	1967) (P. D. Nichols et al., 1986; Volkman et al., 1980)
	Sediment bacteria	(Volkman et al., 1988)
<hr/>		
<i>Sterols*</i>		
26 Δ ^{5,22E}	Phytoplankton	(Schever, 1978)
26 Δ ^{22E}	unspecified	
27 Δ ^{5, 22E}	Phytoplankton	(Volkman et al., 1998)
27 Δ ^{22E}	unspecified	
27 Δ ⁵	Phytoplankton, zooplankton, marine vertebrates and invertebrates, bacteria	(Kanazawa, 2001; Volkman, 1986; Wakeham et al., 1997)
27 Δ ⁰	Cyanobacteria	(Volkman, 2003)
28 Δ ^{5,22E}	Phytoplankton	(Volkman et al., 1998)
28 Δ ^{22E}	unspecified	
28 Δ ^{5,24(28)}	Diatoms	(Volkman et al., 1998)
28 Δ ²⁴⁽²⁸⁾	Phytoplankton	
29 Δ ^{5, 22E}	Phytoplankton	(Volkman, 2003)
29 Δ ^{22E}	unspecified	
29 Stenol	unspecified	
29 Δ ⁵ ethyl	Phytoplankton, blue-green algae	(Volkman, 1986) (Kohlhase and Pohl, 1988)
29 Δ ⁵ dimethyl	Dinoflagellates	
29 Δ ⁰ dimethyl	Dinoflagellates	(Mansour et al., 1999b)
29 Δ ⁰ ethyl	Phytoplankton	
30 Δ ^{22E}	Dinoflagellate	(Venkatesan, 1988; Volkman et al., 1998)
Coprostanol	Whales, seals, sea lions	(Venkatesan et al., 1986; Venkatesan and Santiago, 1989)
<hr/>		
<i>Hydrocarbons</i>		
<i>n</i> -alkane C ₂₁	Phytoplankton	(Blumer et al., 1971)
Predominance of odd <i>n</i> -alkane C ₂₅₋₃₃	Terrestrial higher plant	(Eglinton and Hamilton, 1967)

over even <i>n</i> - alkane		
HBI C _{25:2}	Sea Ice diatoms	(Massé et al., 2011)
HBI C _{25:3, 30:5}	Diatoms	(Fahl and Stein, 2012; Johns et al., 1999; Volkman et al., 1994)
polycyclic aromatic hydrocarbons (PAH)	Fungi	(Jiang et al., 2000)
<hr/>		
<i>Ketones</i>		
Stenones	Degradation of sterols	(Gagosian et al., 1980; Nishimura, 1982)
Hopanones	Bacteria	(Ourisson and Rohmer, 1992)
Wax esters	Zooplankton	(Kattner et al., 1989; R. F. Lee, 1975)
<hr/>		
<i>Core GDGTs</i>		
iGDGT-0	Archaea	(Koga et al., 1993)
iGDGT-1,2,3,4	Archaea	
crenarchaeol	Thaumarchaeota	(Schouten et al., 2007b)
brGDGTs	Soil bacteria	(Weijers et al., 2009)
	Bacteria in anoxic water	(Liu et al., 2014)
	<i>In situ</i> sediment bacteria	(Fietz et al., 2012; Peterse et al., 2009)
OH-GDGTs	Archaea	(Liu et al., 2012)
GDDs	Archaea	(Meador et al., 2014)
Archaeol	Archaea	(Koga et al., 1993)
MeO-Archaeol	Thaumarchaeota	(Elling et al., 2014)*

* LCFAs (long chain fatty acids), 26 $\Delta^{5,22E}$ (24-norcholesta-5,22E-dien-3 β -ol), 26 Δ^{22E} (24-Nor-5 α -cholest-22E-en-3 β -ol), 27 $\Delta^{5,22E}$ (5,22E-dien-3 β -ol), 27 Δ^{22E} (5 α -Cholest-22E-en-3 β -ol), 27 Δ^5

2.3.4 Principal component analysis

To further examine the lipid biomarker composition and distribution along the transect and downcore, we conducted a principal component analysis (PCA). PCA highlighted that the lipid composition transitioned from phytoplankton-rich labile biomarkers in surface sediments to bacteria-rich and recalcitrant biomarkers in bottom sediments (Figure 11). In general, unsaturation and chain length control the reactivity of lipids in sediments (i.e., unsaturated molecules are more labile than saturated molecules, and short carbon chain molecules are more labile than long carbon chain molecules) (Haddad et al., 1992; Meyers and Eadie, 1993; Sun et al., 1997; Wakeham and Canuel,

(cholest-5-en-3 β -ol), 27 Δ^0 (5 α -Cholestan-3 β -ol), 28 $\Delta^{5,22E}$ (24-methylcholesta-5,22E-dien-3 β -ol), 28 Δ^{22E} (24-methyl-5 α -cholest-22E-en-3 β -ol), 28 $\Delta^{5,24(28)}$ (24-methylcholesta-5,24(28)-dien-3 β -ol), 28 $\Delta^{24(28)}$ (24-methylcholest-5-en-3 β -ol), 29 $\Delta^{5,22E}$ (stigmasta-5,22E-dien-3 β -ol), 29 Δ^{22E} (4,24-dimethyl-5 α -cholest-22E-en-3 β -ol), 29 Δ^5 dimethyl (23,24-dimethyl-5 α -cholest-5-en-3 β -ol), 29 Δ^5 ethyl (stigmast-5-en-3 β -ol), 29 Δ^0 dimethyl (23,24-dimethylcholestan-3 β -ol), 29 Δ^0 ethyl (24-ethylcholestan-3 β -ol), 30 Δ^{22E} (4 α ,23,24R-trimethyl-5 α -cholest-22-en-3 β -ol), coprostanol (5 β -cholestan-3 β -ol), iGDGT (isoprenoidal glycerol dialkyl glycerol tetraethers), brGDGTs (branched glycerol dialkyl glycerol tetraethers), OH-GDGTs (hydroxyl glycerol dialkyl glycerol tetraethers), GDDs (glycerol dialkanol diethers), MeO-Archaeol (methoxy-archaeol)

2006). Lipids such as poly-unsaturated fatty acids (PUFAs), mono-unsaturated fatty acids (MUFAs) are relatively labile, while short-chain saturated fatty acids (SCFAs) and *n*-alkanes are relatively recalcitrant and likely preserved in sediments for longer (Cranwell, 1981; Wakeham and Canuel, 2006). In the PCA variable plot, phytoplankton biomarkers such as PUFAs, HBIs, and C₂₈ sterols (Table 3) and other relatively labile biomarkers such as MUFAs were positively loaded on PC2. In contrast, relatively recalcitrant biomarkers such as SCFAs, *n*-alkanes, and bacterial-derived branched fatty acids were negatively loaded on PC2 (Figure 11A). These variations of biomarker loadings contributed to the sample variances. The sample score plot demonstrated that lipid composition changes from the surface to the bottom of the core (Figure 11B). This downcore transition corresponds to the first principal component (PC1) that explained 25% of the lipid composition variance.

Lipid compositions differed among sampling stations, particularly in deeper sediments (Figure 11). Sediment from the most offshore station (K) contains more phytoplankton-rich labile organic matter than the other stations; neighboring Station J contains more recalcitrant and bacterial-rich organic matter than other stations. Station J is somewhat of an 'outlier' in the study area. Although primary productivity at Station J is relatively high in the Larsen A Embayment and comparable to that of Station K (Cape et al., 2014), sediment from Station J had a higher abundance of bacterial biomarkers than sediments from Station K (Figure 10). We hypothesize that lateral transport of

organic matter may be significant at Station J, due to its location near the mouth of Prince Gustav Channel that connects the Larsen A Embayment to the northern Antarctic Peninsula (Figure 1). This could enhance the amount of particulate organic matter delivered to the seafloor. The density of infaunal macro- and meiofauna was greatest at Station J in the embayment (Ribeiro, 2015). We suggest that at Station J, fresh organic matter was intensively grazed by benthic fauna. This could explain the accumulation of more recalcitrant lipid biomarkers such as SCFAs and *n*-alkanes in sediments from Station J compared to the other stations (Figure 11). Moreover, degradation of the fresh organic matter by macro- and meiofauna may stimulate bacterial activity in sediments, explaining the higher contribution of their lipids at Station J compared to the other stations (Figure 10).

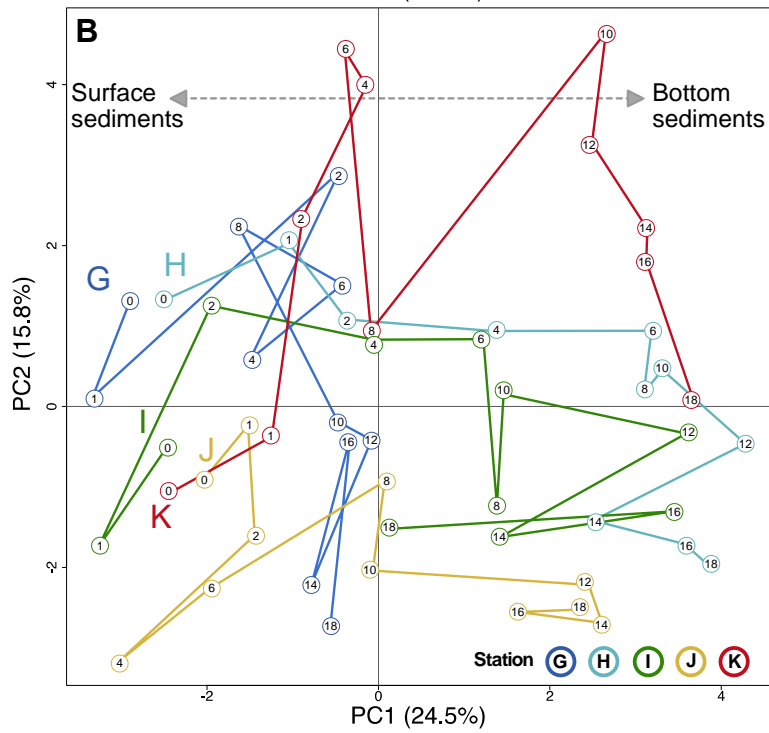
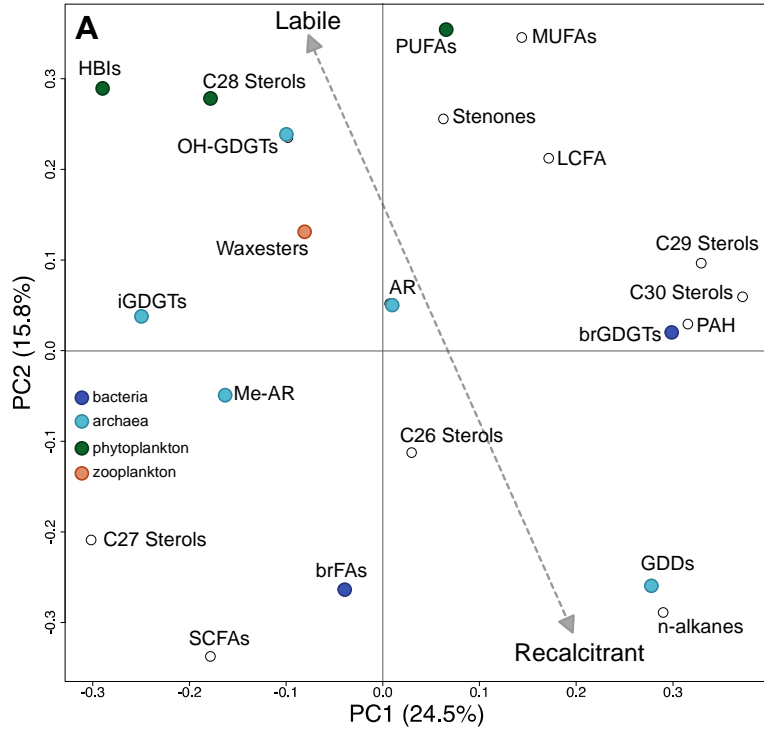


Figure 11: Sediment lipid biomarker variable loadings and sample scores for the first two principal components identified by a PCA model based on relative abundance of fatty acids, sterols, hydrocarbons, ketones and core GDGTs (see material and method for details). (A) Biomarker variable loadings (see Table 3 for abbreviations). Different colors indicate different sources. (B) Sediment sample scores; numbers indicate sediment depths (cm), color indicate sampling stations (see legend) and down core path is indicated by line.

2.5 Conclusions

Lipid biomarker compositions in sediments across the Larsen A Embayment showed that the majority of the organic matter source in the sediments was derived from phytodetritus from the water column. The composition of fatty acids [C_{16} (16:0 and/or 16:1 ω 7), C_{18} (18:0 and/or 18:1 ω 7), and C_{20} (20:5)] and sterols (predominance of 24-methylenecholesterol and sitosterol) was unique compared to other sites in the Southern Ocean likely due to the differences in phytoplankton communities. We also found ^{13}C -enriched sea-ice diatom HBI $C_{25:2}$ as a major hydrocarbon. These lipid compositions demonstrate the importance of organic matter input from sea ice diatoms. The second and third largest lipid sources, bacteria and archaea, could be derived from the water column and *in situ* (sediments). Soil bacteria-derived branched GDGTs compositions and increasing distribution towards offshore and downcore may suggest the *in situ* production of branched GDGTs and potential soil organic matter input by the melting ice shelf and icebergs. The positive correlation between lipid biomarker inventories and time since the ice-shelf collapse indicate increasing lipid accumulation in sediments due to increased primary productivity in the water column following the ice-shelf collapse,

consistent with satellite-based productivity studies. Remote sensing techniques do not capture primary production under sea ice; sediment lipid biomarkers for sea-ice diatoms provide insight into this component of southern ocean productivity.

3. Increasing organic matter flux to the seafloor and reactivity in the sediments following the ice shelf collapse in the Larsen A Embayment, Antarctica

Co-authorship statement

This chapter was conducted as collaborative work. LARISSA 2012 team conducted sample collection. Richard Taylor and David DeMaster (North Carolina State University), conducted ^{210}Pb tracer analysis and ^{14}C dating. Megumi Shimizu conducted sample collection, lipid biomarker analyses, and diagenetic modeling analyses.

3.1 Introduction

Every year, roughly 5% of marine net primary production [2.3 Pg (10^{15}g) carbon] reaches the global seafloor (Dunne et al., 2007). Organic matter flux to the seafloor highly depends on the ocean surface primary productivity. In addition, other factors could influence on organic matter fluxes, carbon export efficiency, including organic matter degradation in sinking particles, grazing of sinking particles in the water column and at the seafloor, and lateral transportation of organic matter. At the seabed, this organic matter sustains benthic fauna and microorganisms, and is ultimately either remineralized as CO_2 or preserved in the fine-grained sediments.

Recent ice melt, including loss of permanent ice and shrinking sea ice extent, has enhanced marine productivity in the Antarctic and Arctic oceans (Arrigo et al., 2008;

Bertolin and Schloss, 2009) and thus is expected to increase the flux of organic matter to the seabed. The extent of Antarctic ice shelves has been decreasing due to recent global warming (Bintanja et al., 2013; Mulvaney et al., 2012). The Antarctic Peninsula region is warming exceptionally fast, with air temperature increasing at a rate of $3.7 \pm 1.6^\circ\text{C}$ century⁻¹, six times greater than the global average rate (Vaughan et al., 2003). Ice shelves along the Antarctic Peninsula, such as Larsen Ice Shelf and Wilkins Ice Shelf, are rapidly disintegrating; more than 2.4×10^4 km² has been lost in past 50 years (National Snow and Ice Data Center, 2010; Peck et al., 2010). The area previously covered by ice shelf is now covered by seasonal sea ice, and is open for the surface primary production during the austral summer. Loss of permanent ice cover changes the water column from an ice-covered, dark sub-ice-shelf environment to a photosynthesis-driven polar ocean system.

In the sub-ice shelf environment, lateral transport from the open ocean system is a source of organic material [apart from localized areas of chemosynthetic production (Domack et al., 2005b)]. Evidence for this includes the presence of diatom frustules throughout Holocene sediments from the Green Peace Trough (in the inner shelf of the Larsen A Embayment) and supports the hypothesis that there is a lateral transport of organic matter underneath the ice shelf (Crawford, 2012). Bioturbation beneath ice shelves (the pre-ice-shelf condition) is incompletely understood. Some studies under the Ross Ice Shelf suggest that there is neither infauna nor bioturbation (T. B. Kellogg and D. E. Kellogg, 1988; Lipps et al., 1979). On the other hand, under the McMurdo Ice Shelf

and the Amery Ice Shelf, organic matter advected beneath the ice shelf could support the abundant and diverse fauna with signs of bioturbated sediments (T. B. Kellogg and D. E. Kellogg, 1988; Post et al., 2007; Riddle et al., 2007).

In the Larsen A Embayment, the ice shelf has collapsed progressively since the mid-19th century, until it finally disappeared in 2000 (Ferrigno, 2006; Rott et al., 1996). Satellite monitoring and field expeditions have documented the increase in surface primary productivity (Bertolin and Schloss, 2009) and the increase in organic matter in surface sediment (Sañé et al., 2011b; 2011a), but measures of the increase in organic matter flux to the seabed after ice-shelf collapse are missing. Organic matter flux to the seabed and carbon burial (sequestration) are key components of the global carbon cycle. In this study, we use lipid biomarkers in sediment cores and diagenetic models to estimate changes in lipid fluxes before and after the ice-shelf disintegration and the importance of this climate change effect on the regional carbon cycle. Our models include multiple modalities (i.e., with and without bioturbation, as well as steady-state and non-steady state sediment profiles) to constrain the estimates of organic matter flux under different assumptions.

Lipids have lower reactivity (high preservation potential) and higher source specificity relative to other organic compound classes (Cranwell, 1982; Hedges, 1995; Wakeham and Canuel, 2006). Lipid biomarker compositions in sediments from beneath the former Larsen A Ice Shelf progress from recalcitrant lipids and bacterial lipids in

deeper sediments to labile lipids of phytoplankton origin in surface sediments (Shimizu et al., in prep). This progression is due to a combination of organic matter degradation in the sediments by microorganisms and increased POC flux to the seabed following ice shelf collapse. Organic matter reactivity in sediments is determined both by the lability of organic matter delivered to the benthic ecosystem and by the environmental conditions under which the organic matter was deposited [e.g., concentrations of dissolved oxygen, and concentrations of other electron acceptors (Canfield, 1994; Canuel and Martens, 1996)].

We estimate lipid fluxes before and after the ice-shelf collapse by applying various models (including biodiffusion-advection-reaction, biodiffusion-reaction, first-order reaction models) to vertical distributions of source-specific organic matter (lipid biomarkers) at five cross-embayment stations. We also estimate the reactivity of individual pelagic lipid biomarkers to understand organic matter diagenesis in the sediments. This approach leads us to an estimate of organic matter flux to the seabed following the ice shelf collapse that is three to four orders of magnitude greater than before ice shelf collapse. The implications are that changing Antarctic ice shelf conditions will increase carbon sequestration in sediments, support a larger biomass of benthic invertebrates and fish, and ultimately, will result in microbial carbon remineralization in the sediments.

3.2 Materials and Methods

3.2.1 Sampling

Sample collection at the Larsen A Embayment site took place as part of a multidisciplinary project, the “Larsen Ice Shelf System, Antarctica” (LARISSA). Sampling was conducted from 7 March to 17 April 2012 from the *RVIB Nathaniel B Palmer* (NBP12-03; M. Vernet, Chief Scientist) off the coast of the East Antarctic Peninsula, Weddell Sea. Sediments were collected using a megacorer at five cross-shelf stations. At each sampling station, one core was devoted to lipid analysis (Shimizu et al., in prep.) and another core was dedicated to ^{210}Pb analysis. Each station represents a different time since exposure to the open-water condition from the ice shelf covered condition: Station G (15 -17 years), Station H (17 – 23 years), Station I (23 – 26 years), Station J (67 - 169 years) (Ferrigno, 2006). Station K serves as a reference station with no ice shelf coverage since 10 ka BP (Davies et al., 2012).

Each core for the lipid analyses was sectioned on board immediately after sample recovery at 0.5-cm intervals to 2 cm depth, 1-cm intervals to 10 cm depth and 2-cm intervals from 10 cm to the bottom of the core (20 cm). Each core for ^{210}Pb analysis was sectioned at 1-cm intervals and stored in the same manner for ^{210}Pb analyses. A peripheral rind on the outside of the core was removed before sampling to eliminate ‘smeared’ sediment during core entry. After sample processing, sectioned sediment samples for lipid analysis were stored at -80 °C. Lipids (hydrocarbons, fatty acids,

sterols) were extracted from sediments, identified and quantified as described in the previous chapter.

3.2.2 Lipid input estimation with diagenetic models

In this study, we assume that vertical distributions of sedimentary organic matter supplied from the water column were controlled by three processes: biodiffusion (bioturbation), advection (sediment accumulation), and reaction (degradation).

The bioturbation process represents the local mixing of sediment through the activity of organisms. Despite the complexity of bioturbation processes, empirical tracer studies repeatedly show that bioturbation can be best mathematically described as random mixing (biodiffusion) (Goldberg and Koide, 1962; Guinasso and Schink, 1975). Diffusion analogy of bioturbation allows us to apply Fick's laws of diffusion to bioturbation (Boudreau, 1986). Biodiffusion rate coefficients and the biodiffusion depth zones in each core were determined by D. DeMaster and R. Taylor (North Carolina State University) using ^{210}Pb tracer distribution following methods in (DeMaster and Cochran, 1982). The top 8 cm at Station G, the top 10 cm at Stations (H to J) and the top 20 cm at Station K are affected by biodiffusion. Due to the low sedimentation rate in the Larsen Embayment [Larsen A: $< 20 \text{ cm kyr}^{-1}$, R. Taylor and D. DeMaster, personal communication; Larsen B: $< 40 \text{ cm kyr}^{-1}$, (Sañé et al., 2011a)] the sediment layer that accumulated after ice-shelf collapse is limited to a maximum of a few centimeters. Bioturbation following ice-shelf collapse mixes newly deposited organic matter to

depths of less than 10 cm in the sediment (Sañé et al., 2011a). We consider that the sediment layers affected by biodiffusion (biodiffusion zone) represent the post-ice-shelf-collapse environment, and the layers not affected by biodiffusion (no biodiffusion zone) represent the pre-ice-shelf-collapse environment.

The advection process represents organic matter supply through sediment accumulation. Long-term sediment burial velocities based on sediment age for each sediment core were determined using organic ^{14}C near the bottom of the cores (20-35 cm) by R. Taylor (NCSU) using methods described in (Fowler et al., 1986). The reaction process represents the microbial and chemical degradation of organic matter in sediments. The reactivity (degradation rate constants) of each lipid biomarker in each sampling station was estimated using reaction models based on first-order kinetics.

Sediments cores were classified into one of three conditions based on assumptions regarding the environmental settings (Table 4). Condition 1 (Station K: 0-20 cm and Station J: 0-10 cm) reflects continuous and constant organic matter supply through biodiffusion and advection with no overlying ice shelf. A biodiffusion-advection-reaction model (Berner, 1980; Boudreau, 1997) was applied to this condition (section 3.2.3.2) to estimate lipid fluxes for the reference station (K) and post-collapse lipid fluxes for Station J.

Condition 2 (Station G: sediment between 0-8 cm, Stations H, I: sediment between 0-10 cm) represents biodiffusion zones and local mixing of post-ice-shelf-

collapse organic material. The depths of sediment accumulated after the ice-shelf collapse are expected to be lower than 0.4 cm (Table 6) and negligible compared to the depths of bioturbated sediment. A biodiffusion-reaction model (Boudreau, 2005) was applied to this condition to estimate post-collapse lipid fluxes for Station G, H, and I. We tested both steady-state (section 3.2.3.3) and non-steady-state (section 3.2.3.4) models for this condition. In the steady-state model, the amount organic matter mixing into the sediments by biodiffusion (bioturbation) is balanced with the amount of organic matter removed by the reaction. However, events such as ice-shelf disintegration would cause an imbalance between the amounts of organic matter introduced and removed. Therefore the downcore lipid distribution after ice-shelf collapse would gradually shift from non-steady state to steady state over the time. We expect that the sediments of the nearshore station (G; most recent loss of ice shelf; 16 years ago) are likely non-steady state, while the more offshore stations, with more time since the collapse, the lipid profiles reached to the steady state. The non-steady-state model allows us to include the change in organic matter vertical distribution with time since the ice-shelf-collapse event.

For Condition 3 (Station G: sediment 8-20 cm; Stations H, I, and J: sediment 10-20 cm), we tested two models with different assumptions about the biodiffusion rate coefficient, namely 1) biodiffusion pre-ice-shelf collapse was zero (no bioturbation) and 2) biodiffusion in the pre-ice-shelf collapse was the same rate as the post-collapse

sediments (as in Condition 2). Biodiffusion rate coefficients in sediments under an ice shelf have not been determined, but an increase in biodiffusion is expected following the transition from ice-shelf to open water regime, given the increase in primary production. A first-order reaction model (Bernier, 1980; 1964) was applied to the case of no biodiffusion (section 3.2.3.5) to estimate pre-collapse lipid fluxes. For the second case with biodiffusion, we applied a biodiffusion-advection-reaction model (section 3.2.3.2).

Table 4: Sediment conditions, stations and sediment datasets, models applied, and their assumptions

CONDITION	Datasets	Models tested	Assumptions
1	Station K (reference) 0-20 cm depths Station J, 0-10 cm depths	Biodiffusion- Advection- Reaction model	Continuous and constant organic matter supply with biodiffusion and sediment accumulation
2	Station G, 0-8 cm depths, Station H and I 0-10 cm depths (biodiffusion zone)	Biodiffusion- Reaction model (steady-state)	Post-ice-shelf-collapse sediment with biodiffusion but negligible sediment accumulation (advection) No change in distribution of organic material in these sediment layers through time (i.e., introduced and remineralized organic matter are in equilibrium)
		Biodiffusion- Reaction model (non-steady- state)	Post-ice-shelf-collapse sediment with biodiffusion but negligible sediment accumulation (advection) Time since ice-shelf collapse is included in the model
3	Station G, 8-20 cm depths, Station H, I, and J	First-order Reaction model	Pre-ice-shelf-collapse sediment with no biodiffusion and advection

10-20 cm depths (no biodiffusion zone)	Biodiffusion- Advection- Reaction model	Pre-ice-shelf-collapse sediment with biodiffusion and advection
---	---	---

All models were applied exclusively to lipid biomarkers exported from the water column (pelagic lipids; Table 5); *in situ* production processes were thus not included in the models. We used the models to estimate the initial lipid concentration for pre- and post-ice shelf collapse datasets, and then converted to fluxes. The lipid flux responses are ratios of post- and pre-fluxes.

Table 5: The lipid biomarkers and their sources used in this study

Lipids	Source	References
Sterol 28 $\Delta^{5,22E}$	Phytoplankton	(Volkman et al., 1998)
Sterol 28 $\Delta^{5,24(28)}$	Diatoms	(Volkman et al., 1998)
Sterol 29 Δ^5 ethyl	Phytoplankton	(Volkman, 1986)
Sterol 29 $\Delta^{5,22E}$	Phytoplankton	(Volkman, 2003)
Sterol 30 Δ^{22E}	Dinoflagellate	(Venkatesan, 1988; Volkman et al., 1998)
HBIs	Diatoms	(Fahl and Stein, 2012; Johns et al., 1999; Massé et al., 2011; Volkman et al., 1994)
FA (20:1 22:1)	Copepods	(Falk-Petersen et al., 1999; Kattner and Hagen, 1995)
FA (24:6 ω 3)	Brittle stars (Ophiuroidea)	(Drazen et al., 2008)
Coprostanol	Marine mammals (whales, seals, and sea lions)	(Venkatesan et al., 1986; Venkatesan and Santiago, 1989)

3.2.3.1 Parameters used in model calculations

Models that take into account biodiffusion, advection and reaction processes depend on sediment parameters (biodiffusion rate coefficients, sediment burial velocity, time since ice-shelf collapse). These values and their sources are summarized in Table 6.

Table 6: Sediment parameters used for modeling lipid biomarker distributions. Biodiffusion rate coefficient D_B , non-steady state model of the distribution of ^{210}Pb activity; determined by R. Taylor (NCSU), sediment burial velocity ω , organic ^{14}C analysis at 20-35 cm depth; determined by R Taylor (NCSU); time since ice-shelf collapse (Ferrigno, 2006), and thickness of sediment layer accumulate after ice shelf collapse that was calculated from sediment burial velocity and time since ice shelf collapse.

Stations	Biodiffusion rate coefficient D_B ($\text{cm}^2 \text{ year}^{-1}$)	Long-term sediment burial velocity ω (cm kyr^{-1})	Time since ice-shelf-collapse (year)	Sediment accumulated after ice-shelf collapse (cm)
G	1.9	< 20	16	0.3
H	5.6	20	20	0.4
I	1.9	7	25	0.1
J	4.9	20	118	2.4
K	4.5	4	NA	NA

3.2.3.2 Biodiffusion-advection-reaction model

The lipid concentrations in sediments that are affected by biodiffusion, advection and reaction can be expressed in a differential equation, under the assumptions of steady state, constant porosity, and the decay of the lipid in proportion to its own concentration (Bernier, 1980; Boudreau, 1997).

$$D_B \frac{d^2 C(x)}{dx^2} - \omega \frac{dC(x)}{dx} - kC(x) = 0 \quad (1)$$

where $C(x)$ is lipid concentration at sediment depth x , D_B is biodiffusion rate coefficient, ω is the sediment burial velocity, and k is the degradation rate constant.

By specifying the flux to the sediment surface as J and applying the Fick's second law of biodiffusion, the first boundary condition implies that.

$$J = \left(-D_B \frac{dC}{dx} + \omega C \right)_{x=0} \quad (2)$$

where C is a concentration of a lipid biomarker. With two other boundary conditions,

$$C_{(x=0)} = C_0$$

$$\left. \frac{dC}{dx} \right|_{x \rightarrow \infty} = 0$$

the known solution of equation (1) as described in Boudreau (1996) is

$$C = C_0 e^{-\alpha x} \quad (3)$$

where

$$\alpha = \frac{-\omega + \sqrt{\omega^2 + 4kD_B}}{2D_B} \quad (4)$$

and

$$C_0 = \frac{J}{D_B \alpha + \omega} \quad (5)$$

where C_0 is the lipid concentration at the time of deposition to surface sediments (x_0). Rearranging equation (3), the model is expressed as a linear regression model

$$\ln(\hat{C}) = -\alpha x + \ln(\hat{C}_0) \quad (6)$$

\hat{C} is the estimated lipid concentration at the sediment depth x and \hat{C}_0 is the estimated average initial lipid input during the dataset time interval. By rearranging equation (4), the rate constant k can be expressed as follows:

$$k = \frac{(2D_B \alpha + \omega)^2 - \omega^2}{4D_B} \quad (7)$$

By rearranging the equation (5), the flux of lipid at the surface sediments can be expressed as follows:

$$J_0 = \hat{C}_0(D_B \alpha + \omega) \quad (8)$$

3.2.3.3 Steady-state biodiffusion-reaction model

The biodiffusion-reaction model was applied to bioturbated zone in Stations (G-J) that was previously covered by the ice shelf. Assuming lipid distribution is controlled by biodiffusion and reaction due to the extremely low advection (Table 4), we removed the advection from the equation (1). The steady-state biodiffusion-reaction model can be expressed as follows:

$$D_B \frac{d^2 C(x)}{dx^2} - kC(x) = 0 \quad (9)$$

Applying the two boundary conditions ($C_{(x=0)} = C_0$ and $dC/dx = 0$ when x reaches ∞), the known solution is

$$C = C_0 e^{-\beta x} \quad (10)$$

where

$$\beta = \sqrt{k/D_B} \quad (11)$$

and

$$C_0 = \frac{J_{post}}{D_B \beta} \quad (12)$$

where J_{post} is the flux of a biomarker at the sediment surface after the ice shelf collapse. By rearranging the equation (11) and (12), the reaction constant and flux were calculated as follows:

$$k = \beta^2 D_B \quad (13)$$

$$J_{post} = C_0 D_B \beta \quad (14)$$

3.2.3.4 Non-steady-state biodiffusion-reaction model

The non-steady-state biodiffusion-reaction model of lipid in below allows us to include the time since the ice-shelf collapse in each station. The model assumes lipid concentrations are initially negligible in sediment but supplied after some arbitrary time ($t = 0$; when ice-shelf broke) at a constant rate (Boudreau, 1997). We assume the lipid concentrations at 0-8 or 0-10 cm sediment depths before the ice-shelf collapse is negligible compared to lipids introduced after the ice-shelf collapse (Table 4). This model also assumes that the biodiffusion is constant and advection can be ignored.

$$\frac{dC}{dt} = D_B \frac{d^2C}{dx^2} - kC \quad (15)$$

with boundary conditions;

$$-D_B \left. \frac{dC}{dx} \right|_0 = J$$

$$C(x, 0) = 0$$

$$\left. \frac{dC}{dx} \right|_{x \rightarrow \infty} = 0$$

To solve the equation, treat C as the sum of a steady-state part (C_{ss}) and a transient part $C_t(x, t)$.

$$C(x, t) = C_{ss}(x) + C_t(x, t) \exp(-kt) \quad (16)$$

where

$$C_{ss}(x) = C_0 \exp\left(-x \sqrt{\frac{k}{D_B}}\right) \quad (17)$$

and

$$C_0 = \frac{J}{D_B k} \quad (15)$$

The reduced transient part of the problem has become

$$\frac{dC_t}{dt} = D_B \frac{d^2 C_t}{dx^2} \quad (19)$$

with boundary conditions,

$$\begin{aligned} \left. \frac{dC_t}{dx} \right|_{x=0} &= 0 \\ \left. \frac{dC_t}{dx} \right|_{x \rightarrow \infty} &= 0 \\ C_t(x, 0) &= -C_0 \exp\left(-x \sqrt{\frac{k}{D_B}}\right) \end{aligned}$$

This can be solved with Separation of Variables (SoV) method for 1-D biodiffusion problems and integration solutions provided by (Ozisik, 1993).

$$C_t(x, t) = -\frac{2C_0}{\pi} \int_0^{\infty} \cos(\beta x) \exp(-D_B \beta^2 t) \int_0^{\infty} \cos(\beta x') \exp\left(-x \sqrt{\frac{k}{D_B}}\right) dx' d\beta \quad (20)$$

The interior integral of this equation can be tabulated (Beyer, 1981) as follows

$$C_t(x, t) = -\frac{2C_0\sqrt{k}}{\pi\sqrt{D_B}} \int_0^{\infty} \frac{\cos(\beta x) \exp(-D_B\beta^2 t)}{\left(\frac{k}{D_B} + \beta^2\right)} d\beta \quad (21)$$

The remaining integral is also tabulated as follows;

$$C_t(x, t) = -\frac{C_0 \exp(kt)}{2} \left[2 \cosh\left(-x \sqrt{\frac{k}{D_B}}\right) - \exp\left(\sqrt{\frac{kx^2}{D_B}}\right) \operatorname{erf}\left(\sqrt{kt} - \frac{x}{2\sqrt{D_B t}}\right) - \exp\left(-\sqrt{\frac{kx^2}{D_B}}\right) \operatorname{erf}\left(\sqrt{kt} + \frac{x}{2\sqrt{D_B t}}\right) \right] \quad (22)$$

This solution was used for non-linear regression using nlmrt package in R (Nash, 2016) to compute the k and C_0 .

3.2.3.2 First-Order Reaction (G) Model

The first-order reaction model was first developed for tracers, but also applicable reactive organic molecules such as lipids (Canuel and Martens, 1996; Westrich and Berner, 1984). For the first-order reaction model (Berner, 1980; 1964), biodiffusion under the ice shelf was assumed to be negligible. With this model, we assume that lipids are degraded by first-order kinetics, and lipid degradation rate is constant. The model is expressed by removing biodiffusion process from the equation (1) as follows:

$$\omega \frac{dC(x)}{dx} + kC = 0 \quad (23)$$

The sediment burial velocity and sediment depths can be replaced with time and equation (23) can be expressed as follows:

$$\frac{dC(t)}{dt} = -kC \quad (24)$$

where t is time. Using the boundary conditions $C_{(t=0)} = C_0$ (Boudreau, 1997), equation (24) is:

$$C = C_0 e^{-kt} \quad (25)$$

C_0 is the lipid concentration at the time of deposition to surface sediments (t_0); we call this initial lipid input concentration. Rearranging equation (25), the model is expressed as a linear regression model.

$$\ln(\hat{C}) = -kt + \ln(\hat{C}_0) \quad (26)$$

\hat{C} is estimated lipid concentration at the sediment age t and \hat{C}_0 is estimated average initial lipid input. Sediment age (t) was calculated from sediment burial velocity (Table 3). Degradation rate constant k was calculated as follows:

$$k = - \frac{\ln\left(\frac{\hat{C}}{\hat{C}_0}\right)}{t} \quad (27)$$

The flux of lipids to the seafloor before the ice shelf collapse was calculated using estimated initial concentration of lipid biomarkers \hat{C}_0 and sediment burial velocity, ω as follows:

$$J_{pre} = \hat{C}_0 \omega \quad (28)$$

3.2.3.3 Sensitivity Analysis

Sensitivity analyses were conducted to determine the range of flux and flux response estimates due to uncertainties of variables (biodiffusion rate coefficient, D_B and sediment burial velocity, ω).

There may be as much as a 50-fold discrepancy of biodiffusion rate coefficients assessed by ^{210}Pb and ^{234}Th (D. DeMaster personal communication, (McClintic et al., 2008). Biodiffusion rate coefficient derived from ^{234}Th (that measures short-term biodiffusion, ~100 days scale) can be higher than those derived from ^{210}Pb (that measures long-term biodiffusion, ~100 years scale) (Smith et al., 1993). The sedimentation rate determined using ^{14}C at > 20 cm depth of the sediment cores could potentially underestimate the post-ice-shelf collapse sedimentation rate. The sediment burial velocity at the Larsen Embayment likely stayed low (<40 cm kyr⁻¹ at the Larsen B Embayment) (Sañé et al., 2011a); the interval sedimentation rate at the surface sediments (0-2 cm) at Larsen A was 0.7 cm / kyr⁻¹ (Domack et al., 2005a). In the Western Antarctic

Peninsula, it ranged between 30 to 150 cm kyr⁻¹ (McClintic et al., 2008), this would be the upper limit of sediment burial velocity uncertainty. We assessed these range of uncertainties of bioturbation rate coefficient (D_B : up to 50-fold) on Condition 1 and 2 datasets and sedimentation rate (ω : up to 40-fold increase) on Condition 1 datasets. We assume the bioturbation before the ice shelf collapse will be none or smaller than what was observed after the ice shelf collapse. We assessed the uncertainty $D_B = 0$ to observed values on Condition 3 datasets.

3.2.3.4 Lipid Flux Response

To estimate the change in organic matter flux between pre and post ice-shelf collapse conditions for Stations G, H, I, J, we calculated a Lipid Flux Response as follows:

$$\text{Lipid Flux Response} = \frac{J_{post}}{J_{pre}} \quad (29)$$

where J_{pre} and J_{post} are lipid fluxes pre- and post- ice-shelf collapse. To obtain these fluxes, we used the initial lipid concentrations (C_0) and converted them to fluxes (Equations 8, 14, and 28). The post-ice-shelf-collapse initial lipid concentrations in the surface sediments ($C_{0,post}$) were obtained by extrapolating from regressions of vertical lipid distributions in Condition 2 datasets (Figure 1, Table 1). The pre-ice-shelf-collapse initial lipid concentrations in the surface sediments ($C_{0,pre}$) were obtained by

extrapolation from regressions of vertical lipid distributions in Condition 3 datasets (Figure 12, Table 4).

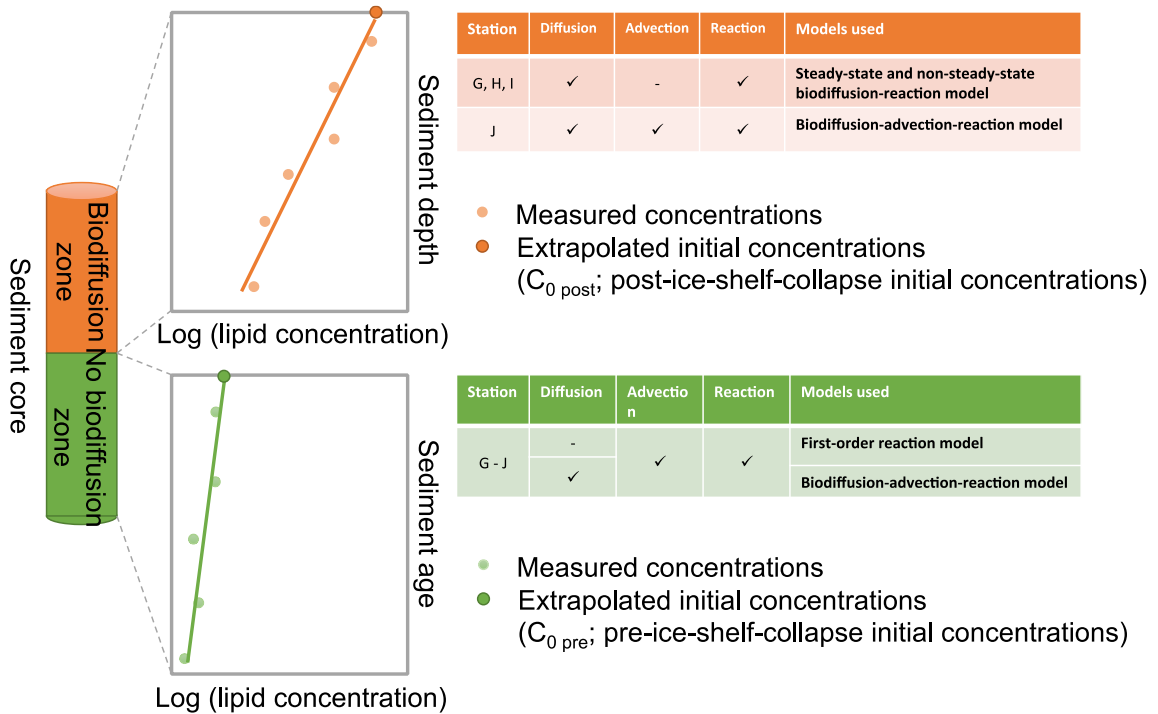


Figure 12: Schematic explanation of the models to estimate initial lipid concentrations for biodiffusion zone sediments and pre-collapse sediments in Station G - J. $C_{0,pre}$: extrapolated initial lipid concentration during the pre-ice-shelf collapse period, $C_{0,post}$: estimated initial lipid concentrations during post-ice-shelf collapse period.

We calculated flux responses for three scenarios by varying the biodiffusion rate coefficient (D_B); 1) the most probable scenario, 2) a conservative scenario (the lowest post-collapse flux estimations / the highest pre-collapse flux estimations), and 3) an extreme scenario (the high post-collapse flux estimations / the lowest pre-collapse flux estimations). Scenario 1 (the most probable estimation) uses measured biodiffusion rate coefficient ($D_B \times 1$) to estimate post-collapse flux and no biodiffusion (the first-order

reaction model) to estimate pre-collapse fluxes. Scenario 2 (the conservative scenario) uses measured biodiffusion rate coefficient ($D_B \times 1$) to estimate both of post- and pre-collapse fluxes. Scenario 3 (the extreme estimation) uses 20-fold of measured biodiffusion rate coefficient ($D_B \times 20$) to estimate post-collapse fluxes, and no biodiffusion (first-order reaction model) to estimate pre-collapse fluxes (Table 7).

Table 7: The combinations of biodiffusion rate coefficients used to calculate three scenarios of lipid flux responses

Scenario	Post-ice-shelf-collapse biodiffusion rate coefficient	Pre-ice-shelf-collapse biodiffusion rate coefficient
1	Measured coefficient ($D_B \times 1$)	No biodiffusion ($D_B = 0$)
2	Measured coefficient ($D_B \times 1$)	Measured coefficient ($D_B \times 1$)
3	20-fold of measured biodiffusion rate coefficient ($D_B \times 20$)	No biodiffusion ($D_B = 0$)

3.2.4 Statistical Analysis

Analysis of variance (ANOVA) was conducted to compare mean fluxes or degradation rate constants across the sampling stations or among lipid biomarkers. If significant variations were evident as a result of the ANOVA, then Tukey–Kramer HSD tests were performed to compare the mean values among sampling stations. For all ANOVA and Tukey–Kramer HSD test results, an alpha level of 0.05 was used as the criterion for statistical significance unless stated otherwise.

3.3 Results

3.3.1 Pelagic lipid distributions and flux at Reference Station K

At the reference station (K, condition 1), concentrations of lipid biomarkers decreased logarithmically downcore (Figure 13), ($R^2 > 0.59$, $p < 0.01$; Table 8). The estimated flux of individual biomarkers determined using a biodiffusion-advection-reaction model ranged between 4 ($C_{24:6}$ fatty acid) to 1353 $\text{ng cm}^{-2} \text{ year}^{-1}$ [polyunsaturated fatty acids (PUFAs)]. The estimated total pelagic lipid flux at the sediment-water interface was 7427 $\text{ng cm}^{-2} \text{ year}^{-1}$.

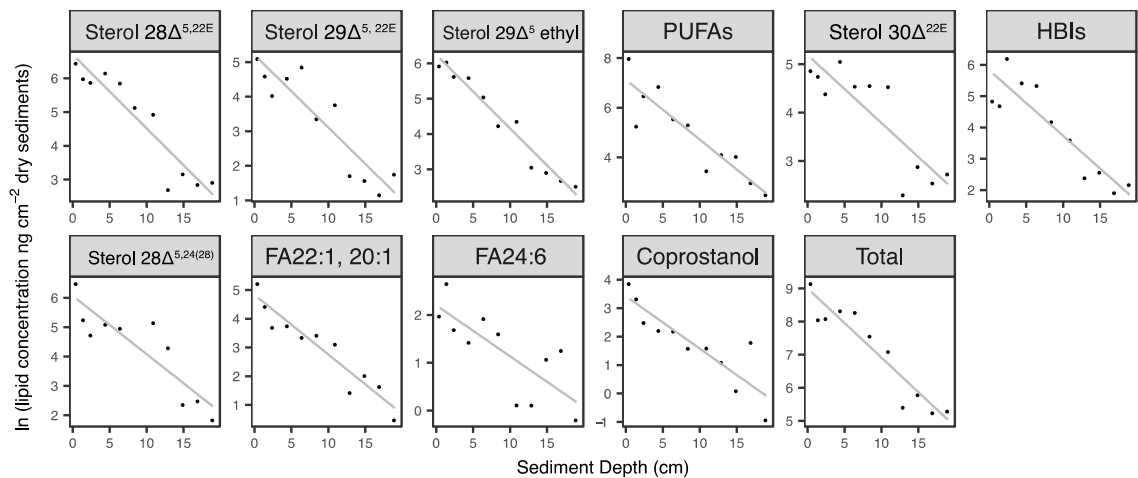


Figure 13: Downcore distribution of lipid biomarkers at the reference station (K). The lipid biomarkers concentrations decrease logarithmically ($R^2 > 0.59$, $p < 0.01$).

3.3.2 Total Pelagic Lipid Flux, Stations G – I post-ice-shelf collapse (biodiffusion zone)

The estimated pelagic total lipid fluxes for Stations G to H ranged between 5700 to 45000 $\text{ng cm}^{-2} \text{ year}^{-1}$. At Station G, the flux estimated by the non-steady-state model

was 13-fold larger than the estimate by the steady-state model (Figure 14). At Stations H and I, the flux estimated by the steady-state model was 1.9 and 1.7-fold larger than the estimate by the non-steady-state model. To determine which model would be appropriate for each dataset, we considered the R^2 values for each model. For Station G, the non-steady-state model fits better ($R^2 = 0.98$, $p=0.002$) than steady-state model ($R^2 = 0.75$, $p=0.06$). The steady-state model fits better for Stations H and I (non-steady-state, Station H: $R^2 = 0.96$, $p<0.001$; Station I: $R^2 = 0.94$, $p<0.001$; steady-state, Station H: $R^2 = 0.98$, $p<0.01$; Station I: $R^2 = 0.95$, $p<0.01$). Therefore, for further analyses, we use the non-steady-state model for Station G and steady-state model for Station H, and I.

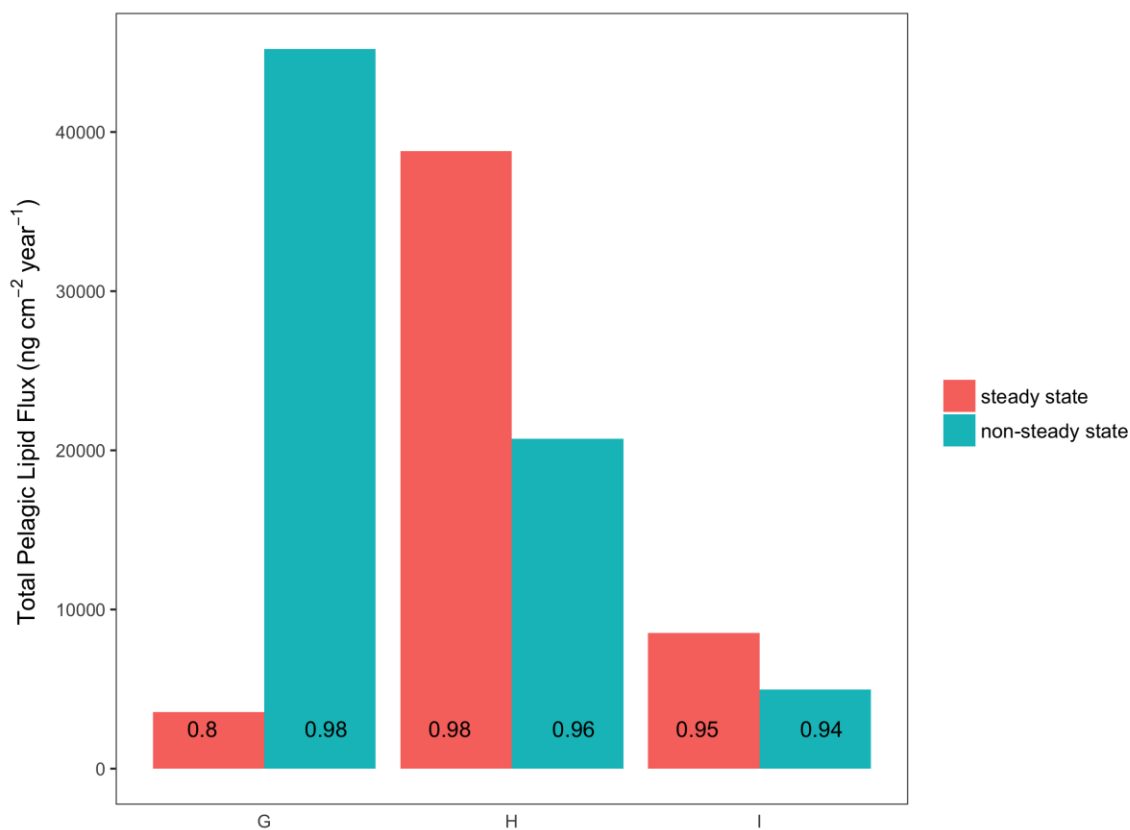


Figure 14: Comparison of estimated total pelagic lipid fluxes applying different models, the steady-state and the non-steady-state biodiffusion-reaction models for biodiffusion zone sediments of Station G, H and I. Values on the bar plots represent the goodness of model fit (R^2).

3.3.3 Pelagic lipid fluxes across the embayment

Post-ice-shelf-collapse total pelagic lipid fluxes estimations ranged between 45000 ng cm⁻² year⁻¹ (Station G) and 5500 ng cm⁻² year⁻¹ (Station I). The individual lipid fluxes ranged between 4 (FA C24:6 at Station I) and 4200 (Cholesterol at Station J) ng cm⁻² year⁻¹.

$^2 \text{ year}^{-1}$ (Table 8). There was no increasing or decreasing pattern of lipid fluxes across the embayment (Figure 15).

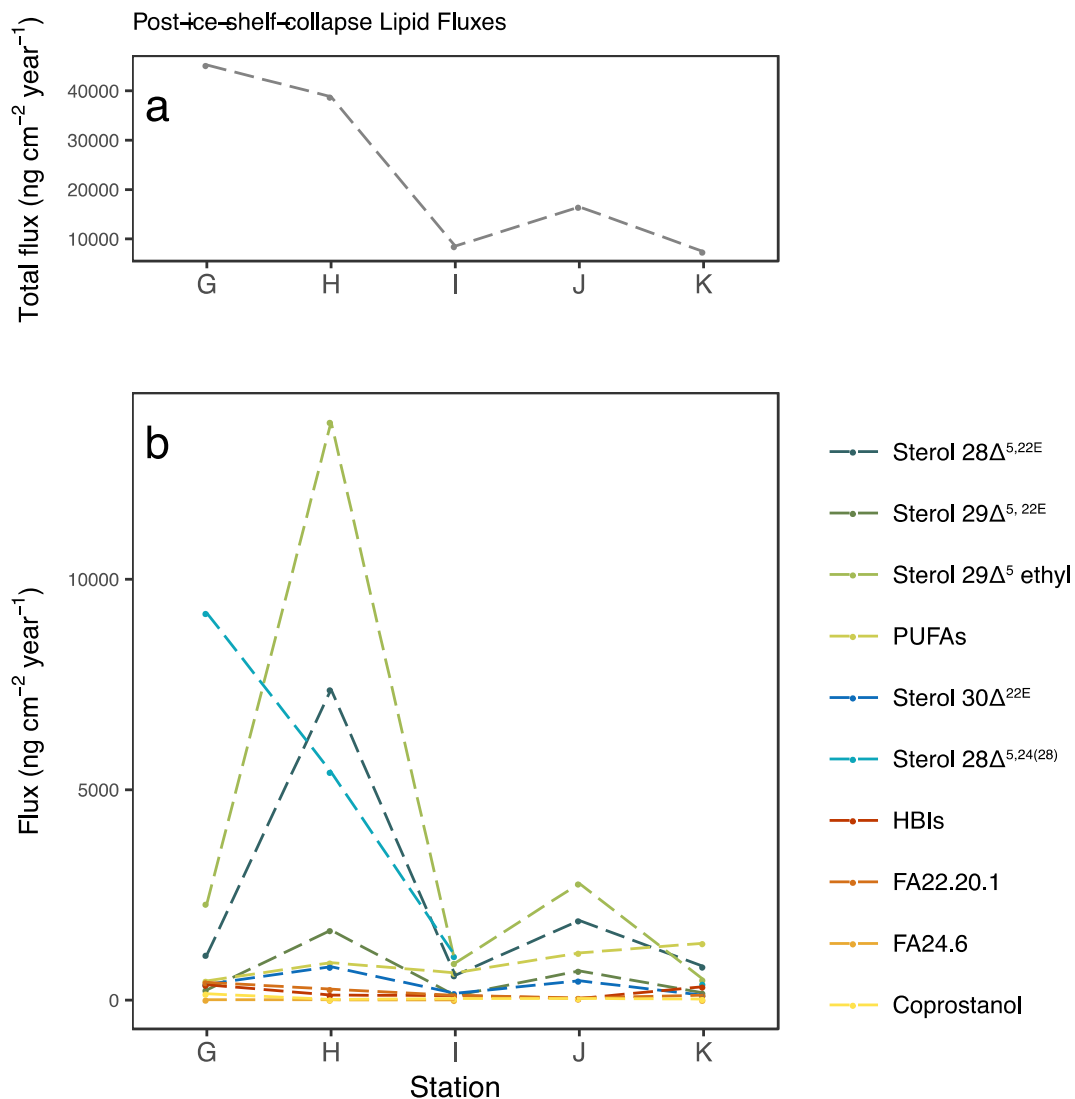


Figure 15: Post-ice-shelf-collapse fluxes of lipid biomarkers across the embayment. a) estimated fluxes of total pelagic lipids; b) estimated fluxes of individual biomarkers; the fluxes for Station G estimated using the non-steady-state biodiffusion-reaction model, for Station H and I using the steady-state biodiffusion reaction model, and for Station J and K using the biodiffusion-advection-reaction model. Only the estimations made from the significant model fitting ($p < 0.1$) were shown here.

Pre-ice-shelf-collapse total pelagic lipid flux estimations ranged from $0.5 \text{ ng cm}^{-2} \text{ year}^{-1}$ (Station I) to $11.0 \text{ ng cm}^{-2} \text{ year}^{-1}$ (Station H) when modeled without biodiffusion

(Figure 16a). In contrast, the total fluxes ranged from 16 to 500 ng cm⁻² year⁻¹ when modeled with biodiffusion (Figure 16c). The estimated total pelagic lipid flux showed decreasing trend towards offshore stations. Individual biomarkers did not show obvious patterns across the embayment for the pre-ice-shelf-collapse sediments (Figure 16b).

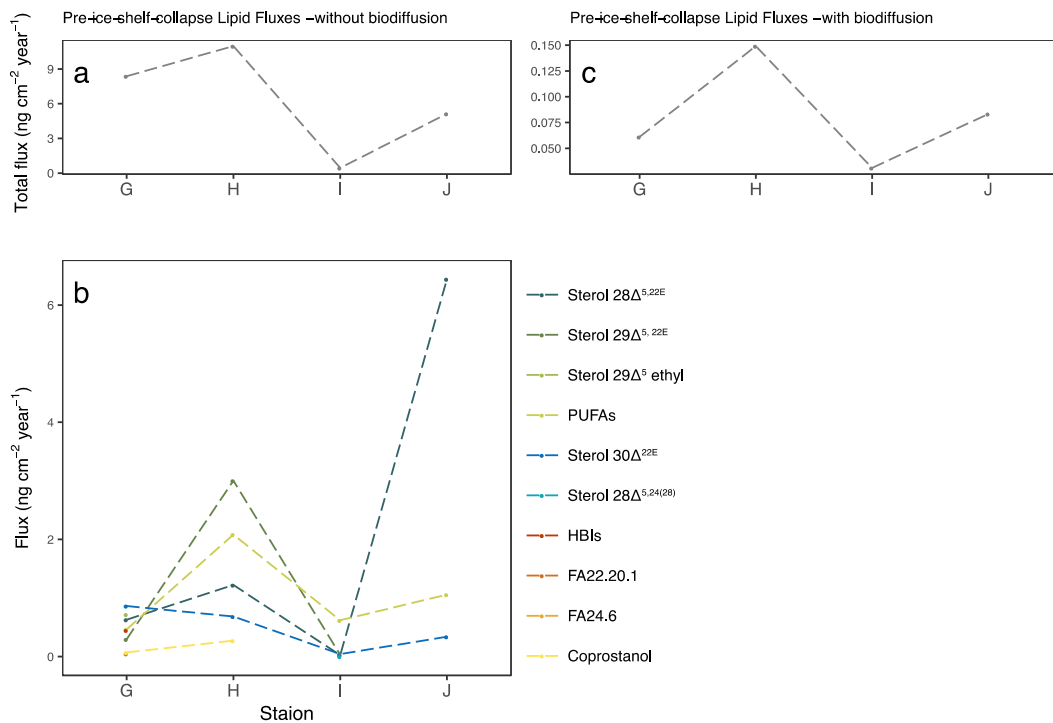


Figure 16: Pre-ice-shelf-collapse fluxes of lipid biomarkers across the embayment. a) fluxes of total pelagic lipids estimated without biodiffusion; d) fluxes of individual lipid biomarkers before the ice shelf collapse; c) fluxes of total pelagic lipids estimated with biodiffusion. Only the estimations made from the significant model fitting ($p < 0.1$) are shown here.

3.3.3 Reactivity (degradation rate constant)

Reactivity (degradation rate constants) of individual pelagic lipids were calculated using equations 7, 13, and 27. The mean post-ice-shelf-collapse degradation

rate constant (Figure 17) ranged between 0.76 yr^{-1} (Station G) and 0.06 yr^{-1} (Station K).

The pre-collapse degradation rate constants were up to three orders of magnitude lower using the model without biodiffusion (first-order degradation model) than using the model with biodiffusion (biodiffusion-advection-reaction model). The post-collapse degradation rate constants were at least three-fold higher than pre-collapse degradation rate constants.

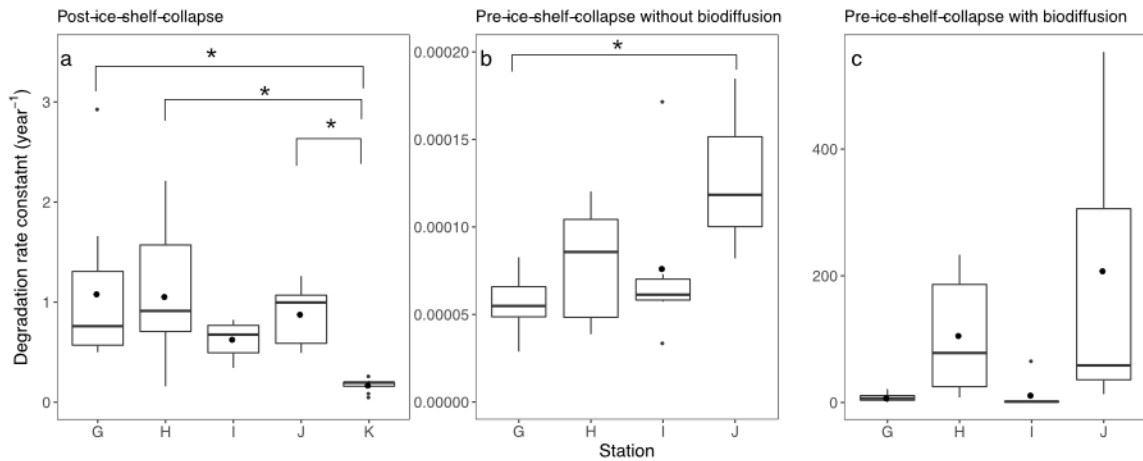


Figure 17: Box plots of estimated lipid degradation rate constants across the sampling stations. a) post-ice-shelf-collapse degradation rate constants. Significance levels; * represents $p < 0.05$; n.s. represents not significant. b) pre-ice-shelf-collapse degradation rate constants estimated without biodiffusion. c) pre-ice-shelf-collapse degradation rate constants estimated with biodiffusion.

3.3.4 Sensitivity Analyses

To understand which variables affect the flux estimation, sensitivity analyses were conducted. Increasing the magnitudes of biodiffusion coefficient (D_B) proportionally increase the flux estimates (Figure 18). Varying the magnitudes of

bio-diffusion coefficient (D_B) up to 50-fold in Conditions 1 affect the flux estimate proportionally (50 fold) (Figure 18a) and in Condition 2 affect the flux estimate exponentially (Figure 18c). Also varying the (D_B) between 0-1 fold in Condition 3 also affect the flux estimates proportionally (17 to 46 folds differences) (Figure 18d). On the contrary, changing the magnitude of ω up to 40 folds had little effect (1.2 folds for Station K, 1.4 folds for Station J) (Figure 18b).

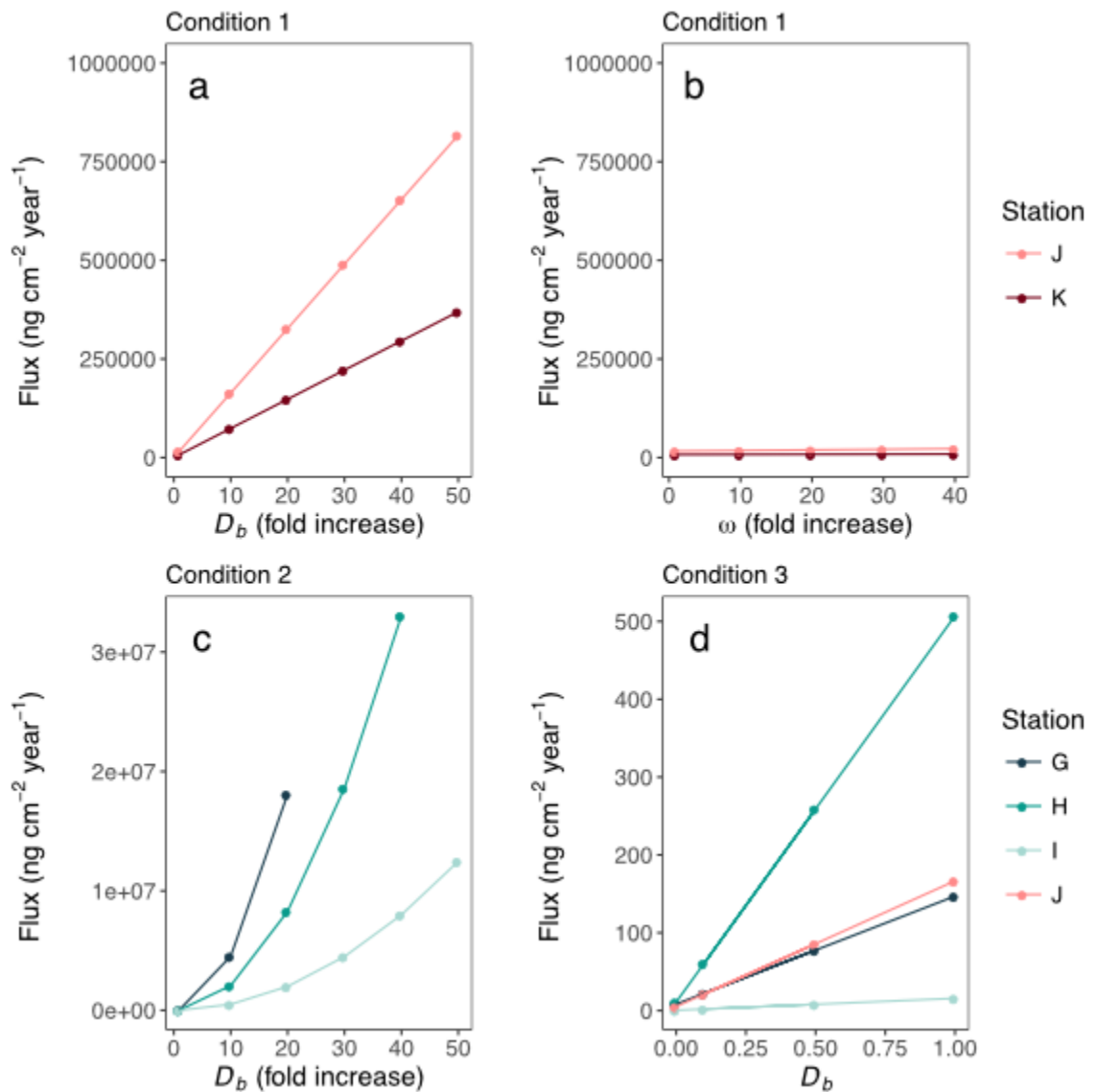


Figure 18: Sensitivity analyses. a and b) The effect of varying the magnitudes of biodiffusion rate coefficient (D_b) and sediment burial velocity (ω) in biodiffusion-advection-reaction model for Condition 1 datasets. c) The effect of varying the magnitudes of D_b in biodiffusion-reaction model for Condition 2 datasets (Station G; non-steady state model and Stations H, and I; steady state model). d) The effect of varying the magnitudes of D_b in first-order reaction model ($D_b = 0$) and in biodiffusion-advection-reaction model ($D_b > 0$) for Condition 3 datasets.

3.3.5 Potential increase in lipid flux following the ice shelf collapse

To quantify the potential changes in lipid fluxes following the ice shelf collapse, we calculated ratios of fluxes (flux responses; equation 29). A flux response > 1 means an increase in pelagic lipid flux following ice-shelf collapse; a flux response < 1 means a decrease in flux.

The three scenarios of biodiffusion coefficients combinations for pre- and post-ice-shelf-collapse fluxes estimations were tested (Table 7). The estimated changes in total pelagic lipid flux with Scenario 1 ranged from 3200 at Station J to 19000 at Station I (Figure 19: Changes in total pelagic lipid flux following ice shelf collapse in Stations G to J. Potential changes in flux at the reference station (K) was 0.6.), indicating a dramatic increase in pelagic lipid flux following the ice-shelf collapse. The potential change in flux at the reference station estimated by biodiffusion-advection-reaction model for top 10 cm and bottom 10 cm sediments) was 0.6. The higher flux changes in Stations G to J than the reference station support the flux change has occurred due to the ice-shelf disintegration. The estimated changes in flux with Scenario 2 ranged from 4 (Station H) to 720 (Station I). The estimated changes in total pelagic lipid flux with Scenario 3 ranged from 750,000 (Station H) to 450,000 (Station I). All flux responses were > 1 , even with conservative estimation, indicating the total pelagic lipid input at all the four stations increased after the ice-shelf collapse event.

Individual biomarkers ranged from 0.4 (HBIs at Station H) to 1770,000 (Sterol $28\Delta^{5,22E}$ at Station I: Table 8). Vertical distributions of some biomarkers (coprostanol, fatty acids $C_{24:6}$, and $C_{22:1,20:1}$) did not significantly fit the models, ($p > 0.10$; Table 8, Table 9). This is likely due to the patchy distribution of the source organisms [i.e., zooplankton, benthic fauna, and marine mammals;(Gutt et al., 2013; 2011)] compared to the phytoplankton, as well as low concentrations of the biomarkers detected. Due to the lack of significance of model fitting, we were not able to determine the flux and the changes in flux following ice-shelf collapse for these biomarkers. All flux changes determined for individual pelagic lipid biomarkers were > 1 except HBIs flux change (0.4) at Station H under the conservative estimation.

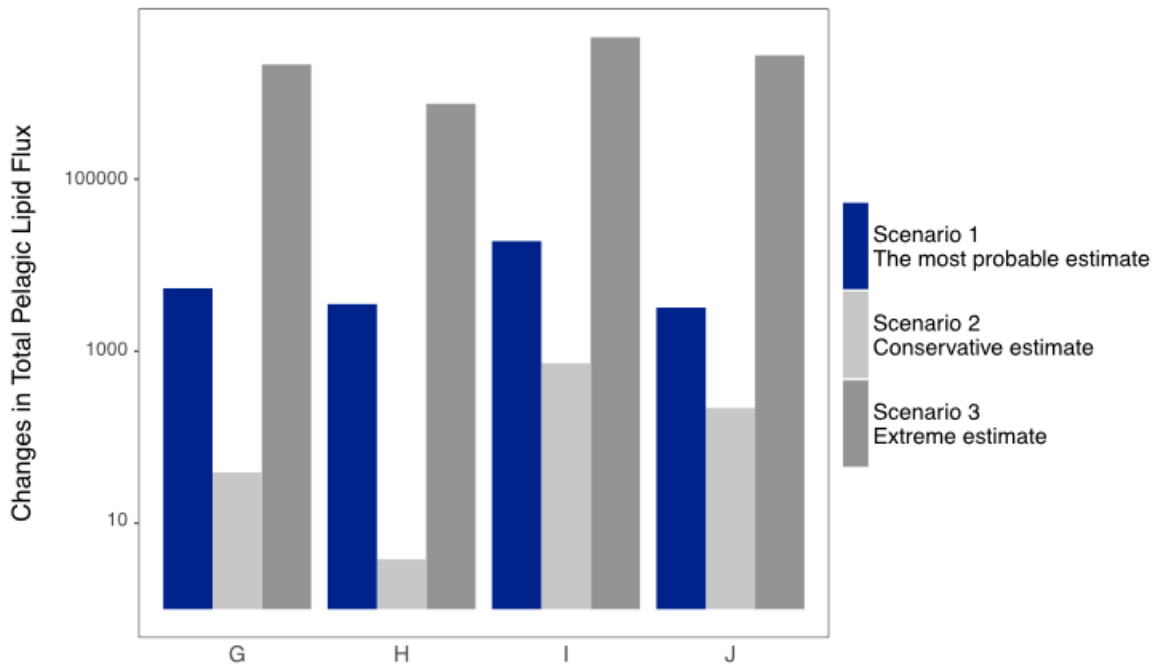


Figure 19: Changes in total pelagic lipid flux following ice shelf collapse in Stations G to J. Potential changes in flux at the reference station (K) was 0.6.

Table 8: Flux and degradation rate constant of lipid biomarkers in post-ice-shelf collapse sediments (top 8 cm for station G, top 10 cm for stations H – J, and whole 20 cm for the reference station K) determined using the diffusion-(advection)-reaction model

	R ²	p value	Flux (ng cm ⁻² yr ⁻¹)	Degradation constant (yr ⁻¹)
Station G (non-steady-state biodiffusion-reaction model)				
Total	0.98	<0.01	45219.00	1.69
Sterol 28Δ ^{5,22E}	0.94	0.01	924.34	0.66
Sterol 29Δ ^{5, 22E}	0.82	0.04	244.01	0.50
Sterol 29Δ ⁵ ethyl	0.96	<0.01	2289.71	1.24
PUFAs	0.98	<0.01	458.28	0.52
Sterol 30Δ ^{22E}	0.87	0.02	373.91	0.60
Sterol 28Δ ^{5,24(28)}	0.99	<0.01	364.86	0.75
HBIs	0.99	0.00	0.00	2.93
FA22.20.1	0.97	<0.01	422.71	1.33
FA24.6	0.89	0.01	10.52	0.56
Coprostanol	0.89	0.03	152.50	1.66
Station H (steady-state biodiffusion-reaction model)				
Total	0.98	<0.01	38810.54	0.76
Sterol 28Δ ^{5,22E}	0.97	<0.01	7382.34	0.65
Sterol 29Δ ^{5, 22E}	0.98	<0.01	1661.05	1.00
Sterol 29Δ ⁵ ethyl	0.88	0.01	13737.60	0.80
PUFAs	0.94	<0.01	890.39	2.98
Sterol 30Δ ^{22E}	0.82	0.01	792.73	0.62
Sterol 28Δ ^{5,24(28)}	0.97	<0.01	5421.85	0.05
HBIs	0.71	0.04	120.08	5.16
FA22.20.1	0.99	<0.01	260.65	0.69
FA24.6	0.83	0.01	8.17	2.14
Coprostanol	0.71	0.03	16.27	0.17
Station I (steady-state biodiffusion-reaction model)				
Total	0.95	<0.01	8540.45	0.46
Sterol 28Δ ^{5,22E}	0.86	0.01	589.05	0.23
Sterol 29Δ ^{5, 22E}	0.91	<0.01	108.11	0.22
Sterol 29Δ ⁵ ethyl	0.94	<0.01	880.18	1.53
PUFAs	0.90	<0.01	649.56	0.21
Sterol 30Δ ^{22E}	0.86	0.01	162.70	0.25
Sterol 28Δ ^{5,24(28)}	0.95	<0.01	1046.53	0.22
HBIs	0.96	<0.01	109.57	0.25

FA22.20.1	0.94	<0.01	113.36	0.31
FA24.6	0.76	0.02	2.67	0.21
Coprostanol	0.94	<0.01	37.37	0.80
Station J (biodiffusion-advection-reaction model)				
Total	0.92	0.01	16499.96	0.96
Sterol 28 $\Delta^{5,22E}$	0.92	0.01	1893.72	1.02
Sterol 29 $\Delta^{5, 22E}$	0.93	0.01	695.54	1.10
Sterol 29 Δ^5 ethyl	0.83	0.03	2770.45	1.06
PUFAs	0.95	<0.01	1121.64	1.26
Sterol 30 Δ^{22E}	0.98	<0.01	461.56	0.97
Sterol 28 $\Delta^{5,24(28)}$	0.90	0.01	2530.23	1.21
HBIs	0.57	0.14	38.67	0.54
FA22.20.1	0.72	0.07	51.82	0.49
FA24.6	0.47	0.20	13.03	0.30
Coprostanol	0.88	0.02	40.55	0.60
Station K (biodiffusion-advection-reaction model)				
Total	0.89	<0.01	7426.92	0.19
Sterol 28 $\Delta^{5,22E}$	0.88	<0.01	797.63	0.21
Sterol 29 $\Delta^{5, 22E}$	0.83	<0.01	172.90	0.20
Sterol 29 Δ^5 ethyl	0.96	<0.01	485.60	0.20
PUFAs	0.82	<0.01	1353.28	0.26
Sterol 30 Δ^{22E}	0.73	<0.01	114.03	0.09
Sterol 28 $\Delta^{5,24(28)}$	0.79	<0.01	385.81	0.18
HBIs	0.82	<0.01	321.13	0.20
FA22.20.1	0.90	<0.01	117.45	0.19
FA24.6	0.59	0.01	4.37	0.05
Coprostanol	0.78	<0.01	25.46	0.15

Table 9: Flux and degradation rate constant of lipid biomarkers in pre-ice-shelf collapse sediments (8-20 cm for station G and 10-20 cm for station H – J) determined using the degradation model

	R ²	p value	First-order reaction model		Biodiffusion-advection-reaction model	
			Flux (ng cm ⁻² yr ⁻¹)	Degradation constant (yr ⁻¹)	Flux (ng cm ⁻² yr ⁻¹)	Degradation constant (yr ⁻¹)
Station G						
Total	0.81	0.02	9.48	5.7E-05	164.29	6.0E-02

Sterol 28 $\Delta^{5,22E}$	0.55	0.09	0.63	5.7E-05	10.96	6.0E-02
Sterol 29 $\Delta^{5,22E}$	0.63	0.06	0.29	6.3E-05	5.63	7.3E-02
Sterol 29 Δ^5						
ethyl	0.72	0.03	0.72	5.1E-05	11.10	4.7E-02
PUFAs	0.85	0.01	0.46	5.2E-05	7.38	5.0E-02
Sterol 30 Δ^{22E}	0.79	0.02	0.86	8.3E-05	21.22	1.2E-01
Sterol 28 $\Delta^{5,24(28)}$	0.18	0.40	0.18	7.9E-05	4.30	1.1E-01
HBIs	0.81	0.01	1.35	4.8E-05	19.76	4.2E-02
FA22,20:1	0.59	0.08	0.05	2.9E-05	0.45	1.6E-02
FA24:6	0.48	0.13	0.53	1.4E-04	21.13	3.2E-01
Coprostanol	0.63	0.06	0.07	7.3E-05	1.56	9.6E-02
Station H						
Total	0.82	0.03	10.90	5.8E-05	479.19	1.3E-01
Sterol 28 $\Delta^{5,22E}$	0.91	0.01	1.22	8.6E-05	78.21	2.9E-01
Sterol 29 $\Delta^{5,22E}$	0.77	0.05	3.00	1.0E-04	233.26	4.3E-01
Sterol 29 Δ^5						
ethyl	0.59	0.13	0.38	3.6E-05	10.19	5.1E-02
PUFAs	0.84	0.08	2.08	1.2E-04	186.33	5.6E-01
Sterol 30 Δ^{22E}	0.87	0.02	0.68	4.8E-05	25.03	9.3E-02
Sterol 28 $\Delta^{5,24(28)}$	0.56	0.14	0.29	7.0E-05	14.97	1.9E-01
HBIs	0.39	0.26	0.72	4.2E-05	23.01	7.0E-02
FA22.20.1	0.38	0.27	0.08	7.1E-05	4.52	2.0E-01
FA24.6	0.04	0.73	0.01	9.8E-06	0.12	4.2E-03
Coprostanol	0.65	0.10	0.27	3.9E-05	8.04	6.0E-02
Station I						
Total	0.88	0.02	0.61	6.2E-05	23.77	3.8E-02
Sterol 28 $\Delta^{5,22E}$	0.89	0.02	0.03	5.7E-05	0.91	3.3E-02
Sterol 29 $\Delta^{5,22E}$	0.90	0.01	0.03	7.3E-05	1.43	5.2E-02
Sterol 29 Δ^5						
ethyl	0.93	0.01	0.03	6.2E-05	1.19	3.8E-02
PUFAs	0.99	0.01	0.62	1.7E-04	65.64	2.9E-01
Sterol 30 Δ^{22E}	0.89	0.01	0.04	6.1E-05	1.65	3.6E-02
Sterol 28 $\Delta^{5,24(28)}$	0.76	0.05	0.00	3.4E-05	0.04	1.1E-02
HBIs	0.49	0.19	0.10	5.5E-05	3.44	3.0E-02
FA22.20.1	0.28	0.36	0.01	4.0E-05	0.23	1.6E-02
FA24.6	0.05	0.85	0.00	-2.5E-05	-0.01	5.8E-03
Coprostanol	0.14	0.53	0.00	5.1E-05	0.14	2.6E-02
Station J						
Total	0.96	<0.01	6.98	8.4E-05	275.44	1.2E-01
Sterol 28 $\Delta^{5,22E}$	0.97	<0.01	6.44	1.8E-04	553.25	5.9E-01

Sterol 29 Δ ^{5, 22E}	0.46	0.21	0.23	8.3E-05	9.03	1.2E-01
Sterol 29 Δ ⁵ ethyl	0.20	0.46	0.45	7.7E-05	16.22	1.0E-01
PUFAs	0.82	0.03	1.06	1.2E-04	58.61	2.5E-01
Sterol 30 Δ ^{22E}	0.67	0.09	0.34	8.2E-05	13.14	1.2E-01
Sterol 28 Δ ^{5,24(28)}	0.39	0.38	0.22	9.8E-05	10.36	1.7E-01
HBIs	0.64	0.10	0.84	7.0E-05	28.16	8.8E-02
FA22.20.1	0.40	0.26	0.11	7.1E-05	3.61	8.9E-02
FA24.6	0.27	0.37	0.05	4.5E-05	1.04	3.7E-02
Coprostanol	0.00	0.98	0.01	-2.0E-06	0.00	-5.4E-06

3.4 Discussion

3.4.1 Biodiffusion rate assumptions and uncertainties in Larsen A Embayment before and after the ice shelf disintegration

Mechanisms and rates of bioturbation in marine sediments are usually assessed by measuring sediment profiles of radiochemical tracers (e.g., ²¹⁰Pb, ²³⁴Th, and ¹³⁷Cs). Naturally occurring ²¹⁰Pb ($t_{1/2} = 22$ years) and bomb-produced ¹³⁷Cs are used for the time scale of ~100 years while naturally occurring ²³⁴Th ($t_{1/2} = 24$ days) is used for time scales on order of ~100 days. Biodiffusion rate coefficients (D_B) represent the intensity of bioturbation and vary depending on the setting. Large rates are typical of coastal sites ($>0.5 \text{ cm}^2 \text{ yr}^{-1}$ and up to $370 \text{ cm}^2 \text{ yr}^{-1}$) (Carpenter et al., 1985; DeMaster et al., 1985; Gerino et al., 1998; Grossi et al., 2003; Legeleux et al., 1994; Sun and Wakeham, 1999), and smaller coefficients ($<0.2 \text{ cm}^2 \text{ yr}^{-1}$) are typical at pelagic/deep sea sites (Table 10) (Cochran, 1985; DeMaster and Cochran, 1982; Legeleux et al., 1994). Biodiffusion rate coefficients in sediments of Antarctic continental shelves ($>0.4 \text{ cm}^2 \text{ yr}^{-1}$ and up to $97 \text{ cm}^2 \text{ yr}^{-1}$) are within the lower range of those of coastal sediments (Table 10). Bioturbation

coefficients (^{210}Pb methodology) in the Larsen B Embayment were ranged 0.43 to 0.55 $\text{cm}^2 \text{yr}^{-1}$ just after the ice-shelf collapse (2006-2007) and likely reflecting the relatively early stage of the transition from pre- to post-ice shelf disintegration (Sañé et al., 2011a).

Table 10: Biodiffusion rate coefficients (D_b) and tracer methodology in coastal, pelagic/deep-sea, and Antarctic continental shelves sediments

Sites	D_b ($\text{cm}^2 \text{yr}^{-1}$)	Method	References
<i>Coastal Sediments</i>			
Puget Sound	0.9 - 370	^{210}Pb	(Carpenter et al., 1985)
East China Sea	24	^{210}Pb , ^{234}Th ^{137}Cs	(DeMaster et al., 1985)
Long Island Sound	0.4 – 15 11	^{234}Th ^{234}Th	(Gerino et al., 1998) (Sun and Wakeham, 1999)
Mediterranean	2.2	Microcosm - Luminophores	(Grossi et al., 2003)
Northeast tropical Atlantic (eutrophic)	0.57	^{210}Pb ^{137}Cs	(Legeleux et al., 1994)
<i>Pelagic/deep-sea sediments</i>			
Equatorial Pacific	0.04 – 0.5	^{210}Pb	(Cochran, 1985) (DeMaster and Cochran, 1982)
South Atlantic/Antarctic	0.04 – 0.16	^{210}Pb	(DeMaster and Cochran, 1982)
Northeast tropical Atlantic (oligotrophic and mesotrophic)	0.01 – 0.03	^{210}Pb , ^{137}Cs	(Legeleux et al., 1994)
<i>Antarctic Continental Shelves sediments</i>			
West Antarctic Peninsula	0.5 - 97	^{234}Th	(McClintic et al., 2008)
Larsen B Embayment	0.43 - 0.55	^{210}Pb	(Sañé et al., 2011a)
Larsen A Embayment	1.9 – 5.6	^{210}Pb	(R.Taylor personal communication)

Because the fresh settling particles could be selectively consumed and degraded at the seafloor, D_B derived from long-term tracers (such as ^{210}Pb) are typically 10-50 times smaller (slower biodiffusion) than D_B derived from short-term tracers (such as ^{234}Th) (McClintic 2008, Lauerman 1997, Smith 1993). In our study, we demonstrated how the uncertainties of biodiffusion rate coefficient (D_B) proportionally or exponentially affect the flux estimates (Figure 18). Underestimating the biodiffusion coefficients could lead to underestimating fluxes proportionally. Despite the uncertainties, knowing the range could help to define the higher and lower end of flux estimates.

3.4.2 *Post-ice-shelf collapse lipid fluxes across the Larsen A Embayment*

The post-ice-shelf-collapse total lipid fluxes ($5.7 - 45 \mu\text{g cm}^{-2} \text{yr}^{-1}$) were higher than lipid fluxes estimated from particulate organic carbon (POC) fluxes (Table 11) in the Western Antarctic Peninsula (Smith et al., 2008) and in the Arctic Ocean (Hargrave et al., 1994), but within the range observed in Ross Sea (Collier et al., 2000). Our estimations were also comparable to lipid fluxes estimated from net community production (NPP) (Li and Cassar, 2016) based carbon fluxes in the Larsen A Embayment ($6.5-8.9 \mu\text{g cm}^{-2} \text{yr}^{-1}$, Table 11).

Our results highlight a trend of decreasing post-ice-shelf-collapse lipid fluxes from nearshore to offshore stations (Stations G to J). In general, organic matter flux directly reflects the productivity at ocean surface (C. Lee and Cronin, 1984; Wakeham and C. Lee, 1993). However, the decreasing trend of total pelagic lipid flux towards

offshore is not consistent with the previously studied increasing trend of primary productivity towards offshore (Cape et al., 2014). Primary productivity at the surface water may not be the most important factor determining the organic matter flux in this system. We suggest that this mismatch is due to the potential underestimation of primary production. The primary productivity measurement through remote sensing does not include the production in sea ice, although the sea ice zone is responsible for 12% of net primary production in the Weddell Sea (Lizotte, 2001). The organic matter input from sea ice community is supported by the sea ice diatom as dominant sediment lipid source (Chapter 2). Estimated flux of one of the potential sea-ice diatom markers, 24-methylenecholesterol also showed decreasing trend towards offshore. Therefore our flux estimation is strongly influenced by organic matter input from sea ice diatom community.

Table 11: POC fluxes in previous studies and the conversion to lipid flux. * POC/POM= 0.5 using elemental ratio (Martiny et al., 2013), contribution of lipids in POM is 1% (Burdige, 2006). Net community production (NCP) and net primary production (NPP) based carbon exports were calculated using adjusted Martin's curve (Grebmeier and Barry, 2007; Martin et al., 1987).

Site	POC flux ($\mu\text{g cm}^{-2} \text{ yr}^{-1}$)	Method	*Estimated Lipid flux ($\mu\text{g cm}^{-2} \text{ yr}^{-1}$)	Reference
Coastal Marine Bay	3650 – 22000	Sediment trap	73 – 440	(Hedges et al., 1988)
NE Pacific (Station ALOHA)	584	Sediment trap	12	(Ruhl et al., 2008)
Western Antarctic Peninsula	18 – 220	Sediment trap	0.4 – 4.4	(Smith et al., 2008)
The Arctic Ocean under the permanent ice	13.4	Sediment trap	2.7	(Hargrave et al., 1994)
Ross Sea	17 – 4500	Sediment trap	0.3 – 90	(Collier et al., 2000)
Pacific deep sea sediments	1.7 – 17.0	Biodiffusion model	0.3 – 3	(Emerson et al., 1985)
Larsen A Station J (NCP: $9.6 \text{ g m}^{-2} \text{ yr}^{-1}$)	$4.4 \text{ g m}^{-2} \text{ yr}^{-1}$	NCP based carbon export	8.9	(Li and Cassar, 2016)
Larsen A Station K (NCP: $6.2 \text{ g m}^{-2} \text{ yr}^{-1}$)	$3.7 \text{ g m}^{-2} \text{ yr}^{-1}$	NCP based carbon export	6.5	(Li and Cassar, 2016)

3.4.3 Factors controlling organic matter reactivity in sediments

The post-ice-shelf collapse reactivity (degradation rate constant) of lipid biomarkers was ~ ten times lower than the fatty acids reactivity at the coastal marine sediments (Canuel and Martens, 1996), but ten times higher than the reactivity at anoxic Black Sea basin sediments (Sun and Wakeham, 1994) and the estuary sediments near Saguenay Fjord in Canada (Louchouart et al., 1997). The mean reactivity at Station K was significantly smaller than the other stations. The pre-ice-shelf collapse reactivity of lipid biomarkers was over 100 times lower than previously reported in the sediment from the Northern Gulf of Mexico which receives recalcitrant organic matter due to intense degradation during POM sinking (Camacho-Ibar and Aveytua-Alcazar, 2003). Variations in reactivity of lipids can be controlled by factors such as quality to the benthic organisms and the environmental conditions under which it was deposited (e.g., concentrations of dissolved oxygen, and concentrations of other electron acceptors) (Canfield, 1994; Canuel and Martens, 1996).

3.4.3.1 Quality of organic matter

In general, the quality (chemical structure) of organic matter is one of the most dominant factors affecting the OM reactivity. For example, Canuel (1996) reported that sterols are more reactive than fatty acids. However, our result showed no significant difference in degradation rate constant among lipid biomarkers ($p > 0.34$). Instead, we

found that significant differences among the sampling stations (Figure 17a) and between the ice shelf conditions (pre- vs post-ice shelf collapse sediments), likely due to the environmental factors discussed below.

3.4.3.2 Oxidation

Oxygen and other electron acceptors play a crucial role in microbial growth and activity. Oxidant concentrations in sediments may be a secondary factor for OM reactivity (Dhakar and Burdige, 1996; Westrich and Berner, 1984), but Cranwell (1994) suggested that the higher oxygen concentration enhances degradation efficiencies of organic matter in sediments where there is a low sedimentation rate. The Larsen A sedimentation rate is extremely low, $< 1 \text{ mm (1000 yr)}^{-1}$ (Table 6), and oxygen penetrates into the upper 8 to 10 cm of sediment at all sampling stations (Figure 20). The difference in reactivity between pre- (below 10 cm) and post-ice-shelf collapse (above 10 cm) sediments could be due to the lower oxygen availability in the sediments deeper than 10 cm below the seafloor. Moreover, the O_2 concentrations in the top 10cm of sediment at Station K were lower than those in sediment cores from other station (Figure 20), which may explain the lower reactivity of lipids at Station K.

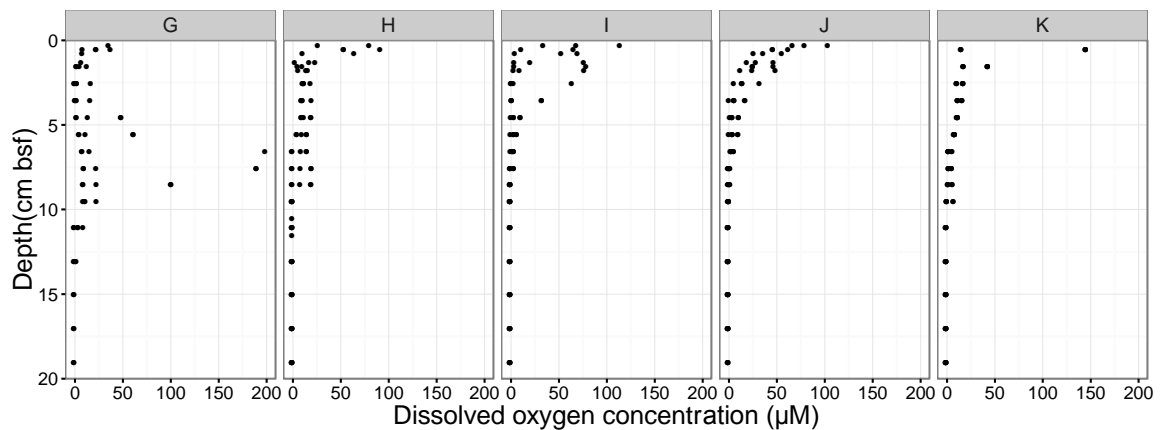


Figure 20: Downcore oxygen concentrations in each sampling stations from G to K

3.4.4 Limitation of diagenetic models

Mathematical modeling of complex processes including biodiffusion, advection, and degradation in a dynamic system is challenging and may require empirical support to quantitate the flux precisely. Our modeling effort was limited by uncertainties of short-term diffusion rate coefficient, short-term sedimentation rate, and potential downcore changes of organic matter degradation coefficient. The sensitivity analyses revealed that the model output (estimations of lipid concentrations and fluxes at the sediment-water interface) are sensitive to the changing diffusion rate coefficient (Figure 18). In addition, the organic matter degradation rate coefficients usually decrease downcore (Middelburg, 1989). Despite that, we used constant degradation coefficient to solve the equations and to obtain estimates of lipid concentrations and fluxes at the sediment-water interface.

3.4.5 Dramatic increase in flux response and ecological implications

Our results revealed that total pelagic lipid fluxes increased by a factor of 19,000 to 150,000 following ice shelf disintegration. This is three to four orders of magnitude greater than seasonal flux variability in Antarctic waters (Smith et al., 2008; Wefer et al., 1988).

This level of lipid flux increase can occur in other Antarctic and Arctic regions where 'permanent' ice disappears. For example, loss of ice shelf around the Antarctic Peninsula increased primary production by 3.5 Tg C year⁻¹ (Peck et al., 2010) and likely resulted in increasing POC flux to the seafloor, that in turn would have influenced the benthic food web. Enhanced POC flux to the seafloor could amplify the activities of benthic organism on a short time scale (< 2 mos) (Veit-Köhler et al., 2011) and alter benthic community composition on long time scales (≥10 yr) (Ruhl et al., 2008).

Substantial increases in organic matter flux will increase carbon burial and alter the biogeochemical cycle in the subsurface. Increasing area of the newly formed open ocean due to ice shelf collapse is correlated with increasing primary productivity and POC flux. Eventually, the permanent ice loss could limit climate change by increasing carbon sequestration (Barnes, 2015; Peck et al., 2010). Peck (2010) estimated that in Antarctic Peninsula Shelf alone generated 0.7 Tg C year⁻¹ of organic matter deposited to the seabed in the past 50 years. The authors suggested that carbon sequestration induced by the shrinking permanent ice coverage could be Earth's largest negative feedback to

the climate change. Our findings of the substantial increase in lipid flux to the seafloor sediments post-ice-shelf collapse are consistent with carbon sequestration, but we do not know how much organic matter is remineralized vs. preserved in the subseafloor.

Mincks (2005) suggested that the low organic carbon concentration and low temperature in Antarctic sediment could limit the bacterial degradation of organic matter and result in the accumulation of organic matter. However, according to Müller (1978), organic carbon accumulation in sediments is dependent on sedimentation rate and $< 0.01\%$ of the biosynthesized organic carbon becomes fossilized in the sediments that accumulate at rates of $< 2\text{-}6 \text{ mm (1000 year)}^{-1}$. As Larsen A sediments accumulate very slowly, $< 1 \text{ mm (1000 year)}^{-1}$, more than 99% of carbon drawn down from the photic zone could be eventually remineralized in the sediments on the time scale of hundreds to thousands of years (Müller and Suess, 1979). The remineralized carbon (CO_2) could dissolve in pore water and seawater as dissolved carbonate, microbial consumption by methanogenesis and acetogenesis, precipitation of authigenic carbonate mineral. Given the increasing trend of depth-integrated TOC concentration from onshore to offshore in the Larsen A (Chapter 2), we suggest that the Larsen A nearshore sediments temporarily accumulate organic carbon (< 50 years), but the labile organic carbon distribution is reaching to the steady state meaning that labile carbon is remineralized in the long term (hundreds to thousands of years).

In summary, we found that the pelagic lipid flux increased after the ice shelf collapse in the four sampling stations in the Larsen A Embayment. The rapid flux increase estimation was supported by the potential flux increase the stations previously covered by ice shelf (> 3000) was greatly higher than the potential flux changes at the reference station (0.6). Our modeling effort was limited by uncertainties of the short-term biodiffusion coefficient, short-term sedimentation rate, and other mathematical constraints such as the assumption of constant downcore diffusion rate coefficient. Further experimental observations of organic matter degradation rate or bacterial respiration rate in sediments collected under ice shelves are needed to expand our understanding of on microbial degradation activity in the under-ice-shelf sediments and to gain a better quantitative measure of organic matter flux under ice shelves.

3.5 Appendix: Flux modeling using TOC

Flux estimation using total organic carbon (TOC) with the diffusion-reaction model and the first-order kinetics model was attempted. When TOC concentrations were converted from weight % to g cm^{-3} , the downcore TOC distribution did not show the systematic decreasing trend (Figure 21) as we found with lipid biomarkers. The surface concentrations were smaller than the concentrations at below surface (2-5 cm) depths. Because the TOC distributions did not fit to the models (Figure S4), the

estimation of TOC flux was not possible. The reason for different downcore distribution between TOC and lipids could be that TOC may be comprised of largely non-reactive and preserved organic matter accumulated before the ice shelf collapse. Lipids represent a relatively small portions of TOC (< 0.008% in the surface sediments) compared to POC that 1-8% is lipids (Burdige, 2006).

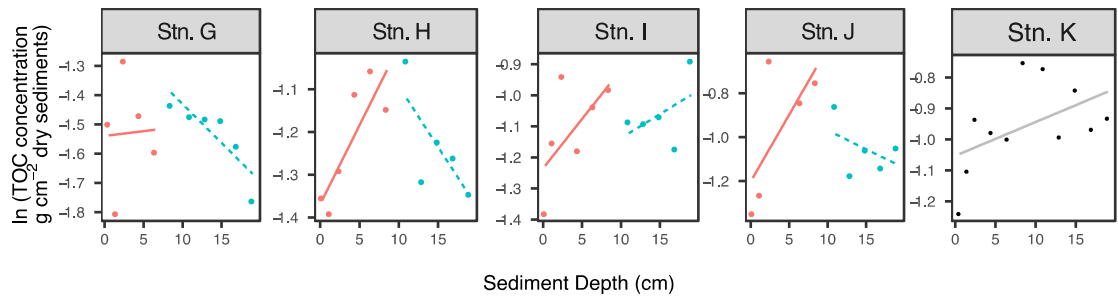


Figure 21: Downcore distribution of total organic carbon across the embayment.

4. Quality and sources of organic matter shape microbial community in sediments after the ice shelf collapse in the Larsen A embayment

This chapter was conducted as collaborative work. Michael L. McCormick (Hamilton University), conducted sample collection, geochemical analyses, DNA extraction, sequence data analyses, and cluster analysis. Dionysios A. Antonopoulos and Jason C. Koval (Argonne National Laboratory) contributed to process the microbial sequence data. Mattias Cape and Maria Vernet (Scripps Institution of Oceanography) provided pigment concentrations in Larsen A sediment samples. Megumi Shimizu conducted the sample collection, geochemical and lipid biomarker analyses, multivariate analyses, cluster analysis, and metagenome prediction (PICRUSt).

4.1 Introduction

Despite surrounding more than 75% of the Antarctic coastline and covering one-third of Antarctica's continental shelf, sub-ice-shelf benthic habitats are among the least studied ecosystems in the world (Barnes and Peck, 2008; A. Clarke et al., 2007; Vick-Majors et al., 2016). Due to the occlusion of light and absence of phytoplankton productivity in overlying waters, these ecosystems depend on the lateral transport of carbon and nutrients that may travel over hundreds of kilometers under ice shelves (Gutt et al., 2011). Much of the labile and nutrient rich content of this material may be degraded in transit leading to sub-ice-shelf ecosystems that are oligotrophic, resembling

deep-sea abyssal plains as reported under the Ross Ice Shelf (Azam et al., 1979). In contrast, under the Amery Ice Shelf, advective currents transport organic matter at least 100 km from open waters at sufficient rates to support a community of diverse sessile suspension feeders, similar to seabed communities in open waters of the Antarctic continental shelf (Post et al., 2014; Riddle et al., 2007).

In recent decades, as a consequence of climate warming, we have seen a rapid retreat of Antarctic ice-shelf systems. This effect has been most dramatic in the Antarctic Peninsula where average air temperatures increased by 0.41 °C per decade since the 1960s, one of the fastest warming regions on Earth (Turner et al., 2005; Vaughan et al., 2003). Because of the temperature increase, the last remnants of the Larsen A Ice Shelf collapsed in 1995, one of the largest ice shelf losses in recorded history, second only to the 2002 collapse of the Larsen B Ice Shelf (Gutt et al., 2011).

Following retreat of the Larsen A ice shelf, the onset of photosynthetic activity in surface waters resulted in chlorophyll-a concentrations similar to those observed in the northern part of the Antarctic Peninsula (Bertolin and Schloss, 2009; Cape et al., 2014; Peck et al., 2010) and delivery of high quality (labile) organic matter to the seabed [(Sañé et al., 2011a), Chapter 2].

Organic matter inputs to sediments provide microbial communities with both a carbon source and an electron donor for anaerobic metabolism and thus can exert a direct influence on community composition. Changes in organic matter input to

sediments can affect the microbial community indirectly by altering the geochemical characteristics of the sediments. In organic-rich sediments, the concentration profiles for oxygen, nitrate, manganese, iron, and sulfate (electron acceptors) are a result of the balance between diffusion of these compounds into the sediment from overlying seawater and their consumption in redox reactions driven primarily by microbial processes linked to the oxidization of particulate and dissolved organic matter. In organic-poor sediments, low sedimentation rate, low organic carbon input and low microbial activity in surface sediments, allow oxygen and other electron acceptors to penetrate more deeply (D'Hondt et al., 2009; Durbin et al., 2009). Organic-lean sediments often select for microbial communities dominated by ammonium-oxidizing Thaumarchaea (Durbin et al., 2010; Durbin and Teske, 2011; Tully and Heidelberg, 2016), while organic-rich sediments result in abundant sulfate reducers, sulfide oxidizers, and anaerobic methane oxidizers (Teske et al., 2011). In the Larsen A Embayment, the increase in organic matter production in the water column following the ice-shelf collapse is expected to have induced rapid changes in the sedimentation regime, redox status, and benthic microbial community composition. Although there is evidence of continuous organic matter supply to the seabed even in the ice-shelf covered period (Crawford, 2012), organic matter input to the seafloor is estimated to have increased by as much as 23,000 fold following ice-shelf collapse (Chapter 2). Understanding the environmental drivers that shaped the benthic microbial communities in the Larsen A

Embayment may shed light on the geochemical and community changes that accompany succession following ice shelf collapse and provide insight into the potential changes that lie ahead for Antarctica's sub-ice shelf benthic habitats as we enter a period of continued climate warming.

To better understand the effects of ice shelf loss on the benthic microbial community and biogeochemical processes in this rapidly changing region we conducted a five-station survey along a 160 km transect following the historical path of retreat of the Larsen A Ice Shelf. Using multivariate analyses, we investigated how a suite of geochemical parameters, including organic matter quality and sources, affected the microbial community structure. Furthermore, we also identified taxonomic groups that potentially play important roles in organic matter degradation, nitrogen cycling and other geochemical processes in Larsen A sediments.

4.2 Materials and Methods

4.2.1 Sampling

Sample collection at the Larsen A Embayment site took place as a part of a multidisciplinary project, the "Larsen Ice Shelf System, Antarctica" (LARISSA). Sampling was conducted from 7 March to 17 April 2012 aboard the *RVIB Nathaniel B Palmer* (NBP12-03) off the coast of the East Antarctic Peninsula, Weddell Sea. Sediments were collected using a megacorer at five cross-shelf stations (Stations G – K) following the historic path of retreat of the Larsen A ice shelf, each station having a different

period of exposure to open water conditions (Figure 1) (Ferrigno, 2006). Water depths varied within a range of 250 m (430 m to 680 m) with the deeper stations occurring closest to shore. Three megacore drops were conducted at each station at spatial intervals of 0.3 to 1.0 km, while interstation distances ranged from 19 to 60 km. A minimum of 5 megacores were collected per station for microbial community analysis (1 or 2 cores per drop), 2 of these cores were also sectioned for geochemical analysis and 1 core for lipids analysis. An additional 3 cores (one per drop) were collected for microprobe profiling of porewater pH and dissolved oxygen. Upon recovery, megacores for geochemical, microprobing or DNA analysis were selected from each drop at 30 cm to 80 cm spacing from the megacore array then capped, wrapped in light blocking thermal insulation and stored at 1 °C until analyzed. Each core for lipid analysis was sectioned on board immediately after sample recovery at 0.5-cm intervals to 2 cm, 1-cm intervals to 10 cm and 2-cm intervals from 10 cm to the bottom of the core (20 cm). After the sample processing, the sectioned sediment samples for lipid were stored at -80 °C until lipid extraction was conducted. Lipids (hydrocarbons, ketones, fatty acids, and sterols) were extracted from sediments and analyzed as described in Chapter 2.

4.2.2 Geochemical analyses

Cores for geochemical analysis were extruded and sectioned at 1 to 2 cm resolution to a depth of 20 cm in a nitrogen-purged glove box maintained at 1 °C to

approximate ambient sediment temperatures (~-1.9 °C). Oxygen levels were monitored and maintained below 0.5% during sample processing. Pore water was collected from each section by centrifugation of sediment in gas-tight Oak Ridge tubes (20 minutes, 10,000 RCF, 4°C). Supernatant was recovered by syringe then filtered (0.22 µm) before analysis. Centrifuge tubes were loaded and unloaded in the anaerobic glove box to avoid sample oxidation. Nutrients, including orthophosphate (PO_4^{3-}), nitrite (NO_2^-), combined nitrate+nitrite ($\text{NO}_2^- + \text{NO}_3^-$), ammonia (NH_3) and silicic acid (H_4SiO_4) were quantified using a five-channel Lachat Instruments QuikChem FIA+ 8000s series autoanalyzer. Samples were stored in the dark, refrigerated at 4 °C for up to 12 hours after collection before being analyzed. Phosphate concentrations were analyzed using modified method of the molybdenum blue procedure (Bernhardt and Wilhelms, 1967). The nitrate + nitrite analysis used the method of Armstrong (1967) with modifications to improve the precision and ease of operation. Nitrite analysis was performed on a separate channel. Ammonia was determined using the indophenol blue method. Silicic acid analysis was based on the method of Armstrong (1967) as adopted by Atlas (1971). Ferrous iron samples were preserved in 0.1 M hydrochloric acid and subsequently analyzed using the Ferrozine assay (Stookey, 1970).

4.2.3 Microprobe analyses

Depth profiles of pH and dissolved oxygen (DO) were acquired on three cores per station (one per megacore drop) using custom built semi-microelectrodes

(Microelectrodes Inc., Maine, USA). Microprobes were calibrated against standards prior to each analysis. Profiles were acquired at 1 mm to 1 cm intervals to a depth of 20 cm.

4.2.4 DNA analysis

Sediment subsamples were collected from the sectioned cores using sterile pre-cut 1 ml syringes and stored at -80 °C. Genomic DNA was extracted from ~0.25 g sediment samples using the PowerSoil DNA Isolation Kit (MoBio, Carlsbad, CA) following the manufacturer's instructions. Genomic DNA was amplified using the Earth Microbiome Project barcoded primer set, adapted for the Illumina MiSeq. The V4 region of the 16S rRNA gene (515F-806R) was amplified with region-specific primers (forward primer: 5'-GTGCCAGCMGCCGCGGTAA-3', reverse primer: 5'-GGACTACHVGGGTWTCTAAT -3') (Caporaso et al., 2011), with the addition of the Illumina barcoded adapter sequences. The coverage of the bacterial and archaeal domains with the primers with two mismatches were 96.1% and 95.6% respectively according to SILVA non-redundant reference database release 117 (SSUr117 RefNR) (Klindworth et al., 2013). Although the primer set covers over 95% of Bacteria and Archaea, it does not cover marine planktonic SAR11 cluster (Apprill et al., 2015; Parada et al., 2016). SAR11 is prevalent in seawater (R. E. Collins et al., 2010; Giovannoni et al., 1990; Rappé et al., 2002), but usually is a minor taxonomic group in marine sediments (Hamdan et al., 2013). The reverse amplification primer contained a twelve base barcode sequence that supports pooling of up to 2,167 different samples in each lane (Caporaso

et al., 2011; 2012). The PCR amplifications were performed in triplicate and then pooled. Following pooling, amplicons from each sample were quantified using PicoGreen (Invitrogen) and a plate reader. Once quantified, volumes of each of the PCR products were pooled into a single tube with equal amplicon representation prior to PCR cleanup using the UltraClean® PCR Clean-Up Kit (MoBio). The final pooled and purified PCR products were quantified again using the Qubit broad range dsDNA quantification kit (Invitrogen) and diluted down to 2nM for sequencing on the Illumina MiSeq. On average 15,000 reads were obtained per sample after removal of singleton sequences (11 million reads total). Average read length was 253 bp. Analysis of high-throughput sequencing data was performed using QIIME v.1.6.0. Taxonomic assignment was performed using GreenGene database (version 13_8) with 97% similarity. The OTU table was obtained after rarefaction based on random subsampling of 2000 sequences per sample.

4.2.5 Statistical Analyses

4.2.5.1 Community diversity

Bray–Curtis dissimilarities (J. R. Bray and Curtis, 1957) between all samples were calculated and used for two-dimensional non-metric multidimensional scaling (NMDS) ordinations (Kruskal, 1964). Stress values below 0.2 indicated that the multidimensional dataset was well represented by the 2D ordination. To quantify the differences in the community compositions, the ANOSIM R statistic was used (K. R.

Clarke and Green, 1988). The ANOSIM R values represent a difference of average rank dissimilarities between and within groups. Analyses were carried out with the vegan package in a software R (Oksanen, 2015).

4.2.5.2 Multivariate analyses – with all environmental variables

Canonical correspondence analysis (CCA) was used to identify the environmental factors associated with differences in community compositions at different sampling stations and depths. The average environmental variables for each station were obtained from 1 to 3 cores, while the average sequence abundance of the rarified OTU table were obtained from 5 to 6 cores recovered from the same stations. The OTU table was standardized by Hellinger transformation (Legendre and Gallagher, 2001). The Hellinger transformation gives low weights to OTUs with low counts and many zeros. The environmental variables for the CCA were chosen from pH, nitrate, nitrite, ammonium, phosphate, iron, silicate, chlorophyll a, oxygen, total organic carbon, and lipid concentrations, and $\delta^{13}\text{C}_{\text{TOC}}$ values in the following manner. First, correlations among the variable were tested. The silicate concentration was removed from the dataset because it significantly covariates with phosphate concentration ($r^2 > 0.81$, $p < 0.001$). Second, the environmental variables were transformed to a normal distribution by using the Box-Cox method (Box and Cox, 1964), and standardized to unit variance and zero mean (Legendre and Gallagher, 2001). Finally, we identified a combination of environmental variables that best explains the variations of the microbial community, by

the automatic forward-backward selection. We used the Akaike Information Criterion (AIC) (Blanchet et al., 2008) with stepwise function with 999 permutation tests at each step of the forward and backward selection. The resulting subset of variables was used as the constrained set of parameters to relate the environmental variables to bacterial and archaeal community composition in the CCA. The significance of the canonical axes was computed using a Monte Carlo test with 999 permutations. Statistical significance of the individual environmental variables was assessed using the marginal effect of the terms tested with 999 permutations.

4.2.5.3 Multivariate analyses – with lipid biomarkers

We performed a redundancy analysis (RDA) to investigate the relationships between the microbial community and lipid biomarkers of non-bacterial or archaeal origin. The variables (% lipid biomarkers) for RDA were chosen in a similar manner as described for CCA. The relative abundances for lipid biomarkers were arcsine transformed (Warton and Hui, 2011), and standardized to unit variance and zero mean. The lipid biomarkers selected by the forward-backward stepwise function were used as the constrained set of parameters for RDA. All the multivariate analyses were conducted using the R package, *vegan* (Oksanen, 2015).

4.2.5.4 Clustering Analysis

Pearson's correlation coefficients were computed between the relative abundance of the 120 most abundant taxa (accounting for >96% of total OTUs and >93% of all DNA

weighted taxonomic abundance) and selected environmental variables and lipid biomarkers that best explain the variation in the microbial community composition. Using the correlation coefficients, hierarchical clustering analyses were performed with Euclidean distances using the R package “pvclust” (Suzuki and Shimodaira, 2006). After multiscale bootstrap resampling (10,000 iterations), approximately unbiased (AU) *P* values were computed (Shimodaira, 2004). Pairwise correlations between each bacterial and archaeal taxa and environmental variables were graphed in a heat map and Euclidean distance clustering dendrogram using R package 'ComplexHeatmap' (Gu et al., 2016).

4.2.6 Metagenome prediction

To predict metagenome-based functions, closed-reference OTU selection was performed in QIIME 1.9.0 (Caporaso et al., 2010) containing the Greengenes reference database version 13_8 (DeSantis et al., 2006). OTU clustering and taxonomy at 97% similarity was carried out in QIIME by closed reference. 72% of sequences were assigned to OTU in the Greengenes version 13_8 database. The resulting OTU table was imported into PICRUSt (Langille et al., 2013) for function prediction and metagenome calculations. The accuracy of the predictions of the metagenomes was assessed by computing NSTI (Nearest Sequenced Taxon Index), which indicates the relation of the DNA sequences in a particular sample to the bacterial and archaeal genomes in a database.

4.3 Results and Discussion

4.3.1 Geochemical distribution

Geochemical profiles revealed downcore gradients as well as cross transect gradients for nearly every measured parameter (Figure 22). Total organic carbon (TOC) was low (below 1% dry wt) in all samples but showed small declines with sediment depth in each core and a steady overall rise in concentration moving offshore from Station G (0.1-0.2 % dry wt) to Stations J and K (0.5-0.8 % dry wt). $\delta^{13}\text{C}_{\text{TOC}}$ values dropped at the surface sediments and remained relatively constant with depth. Station G was an exception; $\delta^{13}\text{C}_{\text{TOC}}$ values were significantly higher below 5 cm sediments compared to other stations.

Lipids, DNA and pigment concentrations (chl-a and pheo), all of which can be considered biomass proxies, showed a similar trend of rising offshore particularly in the near surface sediments (0-1 cm) with chl-a in Station K (22,500 $\mu\text{g/g}$ wet sediment) measuring an order of magnitude higher than the surface sediments of Station G (757 $\mu\text{g/g}$ wet sediment). Pore water pH decreased with depth in all cores and ranged from highs of 7.8 to 7.9 in surface sediments of Stations H and I (mid-transect) to a low of pH 7.1 at 20 cm depth at Station K. Dissolved oxygen was typically decreased sharply within the first 2-4 cm depth at all stations and completely depleted at 10 cm depth. One of the cores at station G showing an anomalous rise in dissolved oxygen between 6-7 cm. This anomaly coincided with a pebbly-coarse granular horizon of presumably high

permeability that we suspect may have been influenced by tidal pumping and irrigation via nearby burrows. Silicate and orthophosphate concentrations were highly correlated with relatively uniform values across the transect at the sediment surface and a near monotonic rise in pore water concentrations moving offshore at depths below 5 cm.

The most striking changes in chemical composition occurred for the inorganic nitrogen species (Figure 22). Nitrate profiles at all stations showed highest concentrations 1-2 cm below the sediment-water interface, indicative of active nitrification and diffusive loss to the overlying water. A nearly symmetric distribution of nitrate was observed across the transect, with a peak concentration $\sim 65 \mu\text{M}$ occurring at Station I. Downcore ammonia concentrations were complementary to the nitrate distribution, showing a trough in concentrations where nitrate values peaked. Anomalously high ammonia concentrations were observed in all surface sediment samples (0-1 cm). We speculate that these values resulted from disruption of intracellular contents of infauna or recently settled diatoms during centrifugation. Artificially elevated concentrations of inorganic nitrogen species have been attributed to cell lysis during pore water separation in other studies (Lomstein et al., 1990; Rysgaard and Glud, 2004). Our sampling occurred approximately two to four weeks following the spring phytoplankton bloom, and freshly deposited layers of diatoms were visible in bottom photos (Craig Smith – yoyo camera images, unpublished data). Dissimilatory reduction of intracellular nitrate to ammonium has been reported in senescing diatoms

(Kamp et al., 2011). Microbial organic matter decomposition also release ammonium to the sediments (Canfield et al., 2010). Furthermore, the distribution of ammonia in the surface sediment layer (0-1 cm) correlates well with the abundance of nematodes and copepods at the same depth across the transect (Ribeiro, 2015).

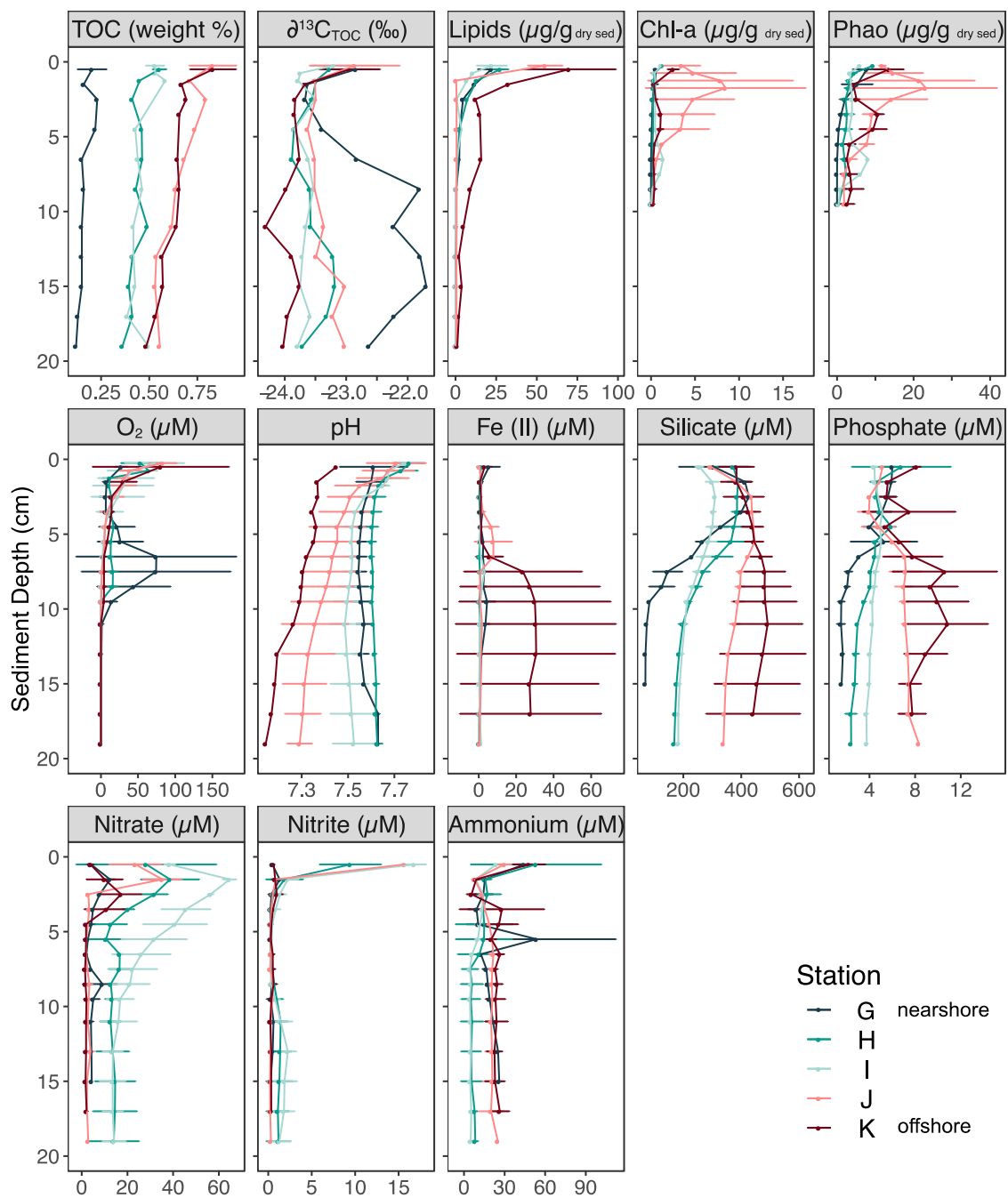


Figure 22. Downcore geochemistry profiles. Colors represent sampling stations. Error bars represent standard deviation (n=3 for O₂, pH, and surface samples of TOC, δ¹³C_{TOC}, and lipids; n=2 for Chl-a, Phao, Fe(II), silicate, phosphate, nitrate, nitrite, and Ammonium concentrations)

4.3.2 Bacterial and Archaeal Distributions and Diversity

Based on the Illumina 16S rRNA gene data, 10 most abundant genus level taxonomic groups dominated about 50% of the total OTUs. These top 10 taxonomic groups were classified within the Gammaproteobacteria, Thaumarchaeota, Alphaproteobacteria, Brocadia, and Deltaproteobacteria (Figure 23). The most abundant taxonomic group in all stations was an unclassified Piscirickettsiaceae. This group was universally (~10%) distributed downcore and across the embayment. Taxonomic groups associated with the family of Cenarchaeaceae including the genus of *Nitrosopumilus*, was the second and third most abundant and especially predominant at Station H and I. Members of the Cenarchaeaceae comprised a total of over 20 % of the community at Station H and I. Unclassified Alphaproteobacteria and the family of Rhodospirillaceae was the fourth most abundant taxa and distributed similarly to Cenarchaeaceae; it was relatively abundant in Station H and I than the other stations. The taxonomic group classified in the genus of *Acinetobacter* was found to be most abundant in the nearshore station (G). The deeper (> 10 cm) sediments at Station G contained 20 - 30% of this taxonomic group. The OTUs closely related to OM60 clade were found mostly in the near surface sediments across the embayment, and relatively abundant at Station G. The *Candidatus Scalindua* group was found to be relatively abundant (> 4%) in the deeper sediments at the offshore stations (J and K). Two

taxonomic groups associated with Deltaproteobacteria were also found to be relatively abundant in Stations J, K, and G than H and I.

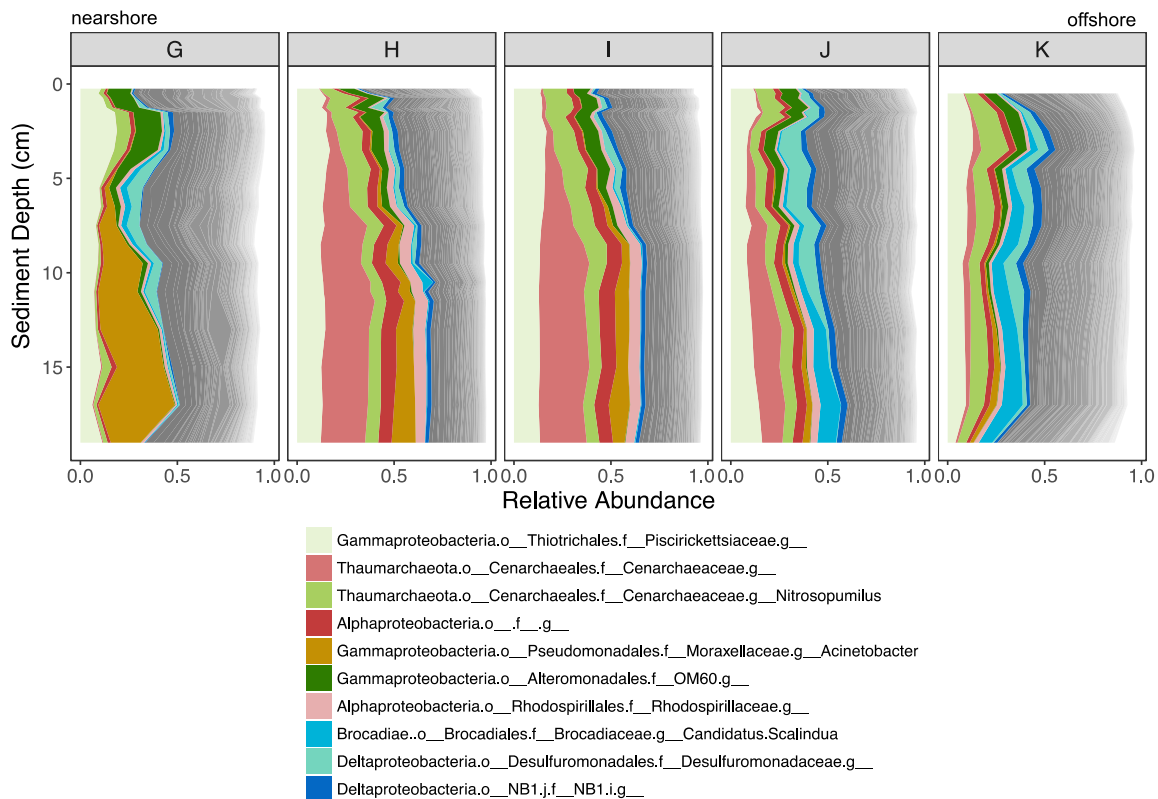


Figure 23: Downcore profiles of the relative abundance of microbial taxonomic groups across the embayment. Top 10 abundant taxa are color coded with the label: o, order; f, family; g, genus

The microbial community composition differed significantly by station (Figure 24a; ANOSIM: $R = 0.36$, $p = 0.006$, 999 permutation) except between Stations H and I (ANOSIM: $R < 0.01$, $p = 0.17$). The community composition differed also between 0-10cm and 10-20 cm sediment depths (Figure 24b; ANOSIM: $R = 0.35$, $p = 0.001$). The surface samples from all stations were clustered relatively closely (ANOSIM: $R = 0.35$, $p = 0.018$),

compared to the deeper sediment samples (ANOSIM: $R = 0.77$, $p = 0.001$) (Figure 24b).

The deeper the sediment cores, the microbial communities are more different among the stations. This reflects that geochemical gradients downcore shape specific niche differentiation for microbial community.

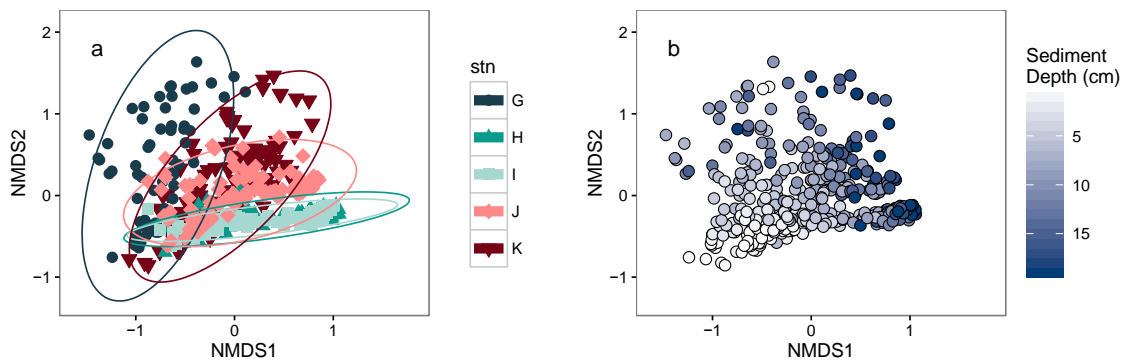


Figure 24: Non-metric multidimensional scaling (NMDS) plot of microbial communities based on Bray-Curtis dissimilarity for 16S rRNA gene libraries. The community profiles from each sample; a) color represents sampling stations. Ellipses represent 95% intervals around centroids for each sampling station. b) color represents sediment depth.

4.3.3 Environmental Drivers of Bacterial and Archaeal Diversity

To identify the environmental drivers of bacterial and archaeal community diversity, a constrained set of environmental variables was identified using stepwise forward-backward selection. After the selection of environmental variables, and testing using Monte Carlo permutation tests, CCA revealed eight environmental variables: lipid concentration, total organic carbon (TOC) concentration, pH, phosphate, ammonium, $\delta^{13}\text{C}_{\text{TOC}}$, NO_2^- : nitrite, NO_3^- : nitrate, that were significantly related to bacterial and

archaeal community composition (Monte Carlo permutation test of marginal effects: lipid: $F= 3.44, p=0.001$; TOC: $F=2.06, p=0.001$; pH: $F= 2.08, p=0.002$; phosphate: $F=2.61, p=0.001$; ammonium: $F=2.46, p=0.001$; $\delta^{13}\text{C}_{\text{TOC}}$: $F= 1.94, p=0.001$; nitrite: $1.61, p=0.010$; nitrate: $F= 1.55, p=0.014$). Under this restricted model, CCA showed that eight variables explained 53% of the variation within the species–environment relationship across the first two canonical axes (Figure 25).

Notably, among the environmental variables evaluated, lipid concentrations and TOC were two of the major drivers of sediment microbial community structure. This is consistent with previous studies that also found organic matter concentrations were one of the major drivers influencing microbial community composition in the organic-lean marine sediments (Bienhold et al., 2012; Jorgensen et al., 2012; Polymenakou et al., 2005). $\delta^{13}\text{C}_{\text{TOC}}$ values that were significantly higher at Station G (Figure 22; $p < 0.001$) also contributed as a driver to microbial community – environment relationship. The $\delta^{13}\text{C}_{\text{TOC}}$ values are dependent on organic matter (OM) sources, growth conditions of OM sources, and fractionation factors during OM degradation. Although the organic matter in Larsen A Embayment is primarily from phytoplankton and algae (chapter 2), growth conditions of the source organisms may be different (e.g. growth in sea ice, spring bloom). The variable growth conditions of phytoplankton may be an explanation of higher $\delta^{13}\text{C}_{\text{TOC}}$ values at Station G than the other stations. The alternative explanation is

fractionation due to degradation. The higher $\delta^{13}\text{C}_{\text{TOC}}$ at Station G could indicate the extensive level of organic matter degradation (Hayes, 1993; Hayes et al., 1989).

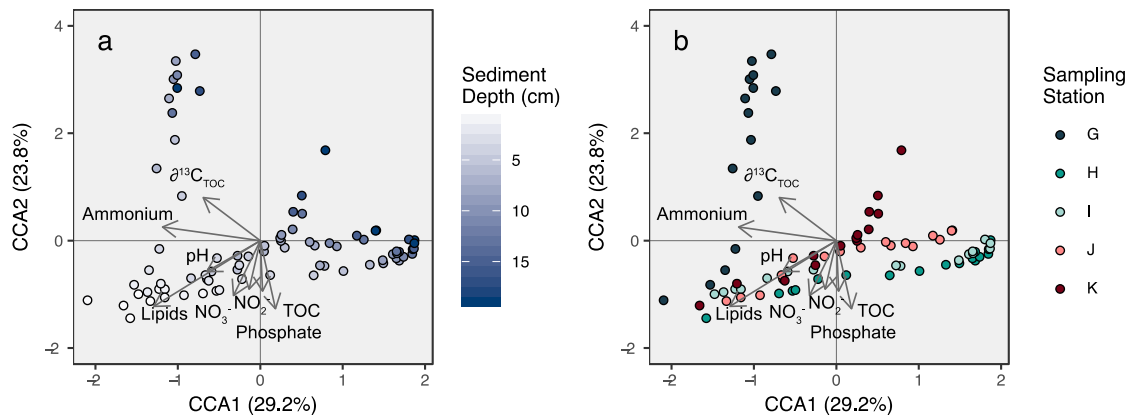


Figure 25: Canonical correspondence analysis (CCA) ordination diagram of axes one and two of the bacterial and archaeal community. CCA was conducted with selected environmental variables (lipid: lipid concentrations, TOC: total organic carbon, pH, phosphate, ammonium, $\delta^{13}\text{C}_{\text{TOC}}$, NO_2^- : nitrite, NO_3^- : nitrate). The percent of the variation in the community explained by each axis is in parenthesis. All the environmental variables were determined to be statistically significant using the marginal effect of the terms ($P < 0.002$). The variables are indicated as vectors. The community profiles from each sample are represented as circles; a) color represents sediment depth, b) color represents sampling stations.

4.3.4 Source and Lability of Organic Matter Shape Microbial Community

To investigate which of the over 40 different contextual parameters (lipid biomarkers) could best explain the microbial community structure, we performed redundancy analyses (RDA). We used non-bacterial or archaeal lipids grouped by similarity of chemical structure (Table 12). The chemical structures of lipid biomarkers primarily determine the lability and reactivity in the sediments. Lability of lipid biomarkers is determined by the chain lengths (i.e., short chain lipids are more labile

than long chain lipids) and a number of unsaturation (i.e., unsaturated molecules are more labile than saturated molecules) (Sun et al., 1997; Wakeham and Canuel, 2006). Although lability estimates are not quantitative, conventional lipids such as poly-unsaturated fatty acids, mono-unsaturated fatty acids are assumed to be relatively labile, while *n*-alkanes are relatively recalcitrant and likely stay in sediments for a longer duration (Cranwell, 1981; Wakeham and Canuel, 2006). In applying this approach, the number of parameters was reduced from 48 lipids to 19 structural groups of lipids (Table 12). The automatic forward-backward selection identified seven lipid groups that best explained the variance of the microbial community. After the selection of lipid groups, and testing using Monte Carlo permutation tests, RDA revealed the seven lipid groups, *n*-alkanes, $\Delta^{5,22}$ sterols, polyaromatic hydrocarbons (PAHs), C₃₀ HBIs, stenones, even-carbon mono-unsaturated fatty acids (MUFAs), and 24-methylenecholesterol (C₂₈ $\Delta^{5,24(28)}$) that were significantly related to bacterial and archaeal community composition in all the sampling stations (Monte Carlo permutation test of marginal effects: *n*-alkanes: F= 4.11, P=0.002; $\Delta^{5,22}$ sterols: F= 6.04, p=0.001; PAHs; F= 3.91, p=0.001; C₃₀ HBIs: F= 2.46, p=0.021; stenones: F = 2.90, p= 0.005; even MUFAs: F=2.75, p=0.011; 24-methylenecholesterol: F=2.65, p=0.008). The lipid groups chosen by the forward-backward selection were used as the constrained variable set to explain bacterial and archaeal community compositions with RDA (Figure 26). The RDA result for all five stations indicated that these lipid groups explained 76% of the microbial community

variation with the first and second axes (RDA1: 55.7%, F= 19.0, $p=0.001$; RDA2: 19.9%, F=6.8, $p=0.01$). The selected lipid groups include general phytoplankton biomarkers (Δ^5 , 22 sterols and even carbon MUFAs) (Volkman et al., 1998) and diatom biomarkers (24-methylenecholesterol and C₃₀ HBIs) (Volkman et al., 1998; 1994). The *n*-alkanes could also be derived from phytoplankton (Chapter 2). Stenones are degradation products of sterols. PAHs, *n*-alkanes, and stenones could be relatively recalcitrant especially in an anoxic environment.

Table 12: Lipid biomarker compound groups that used for RDA and their sources

Compounds and groups of lipids used for forward-backward selection	Lipid compounds contained in groups
<i>Fatty acids</i>	
even MUFAs (phytoplankton)	FAs 16:1 ω 9, 18:1 ω 5,
20 -22 MUFAs (zooplankton)	FAs 20:1, 22:1
PUFAs (phytoplankton)	FAs 20:5 ω 3, 20:4 ω 6, 22:6 ω 3
FA 24:6 ω 3 (Brittle stars - <i>Ophiuroidea</i>)	FA 24:6 ω 3
<i>Sterols</i>	
$\Delta^{5,22E}$ sterols (phytoplankton)	26 $\Delta^{5,22E}$, 27 $\Delta^{5,22E}$, 28 $\Delta^{5,22E}$, 29 $\Delta^{5,22E}$
Δ^{22E} sterols	26 Δ^{22E} , 27 Δ^{22E} , 28 Δ^{22E} , 29 Δ^{22E} , 30 Δ^{22E}
Δ^5 sterols	27 Δ^5 , 29 Δ^5 ethyl, 29 Δ^5 dimethyl
Δ^0 sterols (Dinoflagellates, cyanobacteria)	27 Δ^0 , 29 Δ^0 dimethyl, 29 Δ^0 ethyl
28$\Delta^{5,24(28)}$ (diatoms)	28 $\Delta^{5,24(28)}$
28 $\Delta^{24(28)}$ (phytoplankton)	28 $\Delta^{24(28)}$
Coprostanol (marine mammals)	Coprostanol
<i>Hydrocarbons</i>	
<i>n</i>-alkanes	C ₂₁₋₂₈ <i>n</i> -alkanes
C ₂₅ HBIs (diatoms)	HBI C _{25:2} , C _{25:3} ,

C₃₀ HBIs (diatoms)	HBI C _{30:5}
PAHs (fungi)	PAHs
<hr/>	
<i>Ketones</i>	
Stenones (degradation products of sterols)	Stenones
Wax esters	Wax esters* ¹
<hr/>	

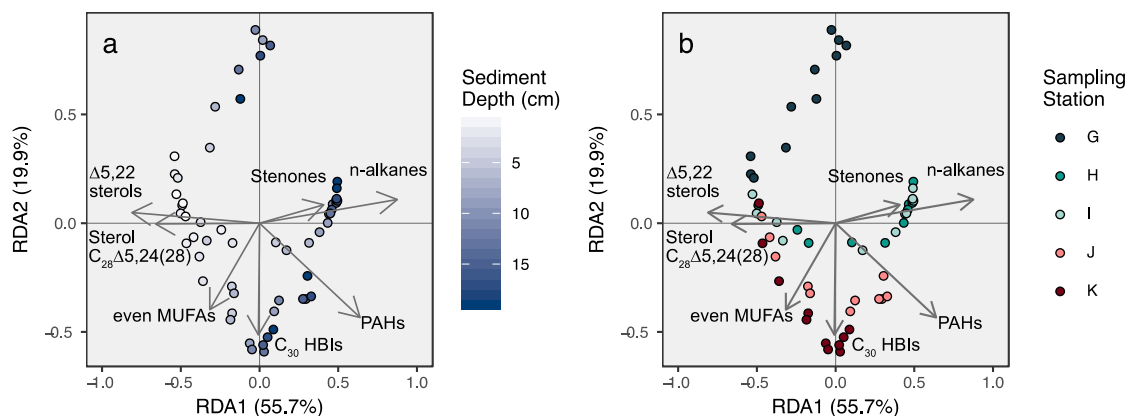


Figure 26: Redundancy analysis (RDA) ordination diagram of axes one and two of the bacterial and archaeal community in samples from five cross-shelf Stations G – K. The percent of the variation in the community explained by each axis is in parenthesis. The variables (*n*-alkane, $\Delta^{5,22}$ sterols, C₃₀ HBIs: highly branched isoprenoids, PAH: polyaromatic hydrocarbons, stenones, even-carbon MUFAs: mono-

¹ MUFAs (mono unsaturated fatty acids), PUFAs (poly unsaturated fatty acids), 26 $\Delta^{5,22E}$ (24-norcholesta-5,22E-dien-3 β -ol), 26 Δ^{22E} (24-Nor-5 α -cholest-22E-en-3 β -ol), 27 $\Delta^{5,22E}$ (5,22E-dien-3 β -ol), 27 Δ^{22E} (5 α -Cholest-22E-en-3 β -ol), 27 Δ^5 (cholest-5-en-3-ol), 27 Δ^0 (5 α -Cholestan-3 β -ol), 28 $\Delta^{5,22E}$ (24-methylcholesta-5,22E-dien-3 β -ol), 28 Δ^{22E} (24-methyl-5 α -cholest-22E-en-3 β -ol), 28 $\Delta^{5,24(28)}$ (24-methylcholesta-5,24(28)-dien-3 β -ol), 28 $\Delta^{24(28)}$ (24-methylcholest-5-en-3 β -ol), 29 $\Delta^{5,22E}$ (stigmasta-5,22E-dien-3 β -ol), 29 Δ^{22E} (4,24-dimethyl-5 α -cholest-22E-en-3 β -ol), 29 Δ^5 dimethyl (23,24-dimethyl-5 α -cholest-5-en-3 β -ol), 29 Δ^5 ethyl (stigmast-5-en-3 β -ol), 29 Δ^0 dimethyl (23,24-dimethylcholestan-3 β -ol), 29 Δ^0 ethyl (24-ethylcholestan-3 β -ol), 30 Δ^{22E} (4 α ,23,24R-trimethyl-5 α -cholest-22-en-3 β -ol), coprostanol (5 β -cholestan-3 β -ol), HBIs (highly branched isoprenoids)

unsaturated fatty acids, sterol $C_{28} \Delta^{5,24(28)}$:24-methylenecholesterol) are indicated as vectors. All of the lipid groups were determined to be statistically significant using the marginal effect of the terms ($P < 0.014$). The community profiles from each sample are represented as circles; a) color represents sediment depth, b) color represents sampling stations. Carbon sources of microbes

4.3.5 Microbial functional clusters

We used correlation coefficients between the environmental variables including lipid compositions and the relative abundance of microbial taxa to conduct Euclidian distance based clustering. The heat map presented in Figure 27 provides a compact view of the microbial clusters of dominant and accompanying taxa that shared similar pairwise correlations with environmental variables and lipid biomarkers. This clustering analysis revealed that the microbial community in the Larsen A sediments was composed of seven functional clusters.

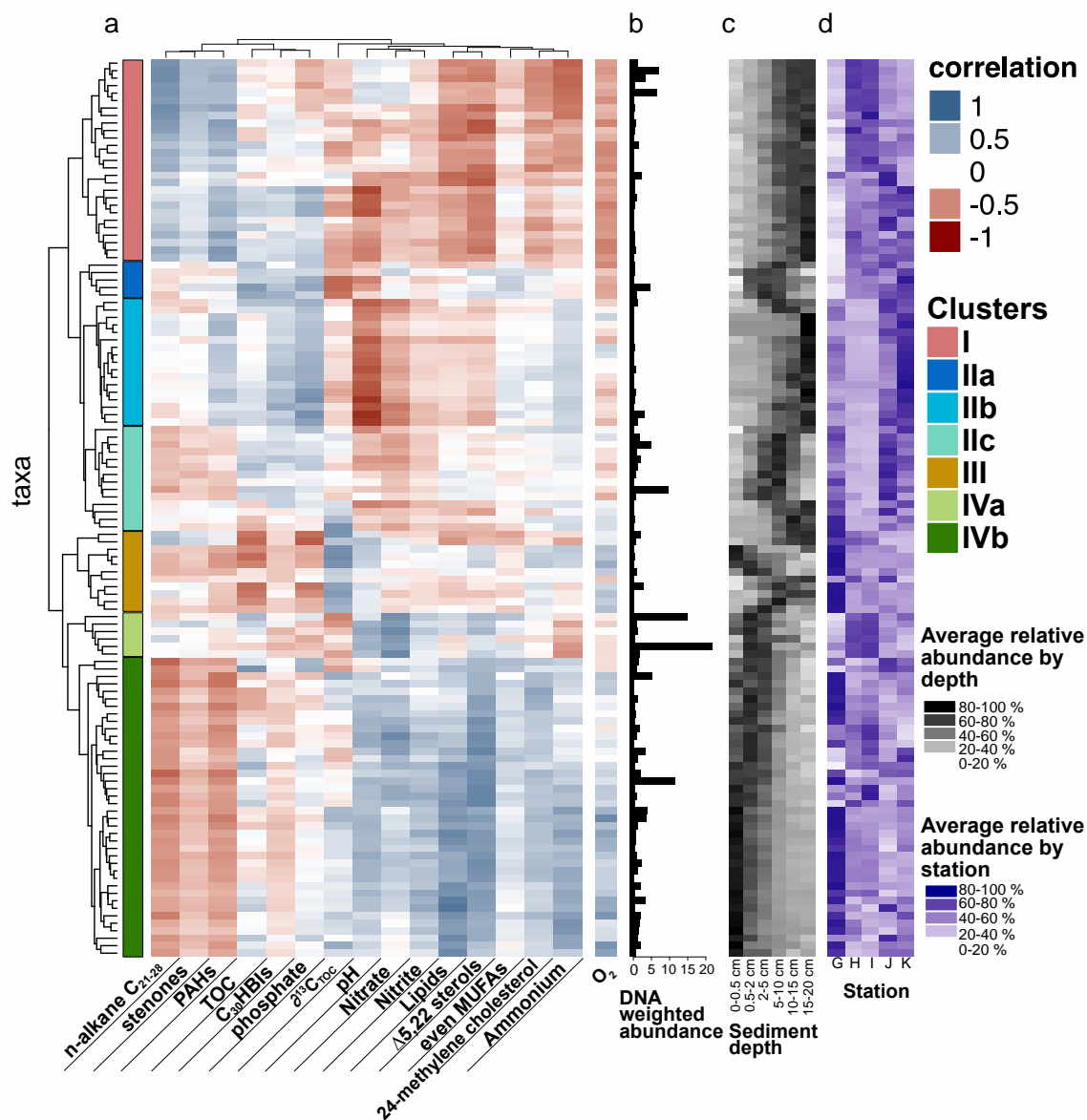


Figure 27: Pearson's correlation coefficients heat maps showing the association between environmental variables and the relative abundance of bacterial and archaeal clusters. a) The top dendrogram defines clusters of environmental variables and relative abundances of lipid biomarkers that best explain the microbial community (based on CCA and RDA). The left dendrogram defines clusters of taxonomic groups sharing similar correlations with environmental and lipid biomarker parameters. b) The bar plot shows DNA-weighted abundance of each taxonomic group. The side

color maps show c) average relative abundances downcore (surface to bottom) and d) across the embayment (Station G to K).

4.3.5.1 Cluster I

Cluster I was composed of taxa that distributed relatively abundant in deeper sediments (> 5 cm) in the mid-embayment (Station H and I) as well as the offshore stations (J and K). This cluster positively correlates with recalcitrant lipid biomarkers (*n*-alkanes, stenones, and PAHs), and negatively correlates with ammonium, nitrite, and lipid concentrations, as well as phytoplankton lipid biomarkers (Figure 27). These correlations suggest that the Cluster I microbes are adapted to metabolize recalcitrant organic matter. The most abundant taxonomic group in Cluster I belongs to unclassified members of the Cenarchaeaceae family. The family of Cenarchaeaceae corresponds to Group I 1a mesophilic Crenarchaeota (Dawson et al., 2006; Jung et al., 2014), initially found as a sponge symbiont (Preston et al., 1996). Cenarchaeaceae is known as chemolithoautotrophic ammonium oxidizer. *Nitrospina* is also a nitrogen-cycle associated taxa included in Cluster I. It is a marine aerobic chemolithoautotrophic nitrite-oxidizing bacteria (Lücker and Daims, 2014; Rani et al., 2017). Besides nitrogen-cycle associated microbes, Cluster I may also represent degraders of recalcitrant or simple organic carbon. Cluster I also includes taxonomic groups classified in the family of Syntrophobacteraceae, the family of Rhodospirillaceae (**Error! Reference source not found.**). Syntrophobacteraceae are sulfate-reducing chemoheterotrophic bacteria which utilize relatively simple organic carbon (Kuever, 2014). Rhodospirillaceae related

organisms were isolated from deep-sea water [*Marispirillum indicum* (Lai et al., 2009)] were shown to degrade crude oil and from coastal sea water [*Pelagibius litoralis* (Choi et al., 2009)] to utilize amino acids.

4.3.5.2 Clusters IIa, IIb, and IIc

Cluster IIa was composed of taxa that distributed relatively abundant in just below the surface to mid-depths sediments (0.5-10 cm) in the offshore (K). Cluster IIb is composed of taxa that found to be relatively abundant in the deeper surface sediments (>15 cm) at Station K, J, and G. Cluster IIc is composed of taxa that distributed relatively abundant in the mid-depths sediments (2-10 cm) at Station J followed by K and G. Clusters IIa, IIb, and IIc correlated positively with TOC concentration, phosphate concentration (which strongly correlates with silicate), and the relative abundance of C₃₀ HBIs, while they are negatively correlated with pH, nitrate, and nitrite.

Cluster IIa, IIb and IIc were dominated by various sulfate-reducing Deltaproteobacteria, such as Desulfuromonadaceae, Desulfobulbaceae, and Desulfobacteraceae (Figure 29). Cluster IIa includes the dominant taxonomic group, uncultured Deltaproteobacteria, NB1-j. It is common in marine sediments and often found along with sulfate reducers (Yanagawa et al., 2013) in sulfate-methane-transition zone (Hamdan et al., 2008). The cluster IIb also includes uncultured Marine Benthic Group – B (MBGB). MBGB was found in a wide range of marine sediments, from the deep sea to the coastal sediments (Teske and Sorensen, 2008). Previous studies

suggested the associations of MBGB with anaerobic oxidation of methane (Knittel et al., 2005b) and sulfate reduction (Fernandez et al., 2016; Robertson et al., 2009). Although we do not have sulfate and sulfide concentrations, the negative correlations between these clusters with nitrate concentrations support that the Cluster II microbes reside below the nitrate reduction zone, sulfate reduction zone of sediments. In addition to the sulfate reducers, one of the dominant taxa within Cluster IIb is *Candidatus Scalindua*, an anoxic ammonium oxidizer (anammox) that uses nitrite as an electron acceptor, (Robertson et al., 2009; Schmid et al., 2003). Although *Candidatus Scalindua* was found in the nitrite depleted samples (Station J and K, > 5 cm, Figure 23), it is feasible to use sulfate as an electron acceptor (sulfate-reducing ammonium oxidation) (Schmidt et al., 2009). If this is the case, it explains that *Candidatus Scalindua* distributed similarly to sulfate-reducing Deltaproteobacteria.

4.3.5.3 Cluster III

Cluster III was composed of taxa that distributed relatively abundant in deeper sediments at Station G. It showed strong positive correlation with $\delta^{13}\text{C}_{\text{TOC}}$ values. The cluster includes taxonomic groups that belong to the genus of *Acinetobacter* and the order of Chromatiales. *Acinetobacter* is capable of utilizing diverse organic compounds as carbon sources; ranging from alcohols, some amino acids, fatty acids, straight-chained hydrocarbons, sugars, and many relatively recalcitrant aromatic compounds such as benzoate (Juni, 1978). *Acinetobacter* is also often found in glaciers (An et al., 2010;

Christner et al., 2003). The relative abundance of *Acinetobacter* showed a positive correlation with *n*-alkanes and stenones, and negative correlations with phytoplankton biomarkers. The order of Chromatiales is better known as phototrophic purple sulfur bacteria (Guyoneaud et al., 1997) but also contains chemotrophic relatives (Imhoff, 2005). Recent studies also suggested that this group is capable of degrading crude oil (Acosta-González et al., 2015; Kostka et al., 2011). Given the capability of these taxonomic groups to degrade relatively recalcitrant organic carbon, the cluster III may be representing functional cluster as degrader of recalcitrant organic matter in organic-lean sediments.

4.3.5.4 Clusters IVa and IVb

Cluster Iva was composed of taxa that distributed relatively abundant in the sediment depths just below the surface (0.5-5 cm) at the mid-embayment (Station H and I). Cluster IVb was composed of taxa that were relatively abundant in the surface sediments (0-5cm) at Station G. Clusters IVa and IVb both positively correlated with pH, nitrate, nitrite, and phytoplankton-related biomarkers such as $\Delta^{5,22}$ sterols and even carbon MUFAs.

Cluster IVa includes two of the most abundant taxa that belong to the family of Piscirickettsiaceae and the genus of *Nitrosopumilus*. The Piscirickettsiaceae, which was the most abundant taxon of this study (~10% of the total sequences), was universally distributed across the embayment and downcore. The Piscirickettsiaceae belongs to

Gammaproteobacteria, and this family includes a broad range of strains that are chemoheterotrophs and chemolithoautotrophs (Kasai et al., 2002). It is often found in hydrothermal vent and cold seeps, where some of the genera are capable of sulfide oxidation or methane oxidation (Nunoura et al., 2012; Sylvan et al., 2012). The bacteria belong to the family of Piscirickettsiaceae were also found in Arctic shelf sediments (Knittel et al., 2005b; Nguyen and Landfald, 2015). An cultured representative isolated from Antarctic sediments, *Thiomicrospira arctic*, is a psychrophilic, obligatory chemolithoautotrophic, sulfur-oxidizing bacteria (Knittel et al., 2005a).

Nitrosopumilus is part of the Marine Group-I Thaumarchaea and widespread in the water column and sediments (Francis et al., 2005; Schleper et al., 2005; Wuchter et al., 2006). Based on the cultured representative of the MG-I Thaumarchaea, *Nitrosopumilus maritimus* is an autotrophic, aerobic ammonia oxidizer (Köenneke et al., 2005), these OTUs are likely ammonia-oxidizing chemolithoautotrophs. Nitrate, a product of ammonia oxidation, showed strong positive correlation with the relative abundance of Cluster IVa, supporting that *Nitrosopumilus* as ammonium-oxidizer as well in our samples. Previous microbial investigations of Antarctic marine sediments using 16S rDNA gene clone libraries revealed that MG-I Thaumarchaea dominates archaeal communities in surface sediments of the continental shelf of the Mertz Glacier Polynya (Bowman et al., 2003) and the Weddell Sea (Gillan and Danis, 2007). Nitrite-oxidizing

Nitrospiraceae was a part of Cluster IVa, indicating the importance of nitrogen-cycle as functions of Cluster IVa.

One of the abundant taxa in Cluster IVb is the OM60 clade. It is an uncultured Gammaproteobacteria that is frequently found in oligotrophic marine waters (Cho and Giovannoni, 2004). This group is also found in Arctic sea ice (R. E. Collins et al., 2010) as well as in Arctic and Antarctic sediments (Ruff et al., 2014; Teske et al., 2011). Some studies suggested that OM60 function as a degrader of phytodetritus and large organic molecules, as it was ubiquitously found in the abyssal sediments in the Southern Ocean where abundant phytodetritus is available in surface sediments (Ruff et al., 2014). In a seawater mesocosm experiment, Sharma and colleagues (2014) found an increase in OM60 clade abundance and its transcripts involved in polysaccharide degradation after adding high molecular dissolved organic carbon. In addition to OM60, Cluster IVb contains the family of Colwelliaceae, the family of Flavobacteriaceae, uncultured Deltaproteobacteria, JTB38 ($r^2 = 0.51$), the order of Oceanospirillales (including the genus of *Candidatus Portiera*), the family of Rhodobacteraceae, the family of Verrucomicrobiaceae (including the genera of *Persicirhabdus* and *Rubritalea*). These are also known as degraders of large molecular weight substrates such as polysaccharides (Bowman, 2014; Martinez-Garcia et al., 2012; Sharma et al., 2014; Williams et al., 2013; J. Yoon et al., 2008) and associated with algal blooms (Fagervold et al., 2014; Rinta-Kanto et al., 2012; Ruff et al., 2014). The higher relative abundance of Cluster IVb microbes in

the surface sediments relative to the bottom sediments as well as the strong correlation with the relative abundances of phytoplankton biomarkers are thus consistent with the hypothesis that these microbes metabolize macromolecules derived from freshly deposited phytodetritus. Therefore we conclude that Cluster IVb represent phytodetritus degraders and may be responding to the increase in phytodetritus flux after the ice shelf collapse.

Our results indicated that the seven functional microbial community clusters represented the horizontal (cross embayment) and the vertical (downcore) diversity in the Larsen A sediments (Figure 28). In the most nearshore Station G, the microbial community was represented by phytodetritus degraders (Cluster IVb) at the top 10 cm sediments, and recalcitrant organic matter degraders (Cluster III) at the bottom 10 cm. This nearshore sediment community may represent the adaptation to the rapid flux increase in the organic matter flux shortly after the ice shelf collapse. In the mid-embayment Station H and I, the microbial community was dominated by nitrogen cycle associated organisms, especially ammonium-oxidizing Thaumarchaea accompanied by nitrite oxidizing bacteria. Although the distribution of *Nitrosopumilus* and Nitrospiraceae (Cluster IVa) in the oxic surface sediments strongly support their function as ammonium and nitrite oxidizers, the distribution of Cenarchaeaceae and Nitrospiraceae (Cluster I) in the anoxic deeper sediments is difficult to interpret. The Cluster I also contain the heterotrophic taxonomic groups that may have the ability to degrade the recalcitrant

and simple organic matter. In the most offshore Station J and K, the microbial community was represented by sulfate-reducing Deltaproteobacteria (Cluster II), in addition to the Cluster IVa and IVb microbes. Sulfate reduction occurs in relatively organic-rich sediments where other electron acceptors are consumed at near surface sediments. This result is consistent with the fact that Station J and K have been ice-shelf free for more than 100 years contained a higher level of organic carbon.

		Station G nearshore ←	Station H and I	Station J and K → offshore
near surface	Cluster and Major taxa	Cluster IVb OM 60	Cluster IVa <i>Nitrosopumilus</i> Nitrospiraceae	Cluster IIa (and IVa + IVb) Deltaproteobacteria NB1
	Potential key functions	phytodetritus degrader	Nitrogen cycle (ammonium oxidation and nitrite oxidation)	Sulfate reduction?
bottom (> 10 cm)	Cluster and Major taxa	Cluster III <i>Acinetobacter</i>	Cluster I Cenarchaeaceae, Nitrospinaceae, Syntrophobacteraceae	Cluster IIb, and IIc Deltaproteobacteria <i>Candidatus Scalindua</i>
	Potential key functions	recalcitrant OM degrader	Nitrogen cycle? recalcitrant OM degrader	Sulfate reduction anaerobic ammonium oxidation

Figure 28: The summary of the horizontal and vertical variability of microbial community characteristics.

Figure 29: Euclidian distance clustering that clusters of taxonomic groups sharing similar correlations with environmental and lipid biomarker parameters. Numbers on the nodes represent approximately unbiased *P* values were computed multiscale bootstrap resampling (10,000 iterations). Taxa labels, k, kingdom; p, phylum; c, class; o, order; f, family; g, genus.

4.3.6 Metagenome prediction

A predicted metagenome was constructed for each sample from the 16S rRNA gene sequences data with PICRUSt (Langille et al., 2013). PICRUSt allows us to predict the potential function of microbial communities. The mean nearest sequence taxon index (NSTI) of samples evaluated here was 0.19 ± 0.05 . This value is high compared to studies done for human microbiome (0.03), indicating that the prediction is less accurate. This is not surprising given that marine sediments in the polar region are poorly sampled and dominated with uncultured OTUs. Although this value is higher than studies done for the human microbiome, it is comparable to previous studies on environmental microbiome samples such as soils (average NSTI = 0.17; Langille et al. 2013), seawater [0.12-0.13; (de Voogd et al., 2015; Polónia et al., 2015)], marine sediments [0.11 - 0.17; (Cleary et al., 2016; de Voogd et al., 2015; Polónia et al., 2015)] and sponges [0.21-0.22, (de Voogd et al., 2015)]. In general, the higher the NSTI values reflect less accurate functional predictions. However, Langille (2013) demonstrated that soil samples (NSTI = 0.17) showed prediction accuracy as high as Human Microbiome Project (NSTI= 0.03). Therefore, we consider predicted microbial function could benefit us to interpret the association between environmental variables and microbial community.

Among the functions (KEGG Orthology groups; KO groups), the Metabolism related category was a dominant function ($60.0 \pm 0.5\%$). Based on NMDS plot (Figure 3) that exhibit community similarity among the surface sediments and diverge among stations in deeper sediments, we made the comparison of 1) between top 10cm and bottom 10 cm of sediments and 2) among station for bottom 10 cm.

The relative abundance of the metabolism related functions revealed several differences among the top and the bottom 10 cm of the sediment cores. The top 10 cm of sediments, for example, were significantly enriched in KO groups related with lipid metabolism and glycan biosynthesis and metabolism ($p < 0.006$, Figure 30, upper). On the other hand, 10-20cm depths sediment samples were significantly enriched in simple carbohydrate metabolism and membrane transfer system such as ABC transporters ($p < 0.001$, Figure 30, lower).

We found that the utilization of different organic matter depends on depths of sediments. For example, fatty acids are metabolized more often at top 10 cm of the sediments than at the bottom 10 cm. On the other hand, the microbial communities at the bottom 10 cm use more simple carbohydrates and a greater potential of fixing carbon. This vertical change of carbon utilization in sediment cores can be considered as microbial succession based on organic matter quality; larger carbohydrate molecules such as fatty acids consumed first after OM reach to the seafloor, low-molecule carbohydrate consumed later at the deeper sediments. McCarren (2010) demonstrated

the temporal succession of marine bacterial community after adding high-molecular-weight dissolved organic matter. The microbial community consumed high-molecular-weight organic matter first, and then used low-molecular-weight organic matter. The vertical change also could be considered as a response to the ice-shelf collapse. The phytodetritus delivered after the ice shelf collapse penetrated the top 10 cm of sediments due to biodiffusion (Chapter 3). The microbial community structure likely shifted to phytodetritus degrader at the surface sediments, and their physiology may be altered as well.

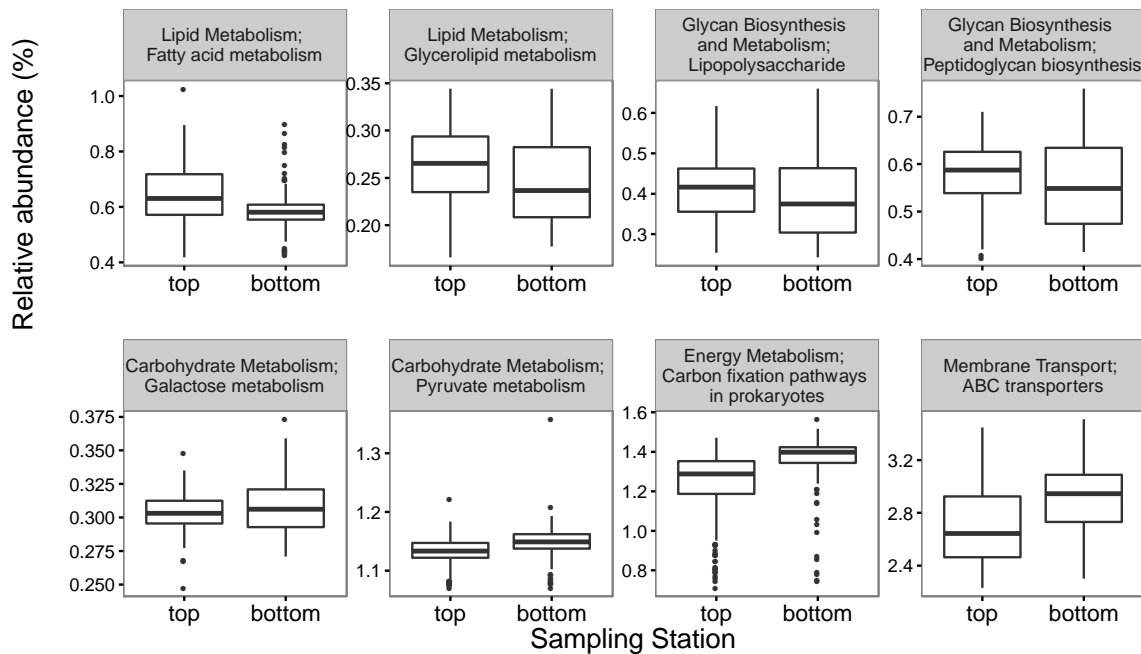


Figure 30: Comparison of the mean relative abundance of KEGG orthologs (KOs) function groups between the top (0-10 cm) and bottom (10-20 cm) of sediment samples. All the relative abundances of KO groups were significantly different between top and bottom ($p < 0.006$).

Among the sampling stations, we found two patterns of predicted function relative abundances among stations. First, Station H and I were significantly enriched in the KO groups including amino acid metabolism, nucleotide metabolism, and ABC transporters (**Error! Reference source not found.**, upper). Second, Station G, J, and K were significantly enriched in the KO groups that are carbohydrate metabolisms such as amino acid sugars and nucleotide sugars metabolism, sulfur metabolism, and glycan biosynthesis (**Error! Reference source not found.**, lower). The difference in the organic matter utilization between Stations H and I, and Stations G, J, and K may be due to their organic matter concentrations and differences in fluxes. Considering that Station G, J,

and K contains a larger amount of phytodetritus (Chapter 2) than other stations, microbial communities in these stations may have more potential to utilize the resources they have. Moreover, the microbes in Station H and I have a higher capacity to metabolize amino acids (Figure 31), possibly recycling amino acids in the organic matter poor environment (Orsi et al., 2013). The higher potential of sulfur metabolism in Stations G, J, and K is consistent with that these Stations contained sulfate-reducing bacteria that belong to Clusters IIa, IIb, and IIc.

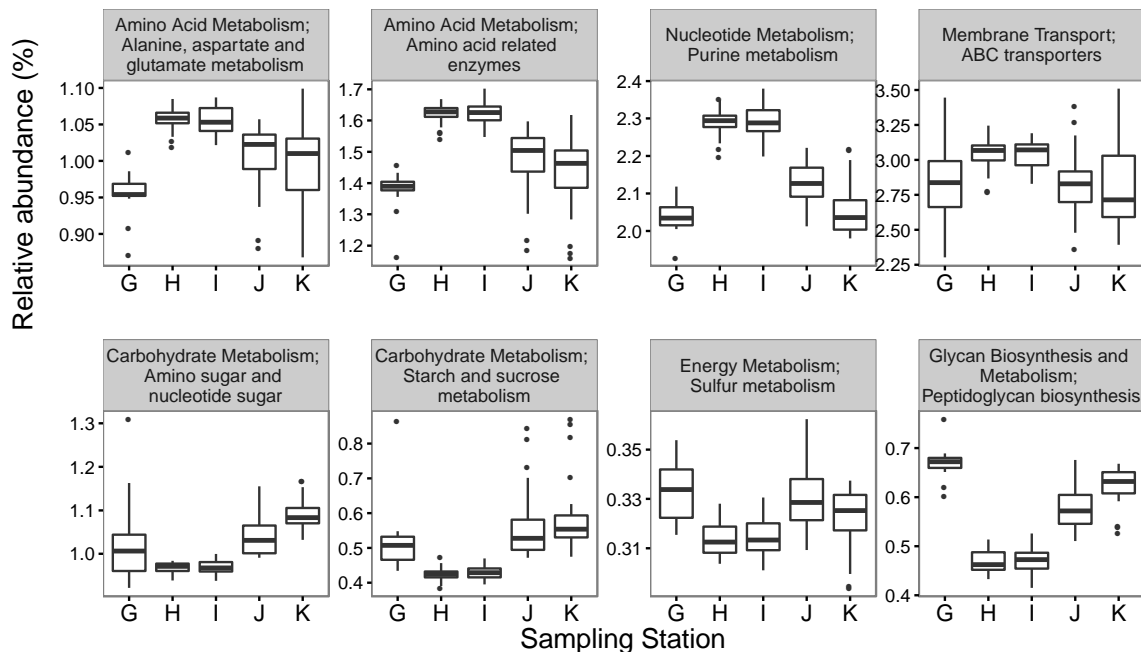


Figure 31: Comparison of the mean relative abundance of KEGG orthologs (KOs) function groups among five sampling stations (G-K). All the relative abundances of KO groups at Station H and I were significantly different from Station G, J and K ($p < 0.05$).

Another interesting observation was that the bacterial communities from bottom 10 cm sediments, particularly in Station H and I, harbored more genes involved in mechanisms of nutrient acquisition, as compared to the top 10 cm of sediment cores. These genes are involved in a production of ATP-binding cassette (ABC) transporters. Biosynthesis of the ABC transporters is energetically costly, and they are synthesized during nutrient limiting conditions. Given the fact that Stations H and I are nutritionally deprived region, higher abundance of ABC transporters gene shows that these stations

are harboring bacterial community with potential but bio-energetically costly adaptive mechanisms for nutrient uptake.

4.4 Conclusions

Organic matter (OM) concentrations, flux and quality, and concentrations of nitrate, nitrite and ammonium concentrations were correlated with relative distributions of microbial functional groups. Our results imply that OM deposition to the seafloor after the ice-shelf collapse indirectly and directly affect the microbial community structure. First, the increasing OM concentrations and fluxes may result in the decrease of electron acceptors and change the dominant microbial processes across the embayment from nitrogen cycle to sulfur-cycle associated processes. Second, OM quality may directly control the vertical community shift from recalcitrant OM degrader in older (deeper) sediments to phytodetritus degrader in newer (surface) sediments. From the point of view of we hypothesize that the microbial communities in the five sampling stations composed of different functional groups represent the microbial succession following the ice shelf disintegration. The most organic-lean mid-embayment stations were inhabited by oligotrophic lineages such as ammonium-oxidizing Thaumarchaea (*Nitrosopumilus*) and degraders of recalcitrant organic carbon. The most nearshore station was inhabited by phytodetritus degraders in the surface sediments and recalcitrant organic matter degraders in the

deeper sediments. The relatively organic- and nutrient-rich offshore stations were inhabited by sulfate-reducing Deltaproteobacteria. This community succession may influence biogeochemical cycles in the sediments and degradation of deposited organic matter. Further investigations are needed to understand the impact of changing microbial community on the organic matter degradation, preservation, and sequestration of organic carbon under the seafloor.

5. Conclusions

This dissertation examined organic matter sources, changes in labile organic matter fluxes, and impact of organic matter flux and quality to microbial community in the Larsen A Embayment, the Weddell Sea. Ocean exposure to sunlight and should enhance biological productivity in surface water and organic matter flux to the seafloor. Organic matter sources are characterized by lipid biomarker compositions (Chapter 2). Then, diagenetic models were applied to lipids vertical distribution to estimate the pre- and post-ice-shelf-collapse lipid fluxes (Chapter 3). By combining lipid composition data with other sediment environmental parameters and microbial sequence data, the influences of contents and quality of organic matter on the microbial community were examined (Chapter 4). This dissertation advances current knowledge of organic matter sources in Antarctic sediments and potential impacts of ice shelf disintegration on organic matter flux and sediment microbial community structure.

One of the highlights of this research is new evidence for the importance of organic matter input to the seafloor from sea-ice diatoms. The Larsen A Embayment is covered by sea ice average 288 days a year in the last two decades. The predominance of C₁₆, C₁₈, and C₂₀ fatty acids, 24-methylenecholesterol, sitosterol, and ¹³C-enriched sea-ice diatom biomarker (C_{25:2} HBIs) support the importance of organic matter inputs from sea-ice diatom community (Chapter 2). Primary production in sea ice may be underestimated by satellite-based primary productivity studies. The role of sea-ice

diatoms is suggested by the mismatch of cross-embayment trends of satellite-based primary productivity and estimated lipid flux after the ice-shelf disintegration (Chapter 3).

Another highlight of this dissertation is finding of potential rapid increase in lipid (labile organic matter) flux following ice-shelf collapse and its impact on sedimentary microbial community structure and processes. Although the diagenetic modeling study has limitations by uncertainties of short-term diffusion rate coefficients and short-term sedimentation rate, and the assumption of constant downcore degradation rate, it suggests over 3000 fold of increase in lipid flux. If true, this scale of flux increase should induce a shift in the microbial community structure in the sediments. The importance of organic matter flux for microbial community structure was supported by multivariate analyses. Organic matter content (total organic carbon and lipid concentrations) and $\delta^{13}\text{C}_{\text{TOC}}$ values, relative abundances of labile and recalcitrant lipid biomarkers, and the concentration of nitrogen species (nitrate, nitrite, and ammonium) correlate with cross-embayment and downcore microbial diversity (Chapter 4). The cross-embayment microbial community diversity could be explained by dominant processes associated with phytodetritus degradation (in the most nearshore), nitrogen cycle (in the mid-embayment), and sulfate reduction (in the offshore). These dominant processes lead the hypothesis that the microbial community may be shifting

from oligotrophic lineages represented by nitrogen-cycle associated community to phytodetritus degraders and then to sulfate-reducers following the ice shelf collapse.

This dissertation contributed novel and valuable scientific information that expands the current knowledge of the sedimentary organic matter sources in Antarctica and potential impact of ice-shelf disintegration on chemical and biological subseafloor environment. Nevertheless, this study was limited by lack of direct measurement, time series sampling or experimental observations. Some of the biggest questions still apparent are those regarding the quantitative measure of changing flux and microbial organic matter degradation rate. While the diagenetic modeling effort presented in Chapter 3 provides estimated lipid flux increases following the ice-shelf collapse, the modeling methods are constrained by uncertainties. Further experimental observations of organic matter degradation rate in sediments collected under ice shelves are needed to expand our understanding of on microbial degradation activity in the under-ice-shelf sediments and to gain a better quantitative measure of organic matter flux under ice shelves.

References

- Acosta-González, A., Martirani-von Abercron, S.-M., Rosselló-Móra, R., Wittich, R.-M., Marqués, S., 2015. The effect of oil spills on the bacterial diversity and catabolic function in coastal sediments: a case study on the Prestige oil spill. *Environ Sci Pollut Res* 22, 15200–15214. doi:10.1007/s11356-015-4458-y
- Albers, C.S., Kattner, G., Hagen, W., 1996. The compositions of wax esters, triacylglycerols and phospholipids in Arctic and Antarctic copepods: evidence of energetic adaptations. *Mar Chem* 55, 347–358. doi:10.1016/S0304-4203(96)00059-X
- Albers, S.-V., Meyer, B.H., 2011. The archaeal cell envelope. *Nat Rev Micro* 9, 414–426. doi:10.1038/nrmicro2576
- An, L.Z., Chen, Y., Xiang, S.R., Shang, T.C., 2010. Differences in community composition of bacteria in four glaciers in western China. *Biogeosciences*.
- Apprill, A., McNally, S., Parsons, R., Webe, L., 2015. Minor revision to V4 region SSU rRNA 806R gene primer greatly increases detection of SAR11 bacterioplankton. *Aquat. Microb. Ecol.* 75, 129–137. doi:10.3354/ame01753
- Armstrong, F.A.J., Stearns, C.R., Strickland, J.D.H., 1967. The measurement of upwelling and subsequent biological process by means of the Technicon Autoanalyzer® and associated equipment. *Deep Sea Research and Oceanographic Abstracts* 14, 381–389. doi:10.1016/0011-7471(67)90082-4
- Arrigo, K.R., van Dijken, G.L., Pabi, S., 2008. Impact of a shrinking Arctic ice cover on marine primary production. *Geophys. Res. Lett.* 35, L19603. doi:10.1029/2008GL035028
- Atkinson, A., Siegel, V., Pakhomov, E., Rothery, P., 2004. Long-term decline in krill stock and increase in salps within the Southern Ocean. *Nature* 432, 100–103. doi:10.1038/nature02950
- Atlas, E.L., 1971. *A Practical Manual for Use of the Technicon Autoanalyzer in Seawater Nutrient Analyses*. Oregon State University.
- Azam, F., Beers, J.R., Campbell, L., Carlucci, A.F., Holm-Hansen, O., Reid, F.M.H., Karl, D.M., 1979. Occurrence and metabolic activity of organisms under the Ross ice shelf, Antarctica, at station j9. *Science* 203, 451–453. doi:10.1126/science.203.4379.451
- Baldock, J.A., Masiello, C.A., Gelinas, Y., Hedges, J.I., 2004. Cycling and composition of organic matter in terrestrial and marine ecosystems. *Mar Chem* 92, 39–64. doi:10.1016/j.marchem.2004.06.016
- Barnes, D.K.A., 2015. Antarctic sea ice losses drive gains in benthic carbon drawdown. *Current Biology* 25, R789–R790. doi:10.1016/j.cub.2015.07.042
- Barnes, D.K.A., Peck, L.S., 2008. Vulnerability of Antarctic shelf biodiversity to predicted regional warming. *Climate Research* 37, 149–163. doi:10.3354/cr00760
- Becker, K.W., Lipp, J.S., Zhu, C., Liu, X.-L., Hinrichs, K.-U., 2013. An improved method for the analysis of archaeal and bacterial ether core lipids. *Org Geochem* 61, 34–44.

- doi:10.1016/j.orggeochem.2013.05.007
- Belt, S.T., Brown, T.A., Ringrose, A.E., Cabedo-Sanz, P., Mundy, C.J., Gosselin, M., Poulin, M., 2013. Quantitative measurement of the sea ice diatom biomarker IP25 and sterols in Arctic sea ice and underlying sediments: Further considerations for palaeo sea ice reconstruction. *Org Geochem* 62, 33–45.
doi:10.1016/j.orggeochem.2013.07.002
- Belt, S.T., Massé, G.G., Vare, L.L., Rowland, S.J., Poulin, M., Sicre, M.A., Sampei, M., Fortier, L., 2008. Distinctive C-13 isotopic signature distinguishes a novel sea ice biomarker in Arctic sediments and sediment traps. *Mar Chem* 112, 158–167.
doi:10.1016/j.marchem.2008.09.002
- Berner, R.A., 1980. *Early Diagenesis*. Princeton University Press.
- Berner, R.A., 1964. An Idealized Model of Dissolved Sulfate Distribution in Recent Sediments. *Geochim Cosmochim Acta* 28, 1497–1503.
- Bernhardt, H., Wilhelms, A., 1967. The continuous determination of low level iron, soluble phosphate and total phosphate with the AutoAnalyzer. *Technicon Symposia*.
- Bertolin, M.L., Schloss, I.R., 2009. Phytoplankton production after the collapse of the Larsen A Ice Shelf, Antarctica. *Polar Biology* 32, 1435–1446. doi:10.1007/s00300-009-0638-x
- Beyer, W.H., 1981. *CRC Standard Mathematical Tables*. CRC.
- Bienhold, C., Boetius, A., Ramette, A., 2012. The energy–diversity relationship of complex bacterial communities in Arctic deep-sea sediments. *ISME J* 6, 724–732.
doi:10.1038/ismej.2011.140
- Bintanja, R., van Oldenborgh, G.J., Drijfhout, S.S., Wouters, B., Katsman, C.A., 2013. Important role for ocean warming and increased ice-shelf melt in Antarctic sea-ice expansion. *Nature Publishing Group* 6, 376–379. doi:10.1038/ngeo1767
- Blanchet, F.G., Legendre, P., Borcard, D., 2008. Forward selection of explanatory variables. <http://dx.doi.org/10.1890/07-0986.1> 89, 2623–2632. doi:10.1890/07-0986.1
- Blumer, M., Guillard, R.R., Chase, T., 1971. Hydrocarbons of Marine Phytoplankton. *Mar Biol* 8, 183–&.
- Borchers, H.W., 2015. Package “pracma.”
- Boudreau, B.P., 2005. Modeling Mixing and Diagenesis, in: *Interactions Between Macro- and Microorganisms in Marine Sediments*. American Geophysical Union, pp. 323–341.
- Boudreau, B.P., 1997. *Diagenetic Models and Their Implementation*. Springer Verlag.
- Boudreau, B.P., 1986. Mathematics of tracer mixing in sediments; I, Spatially-dependent, diffusive mixing. *Am J Sci* 286, 161–198. doi:10.2475/ajs.286.3.161
- Bowman, J.P., 2014. The family colwelliaceae. *The Prokaryotes: Gammaproteobacteria*. doi:10.1007/978-3-642-38922-1_230.pdf
- Bowman, J.P., Bowman, J.P., McCammon, S.A., Gibson, J.A.E., Gibson, J.A.E., Robertson,

- L., Nichols, P.D., 2003. Prokaryotic metabolic activity and community structure in Antarctic continental shelf sediments. *Applied and Environmental Microbiology* 69, 2448–2462. doi:10.1128/aem.69.5.2448-2462.2003
- Box, G., Cox, D.R., 1964. An Analysis of Transformations. *Journal of the Royal Statistical Society Series B* (.... doi:10.2307/2984418
- Bray, E.E., Evans, E.D., 1961. Distribution of n-paraffins as a clue to recognition of source beds. *Geochim Cosmochim Acta* 22, 2–15. doi:10.1016/0016-7037(61)90069-2
- Bray, J.R., Curtis, J.T., 1957. An Ordination of the Upland Forest Communities of Southern Wisconsin. *Ecol Monogr* 27, 325–349. doi:10.2307/1942268
- Buckles, L.K., Villanueva, L., Weijers, J.W.H., Verschuren, D., Sinninghe Damsté, J.S., 2013. Linking isoprenoidal GDGT membrane lipid distributions with gene abundances of ammonia-oxidizing Thaumarchaeota and uncultured crenarchaeotal groups in the water column of a tropical lake (Lake Challa, East Africa). *Environmental Microbiology* 15, 2445–2462. doi:10.1111/1462-2920.12118
- Burdige, D.J., 2006. *Geochemistry of marine sediments*. Princeton University Press.
- Camacho-Ibar, V.F., Aveytua-Alcazar, L., 2003. Fatty acid reactivities in sediment cores from the northern Gulf of California. *Org Geochem*.
- Canfield, D.E., 1994. Factors influencing organic carbon preservation in marine sediments. *Chem Geol* 114, 315–329. doi:10.1016/0009-2541(94)90061-2
- Canfield, D.E., Glazer, A.N., Falkowski, P.G., 2010. The Evolution and Future of Earth's Nitrogen Cycle. *Science* 330, 192–196. doi:10.1126/science.1186120
- Canuel, E.A., Martens, C.S., 1996. Reactivity of recently deposited organic matter: Degradation of lipid compounds near the sediment-water interface. *Geochim Cosmochim Acta* 1–14.
- Cape, M.R., Vernet, M., Kahru, M., 2014. Polynya dynamics drive primary production in the Larsen A and B embayments following ice shelf collapse. *Journal of Geophysical Research: Oceans*.
- Caporaso, J.G., Kuczynski, J., Stombaugh, J., Bittinger, K., Bushman, F.D., Costello, E.K., Fierer, N., Peña, A.G., Goodrich, J.K., Gordon, J.I., Huttley, G.A., Kelley, S.T., Knights, D., Koenig, J.E., Ley, R.E., Lozupone, C.A., McDonald, D., Muegge, B.D., Pirrung, M., Reeder, J., Sevinsky, J.R., Turnbaugh, P.J., Walters, W.A., Widmann, J., Yatsunencko, T., Zaneveld, J., Knight, R., 2010. QIIME allows analysis of high-throughput community sequencing data. *Nat Meth* 7, 335–336. doi:10.1038/nmeth.f.303
- Caporaso, J.G., Lauber, C.L., Walters, W.A., Berg-Lyons, D., Huntley, J., Fierer, N., Owens, S.M., Betley, J., Fraser, L., Bauer, M., Gormley, N., Gilbert, J.A., Smith, G., Knight, R., 2012. Ultra-high-throughput microbial community analysis on the Illumina HiSeq and MiSeq platforms. *ISME J* 6, 1621–1624. doi:10.1038/ismej.2012.8
- Caporaso, J.G., Lauber, C.L., Walters, W.A., Berg-Lyons, D., Lozupone, C.A., Turnbaugh, P.J., Knight, R., 2011. Global Patterns of 16s rRNA diversity at a depth of

- millions of sequences per sample. *proc Natl Acad Sci U S A* 1–7.
doi:10.1073/pnas.1000080107/-/DCSupplemental
- Carpenter, R., Peterson, M.J., Bennett, J.T., 1985. ^{210}Pb -derived sediment accumulation and mixing rates for the greater Puget Sound region. *Marine Geology* 64, 291–312. doi:10.1016/0025-3227(85)90109-4
- Carr, S.A., Vogel, S.W., Dunbar, R.B., Brandes, J., Spear, J.R., Levy, R., Naish, T.R., Powell, R.D., Wakeham, S.G., Mandernack, K.W., 2013. Bacterial abundance and composition in marine sediments beneath the Ross Ice Shelf, Antarctica. *Geobiology* n/a–n/a. doi:10.1111/gbi.12042
- Caspel, M.V., Schröder, M., Huhn, O., Hellmer, H.H., 2015. Precursors of Antarctic Bottom Water formed on the continental shelf off Larsen Ice Shelf. *Deep-Sea Research Part I* 99, 1–9. doi:10.1016/j.dsr.2015.01.004
- Cho, J.-C., Giovannoni, S.J., 2004. Cultivation and growth characteristics of a diverse group of oligotrophic marine Gammaproteobacteria. *Applied and Environmental Microbiology* 70, 432–440. doi:10.1128/AEM.70.1.432-440.2004
- Choi, D.H., Hwang, C.Y., Cho, B.C., 2009. *Pelagibius litoralis* gen. nov., sp. nov., a marine bacterium in the family Rhodospirillaceae isolated from coastal seawater. *INTERNATIONAL JOURNAL OF SYSTEMATIC AND EVOLUTIONARY MICROBIOLOGY* 59, 818–823. doi:10.1099/ijs.0.002774-0
- Christner, B.C., Mosley-Thompson, E., Thompson, L.G., Reeve, J.N., 2003. Bacterial recovery from ancient glacial ice. *Environmental Microbiology* 5, 433–436. doi:10.1046/j.1462-2920.2003.00422.x
- Clarke, A., Murphy, E.J., Meredith, M.P., King, J.C., Peck, L.S., Barnes, D.K.A., Smith, R.C., 2007. Climate change and the marine ecosystem of the western Antarctic Peninsula. *Philosophical Transactions of the Royal Society B: Biological Sciences* 362, 149–166. doi:10.1098/rstb.2006.1958
- Clarke, K.R., Green, R.H., 1988. Statistical design and analysis for a “biological effects” study. *Mar Ecol Prog Ser* 46, 213–226. doi:10.3354/meps046213
- Cleary, D.F.R., Polónia, A.R.M., Sousa, A.I., Lillebø, A.I., Queiroga, H., Gomes, N.C.M., 2016. Temporal dynamics of sediment bacterial communities in monospecific stands of *Juncus maritimus* and *Spartina maritima*. *Plant Biology*. doi:10.1111/plb.12459
- Cochran, J.K., 1985. Particle mixing rates in sediments of the eastern equatorial Pacific: Evidence from ^{210}Pb , $^{239,240}\text{Pu}$ and ^{137}Cs distributions at MANOP sites. *Geochim Cosmochim Acta* 49, 1195–1210. doi:10.1016/0016-7037(85)90010-9
- Collier, R., Dymond, J., Honjo, S., Manganini, S., Francois, R., Dunbar, R.B., 2000. The vertical flux of biogenic and lithogenic material in the Ross Sea: moored sediment trap observations 1996–1998. *Deep Sea Research Part II: Topical Studies in Oceanography* 47, 3491–3520. doi:10.1016/S0967-0645(00)00076-X
- Collins, L.G., Allen, C.S., Pike, J., Hodgson, D.A., Weckström, K., Massé, G.G., 2013. Evaluating highly branched isoprenoid (HBI) biomarkers as a novel Antarctic sea-

- ice proxy in deep ocean glacial age sediments. *Quaternary Science Reviews* 79, 87–98. doi:10.1016/j.quascirev.2013.02.004
- Collins, R.E., Rocap, G., Deming, J.W., 2010. Persistence of bacterial and archaeal communities in sea ice through an Arctic winter. *Environmental Microbiology* 12, 1828–1841. doi:10.1111/j.1462-2920.2010.02179.x
- Corinaldesi, C., Beolchini, F., Dell’Anno, A., 2008. Damage and degradation rates of extracellular DNA in marine sediments: implications for the preservation of gene sequences. *Molecular Ecology* 17, 3939–3951. doi:10.1111/j.1365-294X.2008.03880.x
- Cranwell, P.A., 1982. Lipids of Aquatic Sediments and Sedimenting Particulates. *Prog. Lipid Res.* 21, 271–308.
- Cranwell, P.A., 1981. Diagenesis of free and bound lipids in terrestrial detritus deposited in a lacustrine sediment. *Org Geochem* 3, 79–89. doi:10.1016/0146-6380(81)90002-4
- Crawford, A., 2012. Marine sedimentary record of the greenpeace trough, Larsen A Embayment, Antarctic Peninsula, in: Leventer, A. (Ed.). *Colegate University*.
- Cripps, G.C., 1995. The Occurrence of Monounsaturated n-C-21 and Polyunsaturated C-25 Sedimentary Hydrocarbons in the Lipids of Antarctic Marine Organisms. *Polar Biology* 15, 253–259.
- Cripps, G.C., 1990. Hydrocarbons in the seawater and pelagic organisms of the Southern Ocean. *Polar Biology* 10, 393–402. doi:10.1007/BF00237827
- D'Hondt, S., Spivack, A.J., Pockalny, R., Ferdelman, T.G., Fischer, J.P., Kallmeyer, J., Abrams, L.J., Smith, D.C., Graham, D., Hasiuk, F., Schrum, H., Stancin, A.M., 2009. Subseafloor sedimentary life in the South Pacific Gyre. *proceedings of the National Academy of Sciences* 106, 11651–11656. doi:10.1073/pnas.0811793106
- Dalsgaard, J., St John, M., Kattner, G., Müller-Navarra, D., Hagen, W., 2003. Fatty acid trophic markers in the pelagic marine environment, in: *Advances in Marine ... , Advances in Marine Biology*. Elsevier, pp. 225–340. doi:10.1016/S0065-2881(03)46005-7
- Davies, B.J., Hambrey, M.J., Smellie, J.L., Carrivick, J.L., Glasser, N.F., 2012. Antarctic Peninsula Ice Sheet evolution during the Cenozoic Era. *Quaternary Science Reviews* 31, 30–66. doi:10.1016/j.quascirev.2011.10.012
- Dawson, P., Han, I., Cox, M., Black, C., Simmons, L., 2006. Residence time and food contact time effects on transfer of Salmonella Typhimurium from tile, wood and carpet: testing the five-second rule. *J Appl Microbiol* 0, 061120055200041–???. doi:10.1111/j.1365-2672.2006.03171.x
- de Voogd, N.J., Cleary, D.F.R., Polónia, A.R.M., Gomes, N.C.M., Olson, J., 2015. Bacterial community composition and predicted functional ecology of sponges, sediment and seawater from the thousand islands reef complex, West Java, Indonesia. *FEMS Microbiology Ecology* 91, fiv019. doi:10.1093/femsec/fiv019
- Degens, E.T., 1969. Biogeochemistry of Stable Carbon Isotopes, in: Eglinton, G., Murphy, M.T.J. (Eds.), *Organic Geochemistry*. Springer Berlin Heidelberg, Berlin, Heidelberg,

- pp. 304–329. doi:10.1007/978-3-642-87734-6_14
- Dell'Anno, A., Corinaldesi, C., 2004. Degradation and turnover of extracellular DNA in marine sediments: Ecological and methodological considerations. *Applied and Environmental Microbiology* 70, 4384–4386. doi:10.1128/aem.70.7.4384-4386.2004
- DeMaster, D.J., Cochran, J.K., 1982. Particle mixing rates in deep-sea sediments determined from excess ²¹⁰Pb and ³²Si profiles. *Earth and Planetary Science Letters* 61, 257–271. doi:10.1016/0012-821X(82)90057-7
- DeMaster, D.J., McKee, B.A., Nittrouer, C.A., Jiangchu, Q., Guodong, C., 1985. Rates of sediment accumulation and particle reworking based on radiochemical measurements from continental shelf deposits in the East China Sea. *Continental Shelf Research* 4, 143–158. doi:10.1016/0278-4343(85)90026-3
- DeSantis, T.Z., Hugenholtz, P., Larsen, N., Rojas, M., Brodie, E.L., Keller, K., Huber, T., Dalevi, D., Hu, P., Andersen, G.L., 2006. Greengenes, a chimera-checked 16S rRNA gene database and workbench compatible with ARB. *Applied and Environmental Microbiology* 72, 5069–5072. doi:10.1128/AEM.03006-05
- Dhakar, S.P., Burdige, D.J., 1996. A coupled, non-linear, steady state model for early diagenetic processes in pelagic sediments. *Oceanographic Literature Review* 11, 1098–330. doi:10.2475/ajs.296.3.296
- Diekmann, B., Kuhn, G., 1999. Provenance and dispersal of glacial–marine surface sediments in the Weddell Sea and adjoining areas, Antarctica: ice-rafting versus current transport. *Marine Geology* 158, 209–231. doi:10.1016/S0025-3227(98)00165-0
- Domack, E.W., Duran, D., Leventer, A., Ishman, S.E., Doane, S., McCallum, S., Amblas, D., Ring, J., Gilbert, R., Prentice, M., 2005a. Stability of the Larsen B ice shelf on the Antarctic Peninsula during the Holocene epoch. *Nature* 436, 681–685. doi:10.1038/nature03908
- Domack, E.W., Ishman, S.E., Leventer, A., Sylva, S.P., Willmott, V., Huber, B., 2005b. A chemotrophic ecosystem found beneath Antarctic Ice Shelf. *Eos, Transactions American Geophysical Union* 86, 269–272. doi:10.1029/2005EO290001
- Doney, S.C., Ruckelshaus, M., Emmett Duffy, J., Barry, J.P., Chan, F., English, C.A., Galindo, H.M., Grebmeier, J.M., Hollowed, A.B., Knowlton, N., Polovina, J., Rabalais, N.N., Sydeman, W.J., Talley, L.D., 2012. Climate Change Impacts on Marine Ecosystems. *Annu. Rev. Marine. Sci.* 4, 11–37. doi:10.1146/annurev-marine-041911-111611
- Dowling, N.J.E., Widdel, F., White, D.C., 1986. Phospholipid Ester-linked Fatty Acid Biomarkers of Acetate-oxidizing Sulphate-reducers and Other Sulphide-forming Bacteria. *Journal of General Microbiology*.
- Drazen, J.C., Phleger, C.F., Guest, M.A., Nichols, P.D., 2008. Lipid, sterols and fatty acid composition of abyssal holothurians and ophiuroids from the North-East Pacific Ocean: Food web implications. *Comparative Biochemistry and Physiology Part B* 151, 79–87. doi:10.1016/j.cbpb.2008.05.013

- Ducklow, H.W., Fraser, W., Meredith, M.P., Stammerjohn, S.E., Doney, S.C., Martinson, D.G., Sailley, S., Schofield, O.M., Steinberg, D., Venables, H.J., Amsler, C.D., 2013. West Antarctic Peninsula: An Ice-Dependent Coastal Marine Ecosystem in Transition. *oceanog* 26, 190–203. doi:10.5670/oceanog.2013.62
- Dunne, J.P., Sarmiento, J.L., Gnanadesikan, A., 2007. A synthesis of global particle export from the surface ocean and cycling through the ocean interior and on the seafloor. *Global Biogeochem Cycles* 21, n/a–n/a. doi:10.1029/2006GB002907
- Dunstan, G.A., Volkman, J.K., Barrett, S.M., Leroi, J.M., Jeffrey, S.W., 1994. Essential Polyunsaturated Fatty-Acids From 14 Species of Diatom (Bacillariophyceae). *Phytochemistry* 35, 155–161.
- Durbin, A.M., Durbin, A.M., Biddle, J.F., Martino, A., 2009. Microbial community stratification in TOC-depleted marine subsurface sediments of the Pacific Ocean. *Geochim Cosmochim Acta* 73, 1005–1015. doi:10.1016/j.gca.2009.02.015
- Durbin, A.M., Durbin, A.M., Teske, A.P., 2010. Sediment-associated microdiversity within the Marine Group I Crenarchaeota. *Environ Microbiol Rep* 2, 693–703. doi:10.1111/j.1758-2229.2010.00163.x
- Durbin, A.M., Teske, A.P., 2011. Microbial diversity and stratification of South Pacific abyssal marine sediments. *Environmental Microbiology* 13, 3219–3234. doi:10.1111/j.1462-2920.2011.02544.x
- Eglinton, G., Hamilton, R.J., 1967. Leaf Epicuticular Waxes. *Science* 156, 1322–1335. doi:10.1126/science.156.3780.1322
- Elling, F.J., Könenneke, M., Lipp, J.S., Becker, K.W., Gagen, E.J., Hinrichs, K.-U., 2014. Effects of growth phase on the membrane lipid composition of the thaumarchaeon *Nitrosopumilus maritimus* and their implications for archaeal lipid distributions in the marine environment. *Geochim Cosmochim Acta* 141, 579–597. doi:10.1016/j.gca.2014.07.005
- Elvert, M., Boetius, A., Boetius, A., Knittel, K., Knittel, K., Jørgensen, B.B., 2003. Characterization of specific membrane fatty acids as chemotaxonomic markers for sulfate-reducing bacteria involved in anaerobic oxidation of methane. *Geomicrobiology Journal* 20, 403–419. doi:10.1080/01490450303894
- Emerson, S., Fischer, K., Reimers, C., Heggie, D., 1985. Organic carbon dynamics and preservation in deep-sea sediments. *Deep Sea Research* 32, 1–21. doi:10.1016/0198-0149(85)90014-7
- Fagervold, S.K., Bourgeois, S., Pruski, A.M., Charles, F.C.O., eacute, P.K., Vétion, G., Galand, P.E., 2014. River organic matter shapes microbial communities in the sediment of the Rhône prodelta. *ISME J* 8, 2327–2338. doi:10.1038/ismej.2014.86
- Fahl, K., Kattner, G., 1993. Lipid Content and fatty acid composition of algal communities in sea-ice and water from the Weddell Sea (Antarctica). *Polar Biology* 13, 405–409. doi:10.1007/BF01681982
- Fahl, K., Stein, R., 2012. Modern seasonal variability and deglacial/Holocene change of

- central Arctic Ocean sea-ice cover: New insights from biomarker proxy records. *Earth and Planetary Science Letters* 351, 123–133. doi:10.1016/j.epsl.2012.07.009
- Falk-Petersen, S., Sargent, J.R., Henderson, J., Hegseth, E.N., Hop, H., Okolodkov, Y.B., 1998. Lipids and fatty acids in ice algae and phytoplankton from the Marginal Ice Zone in the Barents Sea. *Polar Biology* 20, 41–47. doi:10.1007/s003000050274
- Falk-Petersen, S., Sargent, J.R., Lønne, O.J., Timofeev, S., 1999. Functional biodiversity of lipids in Antarctic zooplankton: *Calanoides acutus*, *Calanus propinquus*, *Thysanoessa macrura* and *Euphausia crystallorophias* - Springer. *Polar Biology*.
- Fernandez, A.B., Rasuk, M.C., Visscher, P.T., Contreras, M., Novoa, F., Poire, D.G., Patterson, M.M., Ventosa, A., Farias, M.E., 2016. Microbial Diversity in Sediment Ecosystems (Evaporites Domes, Microbial Mats, and Crusts) of Hypersaline Laguna Tebenquiche, Salar de Atacama, Chile. *Front Microbiol* 7, e114570. doi:10.3389/fmicb.2016.01284
- Ferrigno, J.G., 2006. Coastal-Change and Glaciological Map of the Trinity Peninsula Area and South Shetland Islands, Antarctica: 1843–2001. USGS Coastal Change and Glaciological Maps of Antarctica.
- Fietz, S., Hugué, C., Bendle, J., Escala, M., Gallacher, C., Herfort, L., Jamieson, R., Martínez-García, A., McClymont, E.L., Peck, V.L., Prahl, F.G., Rossi, S., Rueda, G., Sanson-Barrera, A., Rosell-Melé, A., 2012. Co-variation of crenarchaeol and branched GDGTs in globally-distributed marine and freshwater sedimentary archives. *Global and Planetary Change* 92–93, 275–285. doi:10.1016/j.gloplacha.2012.05.020
- Fischer, G., Ratmeyer, V., Wefer, G., 2000. Organic carbon fluxes in the Atlantic and the Southern Ocean: relationship to primary production compiled from satellite radiometer data. *Deep Sea Research Part II: Topical Studies in Oceanography* 47, 1961–1997. doi:10.1016/S0967-0645(00)00013-8
- Fowler, A.J., Gillespie, R., Hedges, R.E.M., 1986. Radiocarbon dating of sediments. *Radiocarbon*.
- Francis, C.A., Roberts, K.J., Beman, J.M., Santoro, A.E., Oakley, B.B., 2005. Ubiquity and diversity of ammonia-oxidizing archaea in water columns and sediments of the ocean. *Proc Natl Acad Sci U S A* 102, 14683–14688. doi:10.1073/pnas.0506625102
- Fry, B., 1988. Food web structure on Georges Bank from stable C, N, and S isotopic compositions. *Limnol Oceanogr* 33, 1182–1190. doi:10.4319/lo.1988.33.5.1182
- Fry, B., Sherr, E.B., 1989. $\delta^{13}\text{C}$ Measurements as Indicators of Carbon Flow in Marine and Freshwater Ecosystems, in: *Stable Isotopes in Ecological Research, Ecological Studies*. Springer New York, New York, NY, pp. 196–229. doi:10.1007/978-1-4612-3498-2_12
- Gagosian, R.B., Smith, S.O., Lee, C., Farrington, J.W., Frew, N.M., 1980. Steroid transformations in Recent marine sediments. *Physics and Chemistry of the Earth* 12, 407–419.

- Gerino, M., Aller, R.C., Lee, C., Cochran, J.K., Aller, J.Y., Green, M.A., Hirschberg, D., 1998. Comparison of Different Tracers and Methods Used to Quantify Bioturbation During a Spring Bloom: ²³⁴Thorium, Luminophores and Chlorophylla. *Estuar Coast Shelf Sci* 46, 531–547. doi:10.1006/ecss.1997.0298
- Gibson, J.A.E., Trull, T., Nichols, P.D., Summons, R.E., McMinn, A., 1999. Sedimentation of ¹³C-rich organic matter from Antarctic sea-ice algae: A potential indicator of past sea-ice extent. *Geology* 27, 331–334.
- Gilbert, R., Domack, E.W., 2003. Sedimentary record of disintegrating ice shelves in a warming climate, Antarctic Peninsula. *Geochemistry, Geophysics, Geosystems* 4, n/a–n/a. doi:10.1029/2002gc000441
- Gillan, D.C., Danis, B., 2007. The archaeobacterial communities in Antarctic bathypelagic sediments. *Deep Sea Research Part II: Topical Studies in Oceanography* 54, 1682–1690. doi:10.1016/j.dsr2.2007.07.002
- Giovannoni, S.J., Britschgi, T.B., Moyer, C.L., Field, K.G., 1990. Genetic diversity in Sargasso Sea bacterioplankton. *Nature* 345, 60–63. doi:10.1038/345060a0
- Goldberg, E.D., Koide, M., 1962. Geochronological studies of deep sea sediments by the ionium/thorium method. *Geochim Cosmochim Acta* 26, 417–450. doi:10.1016/0016-7037(62)90112-6
- Grebmeier, J.M., Barry, J.P., 2007. Benthic Processes in Polynyas, in: *Polynyas: Windows to the World*, Elsevier Oceanography Series. Elsevier, pp. 363–390. doi:10.1016/S0422-9894(06)74011-9
- Grossi, V., Caradec, S., Gilbert, F., 2003. Burial and reactivity of sedimentary microalgal lipids in bioturbated Mediterranean coastal sediments. *Mar Chem.*
- Gu, Z., Eils, R., Schlesner, M., 2016. Complex heatmaps reveal patterns and correlations in multidimensional genomic data. *Bioinformatics* 32, 2847–2849. doi:10.1093/bioinformatics/btw313
- Guinasso, N.L., Schink, D.R., 1975. Quantitative estimates of biological mixing rates in abyssal sediments. *Journal of Geophysical Research* 80, 3032–3043. doi:10.1029/JC080i021p03032
- Guo, L., Semiletov, I.P., Gustafsson, O., Ingri, J., Andersson, P., Dudarev, O.V., White, D., 2004. Characterization of Siberian Arctic coastal sediments: Implications for terrestrial organic carbon export. *Global Biogeochem Cycles* 18, n/a–n/a. doi:10.1029/2003GB002087
- Gurr, M.I., Harwood, J.L., Frayn, K.N., 2002. Fatty acid structure and metabolism, in: *Lipid Biochemistry*. Blackwell Publishers Ltd, pp. 1–47.
- Gutt, J., Barratt, I., Domack, E.W., d’Udekem d’Acoz, C., Dimmler, W., Grémare, A., Heilmayer, O., Isla, E., Janussen, D., Jorgensen, E., Kock, K.-H., Sophia Lehnert, L., López-González, P., Langner, S., Linse, K., Eugenia Manjón-Cabeza, M., Meißner, M., Montiel, A., Raes, M., Robert, H., Rose, A., Sañé, E.S., Saucède, T., Scheidat, M., Schenke, H.-W., Seiler, J., Smith, C.R., 2011. Biodiversity change after climate-

- induced ice-shelf collapse in the Antarctic. *Deep Sea Research Part II: Topical Studies in Oceanography* 58, 74–83. doi:10.1016/j.dsr2.2010.05.024
- Gutt, J., Cape, M.R., Dimmler, W., Fillinger, L., Isla, E., Lieb, V., Lundalv, T., Pulcher, C., 2013. Shifts in Antarctic megabenthic structure after ice-shelf disintegration in the Larsen area east of the Antarctic Peninsula. *Polar Biology* 36, 895–906. doi:10.1007/s00300-013-1315-7
- Guyoneaud, R., Matheron, R., Liesack, W., Imhoff, J.F., Caumette, P., 1997. *Thiorhodococcus minus*, gen. nov., sp. nov., a new purple sulfur bacterium isolated from coastal lagoon sediments. *Archives of Microbiology* 168, 16–23. doi:10.1007/s002030050464
- Haddad, R.I., Martens, C.S., Farrington, J.W., 1992. Quantifying early diagenesis of fatty acids in a rapidly accumulating coastal marine sediment. *Org Geochem* 19, 205–216. doi:10.1016/0146-6380(92)90037-X
- Hamdan, L.J., Coffin, R.B., Sikaroodi, M., Greinert, J., Treude, T., Gillevet, P.M., 2013. Ocean currents shape the microbiome of Arctic marine sediments. *ISME J* 7, 685–696. doi:10.1038/ismej.2012.143
- Hamdan, L.J., Gillevet, P.M., Sikaroodi, M., Pohlman, J.W., Plummer, R.E., Coffin, R.B., 2008. Geomicrobial characterization of gas hydrate-bearing sediments along the mid-Chilean margin. *FEMS Microbiology Ecology* 65, 15–30. doi:10.1111/j.1574-6941.2008.00507.x
- Hargrave, B.T., Bodungen, von, B., Stoffyn-Egli, P., Mudie, P.J., 1994. Seasonal variability in particle sedimentation under permanent ice cover in the Arctic Ocean. *Continental Shelf Research* 14, 279–293. doi:10.1016/0278-4343(94)90017-5
- Hayes, J.M., 2001. Fractionation of the Isotopes of Carbon and Hydrogen in Biosynthetic Processes 1–31.
- Hayes, J.M., 1993. Factors controlling ¹³C contents of sedimentary organic compounds: Principles and evidence. *Marine Geology* 113, 111–125. doi:10.1016/0025-3227(93)90153-M
- Hayes, J.M., Popp, B.N., Takigiku, R., Johnson, M.W., 1989. An isotopic study of biogeochemical relationships between carbonates and organic carbon in the Greenhorn Formation. *Geochim Cosmochim Acta* 53, 2961–2972.
- Hedges, J.I., 1995. Sedimentary Organic-Matter Preservation - an Assessment and Speculative Synthesis. *Mar Chem* 49, 81–115. doi:10.1016/0304-4203(95)00008-f
- Hedges, J.I., Clark, W.A., Cowie, G.L., 1988. Fluxes and Reactivities of Organic-Matter in a Coastal Marine Bay. *Limnol Oceanogr* 33, 1137–1152.
- Hinrichs, K.-U., Schneider, R.R., Müller, P.J., Rullkoetter, J., 1999. A biomarker perspective on paleoproductivity variations in two Late Quaternary sediment sections from the Southeast Atlantic Ocean. *Org Geochem* 30, 341–366. doi:10.1016/S0146-6380(99)00007-8
- Hinrichs, K.-U., Summons, R.E., Orphan, V.J., Sylva, S.P., Hayes, J.M., 2000. Molecular

- and isotopic analysis of anaerobic methane-oxidizing communities in marine sediments. *Org Geochem* 31, 1685–1701. doi:10.1016/S0146-6380(00)00106-6
- Hoegh-Guldberg, O., Bruno, J.F., 2010. The Impact of Climate Change on the World's Marine Ecosystems. *Science* 328, 1523–1528. doi:10.1126/science.1189930
- Hopmans, E.C., Weijers, J.W.H., Schefuß, E., Herfort, L., Sinninghe Damsté, J.S., Schouten, S., 2004. A novel proxy for terrestrial organic matter in sediments based on branched and isoprenoid tetraether lipids. *Earth and Planetary Science Letters* 224, 107–116. doi:10.1016/j.epsl.2004.05.012
- Horner-Devine, M.C., Leibold, M.A., Smith, V.H., Bohannon, B.J.M., 2003. Bacterial diversity patterns along a gradient of primary productivity. *Ecol Lett* 6, 613–622. doi:10.1046/j.1461-0248.2003.00472.x
- Huang, W.-Y., Meinschein, W.G., 1979. Sterols as ecological indicators. *Geochim Cosmochim Acta* 43, 739–745. doi:10.1016/0016-7037(79)90257-6
- Huguet, Huguet, C., Hopmans, E.C., Febo-Ayala, W., Thompson, D.H., Sinninghe Damsté, J.S., Schouten, S., 2006. An improved method to determine the absolute abundance of glycerol dibiphytanyl glycerol tetraether lipids. *Org Geochem* 37, 6–6. doi:10.1016/j.orggeochem.2006.05.008
- Imhoff, J.F., 2005. Chromatiales ord. nov., in: *Bergey's Manual® of Systematic Bacteriology*. Springer US, pp. 1–59. doi:10.1007/0-387-28022-7_1
- Ishman, S.E., Szymcek, P., 2003. Foraminiferal distributions in the former Larsen-A ice shelf and Prince Gustav Channel region, eastern Antarctic Peninsula margin: A baseline for Holocene paleoenvironmental change. *Antarctic Research Series* 79, 239–260. doi:doi:10.1029/AR079p0239
- Jiang, C.Q., Alexander, R., Kagi, R.I., Murray, A.P., 2000. Origin of perylene in ancient sediments and its geological significance. *Org Geochem* 31, 1545–1559.
- Johns, L., Wraige, E.J., Belt, S.T., Lewis, C.A., Massé, G.G., Robert, J.-M., Rowland, S.J., 1999. Identification of a C-25 highly branched isoprenoid (HBI) diene in Antarctic sediments, Antarctic sea-ice diatoms and cultured diatoms. *Org Geochem* 30, 1471–1475.
- Jorgensen, S.L., Hannisdal, B., Lanzen, A., Baumberger, T., Flesland, K., Fonseca, R., Øvreås, L., Steen, I.H., Thorseth, I.H., Pedersen, R.B., Schleper, C., 2012. Correlating microbial community profiles with geochemical data in highly stratified sediments from the Arctic Mid-Ocean Ridge. *proc Natl Acad Sci U S A* 109, E2846–E2855. doi:10.1073/pnas.1207574109
- Jung, M.-Y., Park, S.-J., Kim, S.-J., Kim, J.-G., Sinninghe Damsté, J.S., Jeon, C.O., Rhee, S.-K., 2014. A Mesophilic, Autotrophic, Ammonia-Oxidizing Archaeon of Thaumarchaeal Group I.1a Cultivated from a Deep Oligotrophic Soil Horizon. *Applied and Environmental Microbiology* 80, 3645–3655. doi:10.1128/AEM.03730-13
- Juni, E., 1978. Genetics and physiology of *Acinetobacter*. *Annu. Rev. Microbiol.*
- Kamp, A., de Beer, D., Nitsch, J.L., Lavik, G., Stief, P., 2011. Diatoms respire nitrate to

- survive dark and anoxic conditions. *proc Natl Acad Sci U S A* 108, 5649–5654.
doi:10.1073/pnas.1015744108
- Kanazawa, A., 2001. Sterols in marine invertebrates. *Fisheries Science*.
- Kaneda, T., 1991. Iso- and anteiso-fatty acids in bacteria: biosynthesis, function, and taxonomic significance. *Microbiology and Molecular Biology Reviews* 55, 288–302.
- Kasai, Y., Kishira, H., Harayama, S., 2002. Bacteria Belonging to the Genus *Cycloclasticus* Play a Primary Role in the Degradation of Aromatic Hydrocarbons Released in a Marine Environment. *Applied and Environmental Microbiology* 68, 5625–5633. doi:10.1128/AEM.68.11.5625-5633.2002
- Kattner, G., Hagen, W., 1995. Polar herbivorous copepods – different pathways in lipid biosynthesis. *ICES Journal of Marine Science:*
- Kattner, G., Hirche, H.J., Krause, M., 1989. Spatial Variability in Lipid-Composition of Calanoid Copepods From Fram Strait, the Arctic. *Mar Biol* 102, 473–480.
- Kellogg, T.B., Kellogg, D.E., 1988. Antarctic cryogenic sediments: Biotic and inorganic facies of ice shelf and marine-based ice sheet environments. *Palaeogeography, Palaeoclimatology, Palaeoecology* 67, 51–74. doi:10.1016/0031-0182(88)90122-8
- Kelly, J.R., Scheibling, R.E., 2012. Fatty acids as dietary tracers in benthic food webs. *Mar Ecol Prog Ser* 446, 1–22.
- Klindworth, A., Pruesse, E., Schweer, T., Peplies, J., Quast, C., Horn, M., Glöckner, F.O., 2013. Evaluation of general 16S ribosomal RNA gene PCR primers for classical and next-generation sequencing-based diversity studies. *Nucleic Acids Res.* 41, e1. doi:10.1093/nar/gks808
- Knittel, K., Kuever, J., Meyerdierks, A., Meinke, R., Amann, R., Brinkhoff, T., 2005a. *Thiomicrospira arctica* sp. nov. and *Thiomicrospira psychrophila* sp. nov., psychrophilic, obligately chemolithoautotrophic, sulfur-oxidizing bacteria isolated from marine Arctic sediments. *INTERNATIONAL JOURNAL OF SYSTEMATIC AND EVOLUTIONARY MICROBIOLOGY* 55, 781–786. doi:10.1099/ijs.0.63362-0
- Knittel, K., Lösekann, T., Boetius, A., Kort, R., Amann, R., 2005b. Diversity and Distribution of Methanotrophic Archaea at Cold Seeps.
- Koga, Y., Nishihara, M., Morii, H., Akagawamatsushita, M., 1993. Ether Polar Lipids of Methanogenic Bacteria - Structures, Comparative Aspects, and Biosynthesis. *Microbiological Reviews* 57, 164–182.
- Kohlhase, M., Pohl, P., 1988. Saturated and unsaturated sterols of nitrogen-fixing blue-green algae (cyanobacteria). *Phytochemistry* 27, 1735–1740. doi:10.1016/0031-9422(88)80434-5
- Konn, C., Charlou, J.L., Donval, J.P., Holm, N.G., Dehairs, F., Bouillon, S., 2009. Hydrocarbons and oxidized organic compounds in hydrothermal fluids from Rainbow and Lost City ultramafic-hosted vents. *Chem Geol* 258, 299–314. doi:10.1016/j.chemgeo.2008.10.034
- Kostka, J.E., Prakash, O., Overholt, W.A., Green, S.J., Freyer, G., Canion, A., Delgado,

- J., Norton, N., Hazen, T.C., Huettel, M., 2011. Hydrocarbon-Degrading Bacteria and the Bacterial Community Response in Gulf of Mexico Beach Sands Impacted by the Deepwater Horizon Oil Spill. *Applied and Environmental Microbiology* 77, 7962–7974. doi:10.1128/AEM.05402-11
- Köenneke, M., Bernhard, A.E., la Torre, de, J.R., Walker, C.B., Waterbury, J.B., Stahl, D.A., 2005. Isolation of an autotrophic ammonia-oxidizing marine archaeon. *Nature* 437, 543–546. doi:10.1038/nature03911
- Kruskal, J.B., 1964. Nonmetric multidimensional scaling: A numerical method. *Psychometrika* 29, 115–129. doi:10.1007/BF02289694
- Kuever, J., 2014. The Family Syntrophobacteraceae, in: *The Prokaryotes*. Springer Berlin Heidelberg, pp. 289–299. doi:10.1007/978-3-642-39044-9_268
- Kvenvolden, K.A., Rapp, J.B., Golan-Bac, M., Hostettler, F.D., 1987. Multiple sources of alkanes in Quaternary oceanic sediment of Antarctica. *Org Geochem* 11, 291–302. doi:10.1016/0146-6380(87)90040-4
- Lai, Q., Yuan, J., Gu, L., Shao, Z., 2009. *Marispirillum indicum* gen. nov., sp. nov., isolated from a deep-sea environment. *INTERNATIONAL JOURNAL OF SYSTEMATIC AND EVOLUTIONARY MICROBIOLOGY* 59, 1278–1281. doi:10.1099/ijs.0.003889-0
- Lamb, A.L., Wilson, G.P., Leng, M.J., 2006. A review of coastal palaeoclimate and relative sea-level reconstructions using $\delta^{13}\text{C}$ and C/N ratios in organic material. *Earth-Science Reviews* 75, 29–57. doi:10.1016/j.earscirev.2005.10.003
- Langille, M.G.I., Zaneveld, J., Caporaso, J.G., McDonald, D., Knights, D., Reyes, J.A., Clemente, J.C., Burkepille, D.E., Thurber, R.L.V., Knight, R., Beiko, R.G., Huttenhower, C., 2013. Predictive functional profiling of microbial communities using 16S rRNA marker gene sequences. *Nature Biotechnology* 31, 814–821. doi:10.1038/nbt.2676
- Lee, C., Cronin, C., 1984. Particulate amino acids in the sea: Effects of primary productivity and biological decomposition. *J Mar Res* 42, 1075–1097. doi:10.1357/002224084788520710
- Lee, R.F., 1975. Lipids of Arctic Zooplankton. *Comp. Biochem. Physiol., B* 51, 263–266.
- Legeleux, F., Reyss, J.-L., Schmidt, S., 1994. Particle mixing rates in sediments of the northeast tropical Atlantic: Evidence from ^{210}Pb xs, ^{137}Cs , ^{228}Th xs and ^{234}Th xs downcore distributions. *Earth and Planetary Science Letters* 128, 545–562. doi:10.1016/0012-821X(94)90169-4
- Legendre, P., Gallagher, E.D., 2001. Ecologically meaningful transformations for ordination of species data - Springer. *Oecologia*.
- Levin, L.A., Gage, J.D., 1998. Relationships between oxygen, organic matter and the diversity of bathyal macrofauna. *Deep Sea Research Part II: Topical Studies in Oceanography* 45, 129–163. doi:10.1016/S0967-0645(97)00085-4
- Li, Z., Cassar, N., 2016. Satellite estimates of net community production based on O_2/Ar

- observations and comparison to other estimates. *Global Biogeochem Cycles* 30, 735–752. doi:10.1002/2015GB005314
- Lincoln, S.A., Wai, B., Eppley, J.M., Church, M.J., Summons, R.E., DeLong, E.F., 2014. Planktonic Euryarchaeota are a significant source of archaeal tetraether lipids in the ocean. *proc Natl Acad Sci U S A* 111, 9858–9863. doi:10.1073/pnas.1409439111
- Lipps, J.H., Ronan, T.E., DeLaca, T.E., 1979. Life below the ross ice shelf, antarctica. *Science* 203, 447–449. doi:10.1126/science.203.4379.447
- Liu, X.-L., Lipp, J.S., Hinrichs, K.-U., 2011. Distribution of intact and core GDGTs in marine sediments. *Org Geochem* 42, 368–375. doi:10.1016/j.orggeochem.2011.02.003
- Liu, X.-L., Lipp, J.S., Simpson, J.H., Lin, Y.-S., Summons, R.E., Hinrichs, K.-U., 2012. Mono- and dihydroxyl glycerol dibiphytanyl glycerol tetraethers in marine sediments: Identification of both core and intact polar lipid forms. *Geochim Cosmochim Acta* 89, 102–115. doi:10.1016/j.gca.2012.04.053
- Liu, X.-L., Zhu, C., Wakeham, S.G., Hinrichs, K.-U., 2014. In situ production of branched glycerol dialkyl glycerol tetraethers in anoxic marine water columns. *Mar Chem* 166, 1–8. doi:10.1016/j.marchem.2014.08.008
- Lizotte, M.P., 2001. The Contributions of Sea Ice Algae to Antarctic Marine Primary Production. *Integrative and Comparative Biology* 41, 57–73. doi:10.1093/icb/41.1.57
- Lomstein, E., Jensen, M.H., Sørensen, J., 1990. Intracellular NH₄ and NO₃ pools associated with deposited phytoplankton in a marine sediment (Aarhus Bight, Denmark). *Mar Ecol Prog Ser*.
- Londry, K.L., Jahnke, L.L., Marais, Des, D.J., 2004. Stable carbon isotope ratios of lipid biomarkers of sulfate-reducing bacteria. *Applied and Environmental Microbiology* 70, 745–751. doi:10.1128/AEM.70.2.745-751.2004
- Lorenz, M.G., Wackernagel, W., 1994. Bacterial gene-transfer by natural genetic-transformation in the environment. *Microbiological Reviews* 58, 563–602.
- Louchouart, P., Lucotte, M., Canuel, R., Gagné, J.-P., Richard, L.-F., 1997. Sources and early diagenesis of lignin and bulk organic matter in the sediments of the Lower St. Lawrence Estuary and the Saguenay Fjord. *Mar Chem* 58, 3–26. doi:10.1016/S0304-4203(97)00022-4
- Löder, M.G.J., Meunier, C., Wiltshire, K.H., Boersma, M., Aberle, N., 2011. The role of ciliates, heterotrophic dinoflagellates and copepods in structuring spring plankton communities at Helgoland Roads, North Sea. *Mar Biol* 158, 1551–1580. doi:10.1007/s00227-011-1670-2
- Lu, Z.L., Rickaby, R.E.M., Kennedy, H., Kennedy, P., Pancost, R.D., Shaw, S., Lennie, A., Wellner, J.S., Anderson, J.B., 2012. An ikaite record of late Holocene climate at the Antarctic Peninsula. *Earth and Planetary Science Letters* 325, 108–115. doi:10.1016/j.epsl.2012.01.036
- Lücker, S., Daims, H., 2014. The Family Nitrospinaceae, in: *The Prokaryotes*. Springer Berlin Heidelberg, pp. 231–237. doi:10.1007/978-3-642-39044-9_402

- Mackie, P.R., Platt, H.M., Hardy, R., 1978. Hydrocarbons in the marine environment: II. Distribution of n-alkanes in the fauna and environment of the sub-antarctic island of South Georgia. *Estuarine and Coastal Marine Science* 6, 301–313. doi:10.1016/0302-3524(78)90018-X
- Magen, C., Chaillou, G., Crowe, S.A., Mucci, A., Sundby, B., Gao, A., Makabe, R., Sasaki, H., 2010. Origin and fate of particulate organic matter in the southern Beaufort Sea – Amundsen Gulf region, Canadian Arctic. *Estuar Coast Shelf Sci* 86, 31–41. doi:10.1016/j.ecss.2009.09.009
- Mansour, M.P., Volkman, J.K., Holdsworth, D.G., Jackson, A.E., Blackburn, S.I., 1999a. Very-long-chain (C28) highly unsaturated fatty acids in marine dinoflagellates. *Phytochemistry* 50, 541–548. doi:10.1016/S0031-9422(98)00564-0
- Mansour, M.P., Volkman, J.K., Jackson, A.E., Blackburn, S.I., 1999b. The fatty acid and sterol composition of five marine dinoflagellates. *Journal of Phycology* 35, 710–720. doi:10.1046/j.1529-8817.1999.3540710.x
- Martin, J.H., Knauer, G.A., Karl, D.M., Broenkow, W.W., 1987. VERTEX: carbon cycling in the northeast Pacific. *Deep Sea Research* 34, 267–285. doi:10.1016/0198-0149(87)90086-0
- Martinez-Garcia, M., Brazel, D.M., Swan, B.K., Arnosti, C., Chain, P.S.G., Reitenga, K.G., Xie, G., Poulton, N.J., Gomez, M.L., Masland, D.E.D., Thompson, B., Bellows, W.K., Ziervogel, K., Lo, C.-C., Ahmed, S., Gleasner, C.D., Detter, C.J., Stepanauskas, R., 2012. Capturing Single Cell Genomes of Active Polysaccharide Degraders: An Unexpected Contribution of Verrucomicrobia. *PLoS One* 7, e35314. doi:10.1371/journal.pone.0035314
- Martiny, A.C., Pham, C.T.A., Primeau, F.W., Vrugt, J.A., Moore, J.K., Levin, S.A., Lomas, M.W., 2013. Strong latitudinal patterns in the elemental ratios of marine plankton and organic matter. *Nature Publishing Group* 6, 279–283. doi:10.1038/ngeo1757
- Massé, G.G., Belt, S.T., Crosta, X., Schmidt, S., Snape, I., Thomas, D.N., Rowland, S.J., 2011. Highly branched isoprenoids as proxies for variable sea ice conditions in the Southern Ocean. *Antarctic Science* 23, 487–498. doi:10.1017/s0954102011000381
- Matsumoto, G., Torii, T., Hanya, T., 1982. High abundance of algal 24-ethylcholesterol in Antarctic lake sediment. *Nature* 299, 52–54. doi:10.1038/299052a0
- McCaffrey, M.A., Farrington, J.W., Repeta, D.J., 1989. Geochemical Implications of the Lipid-Composition of *Thioploca* Spp From the Peru Upwelling Region 15-Degrees-S. *Org Geochem* 14, 61–68.
- McCarren, J., Becker, J.W., Repeta, D.J., Shi, Y., Young, C.R., Malmstrom, R.R., Chisholm, S.W., DeLong, E.F., 2010. Microbial community transcriptomes reveal microbes and metabolic pathways associated with dissolved organic matter turnover in the sea. *proc Natl Acad Sci U S A* 107, 16420–16427. doi:10.1073/pnas.1010732107
- McClintic, M.A., DeMaster, D.J., Thomas, C.J., 2008. Testing the FOODBANCS hypothesis: Seasonal variations in near-bottom particle flux, bioturbation intensity,

- and deposit feeding based on ^{234}Th measurements. *Deep Sea Research Part II: Topical Studies in Oceanography*.
- Meador, T.B., Zhu, C., Elling, F.J., Könenneke, M., Hinrichs, K.-U., 2014. Identification of isoprenoid glycosidic glycerol dibiphytanol diethers and indications for their biosynthetic origin. *Org Geochem* 69, 70–75. doi:10.1016/j.orggeochem.2014.02.005
- Meyers, P.A., 1994. Preservation of elemental and isotopic source identification of sedimentary organic matter. *Chem Geol* 114, 289–302. doi:10.1016/0009-2541(94)90059-0
- Meyers, P.A., Eadie, B.J., 1993. Sources, degradation and recycling of organic matter associated with sinking particles in Lake Michigan. *Org Geochem* 20, 47–56. doi:10.1016/0146-6380(93)90080-U
- Middelburg, J.J., 1989. A Simple rate model for organic-matter decomposition in marine-sediments. *Geochim Cosmochim Acta* 53, 1577–1581. doi:10.1016/0016-7037(89)90239-1
- Mincks, S.L., Mincks, S.L., Smith, C.R., DeMaster, D.J., 2005. Persistence of labile organic matter and microbial biomass in Antarctic shelf sediments: Evidence of a sediment food bank. *Mar Ecol Prog Ser*.
- Mincks, S.L., Smith, C.R., Jeffreys, R.M., Sumida, P.Y.G., 2008. Trophic structure on the West Antarctic Peninsula shelf: Detritivory and benthic inertia revealed by $\delta^{13}\text{C}$ and $\delta^{15}\text{N}$ analysis. *Deep Sea Research Part II: Topical Studies in Oceanography* 55, 2502–2514. doi:10.1016/j.dsr2.2008.06.009
- Moodley, L., Middelburg, J.J., Boschker, H., 2002. Bacteria and Foraminifera: key players in a short-term deep-sea benthic response to phytodetritus. *Mar Ecol Prog Ser*.
- Mulvaney, R., Abram, N.J., Hindmarsh, R.C.A., Arrowsmith, C., Fleet, L., Triest, J., Sime, L.C., Alemany, O., Foord, S., 2012. Recent Antarctic Peninsula warming relative to Holocene climate and ice-shelf history. *Nature* 489, 141–144. doi:10.1038/nature11391
- Müller, P.J., Suess, E., 1979. Productivity, sedimentation rate, and sedimentary organic matter in the oceans—I. Organic carbon preservation. *Deep Sea Research* 26, 1347–1362. doi:10.1016/0198-0149(79)90003-7
- Nash, J.C., 2016. Package “nlmrt” 1–31.
- National Snow and Ice Data Center, 2010. SOTC: Ice Shelves [WWW Document]. nsidc.org. URL <http://nsidc.org/cryosphere/sotc/iceshelves.html> (accessed 4.11.14).
- Nguyen, T.T., Landfald, B., 2015. Polar front associated variation in prokaryotic community structure in Arctic shelf seafloor. *Front Microbiol* 6, 17. doi:10.3389/fmicb.2015.00017
- Nichols, D.S., Nichols, P.D., Sullivan, C.W., 1993. Fatty acid, sterol and hydrocarbon composition of Antarctic sea ice diatom communities during the spring bloom in McMurdo Sound. *Antarctic Science*.
- Nichols, P.D., Palmisano, A.C., Rayner, M.S., Smith, G.A., White, D.C., 1989. Changes in the lipid composition of Antarctic sea-ice diatom communities during a spring

- bloom: an indication of community physiological status. *Antarctic Science* 1, 133–140. doi:10.1017/S0954102089000209
- Nichols, P.D., Palmisano, A.C., Smith, G.A., White, D.C., 1986. Lipids of the antarctic sea ice diatom *Nitzschia cylindrus*. *Phytochemistry*.
- Nichols, P.D., Palmisano, A.C., Volkman, J.K., Smith, G.A., White, D.C., 1988. Occurrence of an isoprenoid C₂₅ diunsaturated alkene and high neutral lipid content in antarctic sea-ice diatom communities. *Journal of Phycology* 24, 90–96. doi:10.1111/j.1529-8817.1988.tb04459.x
- Nishimura, M., 1982. 5 β -isomers of stanols and stanones as potential markers of sedimentary organic quality and depositional paleoenvironments. *Geochim Cosmochim Acta* 46, 423–432. doi:10.1016/0016-7037(82)90233-2
- Nunoura, T., Takaki, Y., Kazama, H., Hirai, M., Ashi, J., Imachi, H., Takai, K., 2012. Microbial Diversity in Deep-sea Methane Seep Sediments Presented by SSU rRNA Gene Tag Sequencing. *Microbes and Environments* 27, 382–390. doi:10.1264/jsme2.ME12032
- Oksanen, J., 2015. Multivariate Analysis of Ecological Communities in R: vegan tutorial [WWW Document]. URL (accessed 1.5.16).
- Oksanen, J., Kindt, R., Legendre, P., 2008. The vegan package, ... ecology package.
- Orcutt, D.M., Parker, B.C., Lusby, W.R., 1986. Lipids in blue-green algal mats (modern stromatolites) from Antarctic oasis lakes. *Journal of Phycology* 22, 523–530. doi:10.1111/j.1529-8817.1986.tb02496.x
- Orsi, W.D., Edgcomb, V.P., Christman, G.D., Biddle, J.F., 2013. Gene expression in the deep biosphere. *Nature* 499, 205–208. doi:10.1038/nature12230
- Ourisson, G., Rohmer, M., 1992. Hopanoids. 2. Biohopanoids: a novel class of bacterial lipids. *Acc. Chem. Res.* 25, 403–408. doi:10.1021/ar00021a004
- Ozisik, M.N., 1993. *Heat Conduction*. John Wiley & Sons.
- Pachauri, R.K., 2008. Climate change 2007. Synthesis report. Contribution of Working Groups I, II and III to the fourth assessment report. Intergovernmental Panel on Climate Change, Geneva (Switzerland).
- Pancost, R.D., Sinninghe Damsté, J.S., 2003. Carbon isotopic compositions of prokaryotic lipids as tracers of carbon cycling in diverse settings. *Chem Geol* 195, 29–58. doi:10.1016/S0009-2541(02)00387-X
- Parada, A.E., Needham, D.M., Fuhrman, J.A., 2016. Every base matters: assessing small subunit rRNA primers for marine microbiomes with mock communities, time series and global field samples. *Environmental Microbiology* 18, 1403–1414. doi:10.1111/1462-2920.13023
- Parkes, R.J., Taylor, J., 1983. The relationship between fatty acid distributions and bacterial respiratory types in contemporary marine sediments. *Estuarine*.
- Parrish, C.C., Thompson, R.J., Deibel, D., 2005. Lipid classes and fatty acids in plankton and settling matter during the spring bloom in a cold ocean coastal environment.

- Mar Ecol Prog Ser 286, 57–68.
- Pearson, A., Ingalls, A.E., 2013. Assessing the Use of Archaeal Lipids as Marine Environmental Proxies. *Annu. Rev. Earth Planet. Sci.* 41, 359–384.
doi:10.1146/annurev-earth-050212-123947
- Peck, L.S., Barnes, D.K.A., Cook, A.J., Fleming, A.H., Clarke, A., 2010. Negative feedback in the cold: ice retreat produces new carbon sinks in Antarctica. *Glob Chang Biol* 16, 2614–2623. doi:10.1111/j.1365-2486.2009.02071.x
- Peterse, F., Kim, J.-H., Schouten, S., Kristensen, D.K., Koç, N., Sinninghe Damsté, J.S., 2009. Constraints on the application of the MBT/CBT palaeothermometer at high latitude environments (Svalbard, Norway). *Org Geochem* 40, 692–699.
doi:10.1016/j.orggeochem.2009.03.004
- Platt, H.M., Mackie, P.R., 1980. Distribution and fate of aliphatic and aromatic hydrocarbons in Antarctic fauna and environment. *Helgoländer Meeresuntersuchungen* 33, 236–245. doi:10.1007/BF02414749
- Polónia, A.R.M., Cleary, D.F.R., Freitas, R., Voogd, N.J., Gomes, N.C.M., 2015. The putative functional ecology and distribution of archaeal communities in sponges, sediment and seawater in a coral reef environment. *Molecular Ecology* 24, 409–423.
doi:10.1111/mec.13024
- Polymenakou, P.N., Bertilsson, S., Tselepides, A., Stephanou, E.G., 2005. Bacterial community composition in different sediments from the Eastern Mediterranean Sea: a comparison of four 16S ribosomal DNA clone libraries. *Microb Ecol* 50, 447–462.
doi:10.1007/s00248-005-0005-6
- Popp, B.N., Trull, T., Kenig, F., Wakeham, S.G., Rust, T.M., Tilbrook, B.D., Griffiths, B., Wright, S.W., Marchant, H.J., Bidigare, R.R., 1999. Controls on the carbon isotopic composition of Southern Ocean phytoplankton. *Global Biogeochem Cycles* 13, 827–843.
- Post, A.L., Galton-Fenzi, B.K., Riddle, M.J., Herraiz-Borreguero, L., O'Brien, P.E., Hemer, M.A., McMin, A., Rasch, D., Craven, M., 2014. Modern sedimentation, circulation and life beneath the Amery Ice Shelf, East Antarctica. *Continental Shelf Research* 74, 77–87. doi:10.1016/j.csr.2013.10.010
- Post, A.L., Hemer, M.A., O'Brien, P.E., Roberts, D., Craven, M., 2007. History of benthic colonisation beneath the Amery Ice Shelf, East Antarctica. *Mar Ecol Prog Ser* 344, 29–37. doi:10.3354/meps06966
- Preston, C.M., Wu, K.Y., Molinski, T.F., DeLong, E.F., 1996. A psychrophilic crenarchaeon inhabits a marine sponge: *Cenarchaeum symbiosum* gen. nov., sp. nov. *proc Natl Acad Sci U S A* 93, 6241–6246.
- Pudsey, C.J., Evans, J., 2001. First survey of Antarctic sub-ice shelf sediments reveals mid-Holocene ice shelf retreat. *Geology*.
- Rani, S., Koh, H.-W., Rhee, S.-K., Fujitani, H., Park, S.-J., 2017. Detection and Diversity of the Nitrite Oxidoreductase Alpha Subunit (nxrA) Gene of Nitrospina in Marine

- Sediments. *Microb Ecol* 73, 111–122. doi:10.1007/s00248-016-0897-3
- Rappé, M.S., Connon, S.A., Vergin, K.L., Giovannoni, S.J., 2002. Cultivation of the ubiquitous SAR11 marine bacterioplankton clade. *Nature* 418, 630–633. doi:10.1038/nature00917
- Rau, G.H., Sullivan, C.W., Gordon, L.I., 1991. $\delta^{13}\text{C}$ and $\delta^{15}\text{N}$ variations in Weddell Sea particulate organic matter. *Mar Chem* 35, 355–369. doi:10.1016/S0304-4203(09)90028-7
- Rau, G.H., Takahashi, T., Desmarais, D.J., Repeta, D.J., Martin, J.H., 1992. The relationship between of $\delta^{13}\text{C}$ organic matter and $[\text{CO}_2(\text{aq})]$ in ocean surface water. *Geochim Cosmochim Acta* 56, 1413–1419.
- Ribeiro, M.C.H., 2015. Comunidade bêntica da área da plataforma de gelo Larsen A (Antártica) 17 anos após sua desintegração, com ênfase na meiofauna . UNIVERSIDADE DE SÃO PAULO.
- Riddle, M.J., Craven, M., Goldsworthy, P.M., Carsey, F., 2007. A diverse benthic assemblage 100 km from open water under the Amery Ice Shelf, Antarctica. *Paleoceanography* 22, n/a–n/a. doi:10.1029/2006PA001327
- Rinta-Kanto, J.M., Sun, S., Sharma, S., Kiene, R.P., Moran, M.A., 2012. Bacterial community transcription patterns during a marine phytoplankton bloom. *Environmental Microbiology* 14, 228–239. doi:10.1111/j.1462-2920.2011.02602.x
- Robertson, C.E., Spear, J.R., Harris, J.K., Pace, N.R., 2009. Diversity and stratification of archaea in a hypersaline microbial mat. *Applied and Environmental Microbiology* 75, 1801–1810. doi:10.1128/AEM.01811-08
- Rott, H., Rott, H., Skvarca, P., Nagler, T., 1996. Rapid collapse of northern Larsen Ice Shelf, Antarctica. *Science* 271, 788–792. doi:10.1126/science.271.5250.788
- Ruff, S.E., Probandt, D., Zinkann, A.-C., Iversen, M.H., Klaas, C., Würzberg, L., Krombholz, N., Wolf-Gladrow, D., Amann, R., Knittel, K., 2014. Indications for algae-degrading benthic microbial communities in deep-sea sediments along the Antarctic Polar Front. *Deep Sea Research Part II: Topical Studies in Oceanography* 108, 6–16. doi:10.1016/j.dsr2.2014.05.011
- Ruhl, H.A., Ellena, J.A., Smith, K.L., Jr., 2008. Connections between climate, food limitation, and carbon cycling in abyssal sediment communities. *proc Natl Acad Sci U S A* 105, 17006–17011. doi:10.1073/pnas.0803898105
- Rysgaard, S., Glud, R.N., 2004. Denitrification and anammox activity in Arctic marine sediments. *Limnol Oceanogr.*
- Sackett, W.M., 1986. Organic-Carbon in Sediments Underlying the Ross Ice Shelf. *Org Geochem* 9, 135–137.
- Sackett, W.M., Eckelmann, W.R., Bender, M.L., Be, A.W.H., 1965. Temperature Dependence of Carbon Isotope Composition in Marine Plankton and Sediments. *Science* 148, 235–237. doi:10.1126/science.148.3667.235
- Sañé, E.S., Isla, E., Gerdes, D., Montiel, A., Gili, J.M., 2012. Benthic macrofauna

- assemblages and biochemical properties of sediments in two Antarctic regions differently affected by climate change. *Continental Shelf Research* 35, 53–63. doi:10.1016/j.csr.2011.12.008
- Sañé, E.S., Isla, E., Grémare, A., Gutt, J., Vétion, G., DeMaster, D.J., 2011a. Pigments in sediments beneath recently collapsed ice shelves: The case of Larsen A and B shelves, Antarctic Peninsula. *Journal of Sea Research* 65, 94–102. doi:10.1016/j.seares.2010.07.005
- Sañé, E.S., Isla, E., Pruski, A.M., Barcena, M.A., Vétion, G., DeMaster, D.J., 2011b. Diatom valve distribution and sedimentary fatty acid composition in Larsen Bay, Eastern Antarctica Peninsula. *Continental Shelf Research* 31, 1161–1168. doi:10.1016/j.csr.2011.04.002
- Scambos, T.A., Bohlander, J.A., Shuman, C.A., Skvarca, P., 2004. Glacier acceleration and thinning after ice shelf collapse in the Larsen B embayment, Antarctica. *Geophys. Res. Lett.* 31. doi:10.1029/2004GL020670
- Scambos, T.A., Fricker, H.A., Liu, C.-C., Bohlander, J., Fastook, J., Sargent, A., Massom, R., Wu, A.-M., 2009. Ice shelf disintegration by plate bending and hydro-fracture: Satellite observations and model results of the 2008 Wilkins ice shelf break-ups. *Earth and Planetary Science Letters* 280, 51–60. doi:10.1016/j.epsl.2008.12.027
- Schever, P., 1978. *Marine Natural Products V2*. Academic PRESS LTD.
- Schleper, C., Jurgens, G., Jonuscheit, M., 2005. Genomic studies of uncultivated archaea. *Nat Rev Micro* 3, 479–488. doi:10.1038/nrmicro1159
- Schmid, M., Walsh, K., Webb, R., Rijpstra, W.I.C., van de Pas-Schoonen, K.T., Verbruggen, M.J., Hill, T., Moffett, B., Fuerst, J.A., Schouten, S., Sinninghe Damsté, J.S., Harris, J., Shaw, P.M., Jetten, M., Strous, M., 2003. Candidatus “*Scalindua brodae*,” sp. nov., Candidatus ‘*Scalindua wagneri*’, sp. nov., Two New Species of Anaerobic Ammonium Oxidizing Bacteria. *Systematic and Applied Microbiology* 26, 529–538. doi:10.1078/072320203770865837
- Schmidt, F., Elvert, M., Koch, B.P., Witt, M., Hinrichs, K.-U., 2009. Molecular characterization of dissolved organic matter in pore water of continental shelf sediments. *Geochim Cosmochim Acta* 73, 3337–3358. doi:10.1016/j.gca.2009.03.008
- Schofield, O.M., Ducklow, H.W., Martinson, D.G., Meredith, M.P., Moline, M.A., Fraser, W.R., 2010. How Do Polar Marine Ecosystems Respond to Rapid Climate Change? *Science* 328, 1520–1523. doi:10.1126/science.1185779
- Schouten, S., Hopmans, E.C., Schefuss, E., Sinninghe Damsté, J.S., 2002. Distributional variations in marine crenarchaeotal membrane lipids: a new tool for reconstructing ancient sea water temperatures? *Earth and Planetary Science Letters* 204, 265–274. doi:10.1016/s0012-821x(02)00979-2
- Schouten, S., Hopmans, E.C., Sinninghe Damsté, J.S., 2013. The organic geochemistry of glycerol dialkyl glycerol tetraether lipids: A review. *Org Geochem* 54, 19–61. doi:10.1016/j.orggeochem.2012.09.006

- Schouten, S., Ossebaar, J., Brummer, G.J., Elderfield, H., 2007a. Transport of terrestrial organic matter to the deep North Atlantic Ocean by ice rafting. *Org Geochem*.
- Schouten, S., van der Meer, M.T.J., Hopmans, E.C., Rijpstra, W.I.C., Reysenbach, A.-L., Reysenbach, A.L., Ward, D.M., Ward, D.M., Sinninghe Damsté, J.S., 2007b. Archaeal and bacterial glycerol dialkyl glycerol tetraether lipids in hot springs of yellowstone national park. *Applied and Environmental Microbiology* 73, 6181–6191. doi:10.1128/AEM.00630-07
- Schubotz, F., Lipp, J.S., Elvert, M., Hinrichs, K.-U., 2011. Stable carbon isotopic compositions of intact polar lipids reveal complex carbon flow patterns among hydrocarbon degrading microbial communities at the Chapopote asphalt volcano. *Geochim Cosmochim Acta* 75, 4399–4415. doi:10.1016/j.gca.2011.05.018
- Sharma, A.K., Becker, J.W., Ottesen, E.A., Bryant, J.A., Duhamel, S., Karl, D.M., Cordero, O.X., Repeta, D.J., DeLong, E.F., 2014. Distinct dissolved organic matter sources induce rapid transcriptional responses in coexisting populations of *Prochlorococcus*, *Pelagibacter* and the OM60 clade. *Environmental Microbiology* 16, 2815–2830. doi:10.1111/1462-2920.12254
- Shaw, P.M., Jones, G.J., Smith, J.D., Johns, R.B., 1989. Intraspecific Variations in the Fatty-Acids of the Diatom *Skeletonema-Costatum*. *Phytochemistry* 28, 811–815.
- Shimodaira, H., 2004. Approximately unbiased tests of regions using multistep-multiscale bootstrap resampling. *Ann. Statist.* 32, 2616–2641. doi:10.1214/009053604000000823
- Sinninghe Damsté, J.S., Rijpstra, W.I.C., Coolen, M.J.L., Schouten, S., Volkman, J.K., 2007. Rapid sulfurisation of highly branched isoprenoid (HBI) alkenes in sulfidic Holocene sediments from Ellis Fjord, Antarctica. *Org Geochem* 38, 128–139. doi:10.1016/j.orggeochem.2006.08.003
- Sinninghe Damsté, J.S., Rijpstra, W.I.C., Hopmans, E.C., Prahl, F.G., Wakeham, S.G., Schouten, S., 2002a. Distribution of membrane lipids of planktonic Crenarchaeota in the Arabian Sea. *Applied and Environmental Microbiology* 68, 2997–3002. doi:10.1128/AEM.68.6.2997-3002.2002
- Sinninghe Damsté, J.S., Schouten, S., Hopmans, E.C., van Duin, A.C.T., Geenevasen, J.A.J., 2002b. Crenarchaeol: the characteristic core glycerol dibiphytanyl glycerol tetraether membrane lipid of cosmopolitan pelagic crenarchaeota. *The Journal of Lipid Research* 43, 1641–1651. doi:10.1194/jlr.M200148-JLR200
- Skerratt, J.H., Nichols, P.D., McMeekin, T.A., Burton, H.R., 1995. Seasonal and inter-annual changes in planktonic biomass and community structure in eastern Antarctica using signature lipids. *Mar Chem*.
- Smetacek, V., Klaas, C., Strass, V.H., Assmy, P., Montresor, M., Cisewski, B., Savoye, N., Webb, A., d'Ovidio, F., Arrieta, J.M., Bathmann, U., Bellerby, R., Berg, G.M., Croot, P., Gonzalez, S., Henjes, J., Herndl, G.J., Hoffmann, L.J., Leach, H., Losch, M., Mills, M.M., Neill, C., Peeken, I., Röttgers, R., Sachs, O., Sauter, E., Schmidt, M.M.,

- Schwarz, J., Terbrüggen, A., Wolf-Gladrow, D., 2012. Deep carbon export from a Southern Ocean iron-fertilized diatom bloom. *Nature* 487, 313–319.
doi:10.1038/nature11229
- Smith, C.R., Mincks, S.L., Mincks, S., DeMaster, D.J., 2008. The FOODBANCS project: Introduction and sinking fluxes of organic carbon, chlorophyll-a and phytodetritus on the western Antarctic Peninsula continental shelf. *Deep Sea Research Part II: Topical Studies in Oceanography*.
- Smith, C.R., Mincks, S.L., Mincks, S., DeMaster, D.J., 2006. A synthesis of benthic-pelagic coupling on the Antarctic shelf: Food banks, ecosystem inertia and global climate change. *Deep Sea Research Part II: Topical Studies in Oceanography* 53, 875–894.
doi:10.1016/j.dsr2.2006.02.001
- Smith, C.R., Pope, R.H., DeMaster, D.J., Magaard, L., 1993. Age-Dependent Mixing of Deep-Sea Sediments. *Geochim Cosmochim Acta* 57, 1473–1488.
- Stookey, L.L., 1970. Ferrozine---a new spectrophotometric reagent for iron. *Anal. Chem.* 42, 779–781. doi:10.1021/ac60289a016
- Sun, M.-Y., Wakeham, S.G., 1999. Diagenesis of planktonic fatty acids and sterols in Long Island Sound sediments: Influences of a phytoplankton bloom and bottom water oxygen content. *J Mar Res* 57, 357–385. doi:10.1357/002224099321618254
- Sun, M.-Y., Wakeham, S.G., 1994. Molecular evidence for degradation and preservation of organic matter in the anoxic Black Sea Basin. *Geochim Cosmochim Acta* 58, 3395–3406. doi:10.1016/0016-7037(94)90094-9
- Sun, M.-Y., Wakeham, S.G., Lee, C., 1997. Rates and mechanisms of fatty acid degradation in oxic and anoxic coastal marine sediments of Long Island Sound, New York, USA. *Geochim Cosmochim Acta* 61, 341–355. doi:10.1016/S0016-7037(96)00315-8
- Suzuki, R., Shimodaira, H., 2006. Pvclust: an R package for assessing the uncertainty in hierarchical clustering. *Bioinformatics* 22, 1540–1542.
doi:10.1093/bioinformatics/btl117
- Sylvan, J.B., Toner, B.M., Edwards, K.J., 2012. Life and Death of Deep-Sea Vents: Bacterial Diversity and Ecosystem Succession on Inactive Hydrothermal Sulfides. *mBio* 3, e00279–11. doi:10.1128/mBio.00279-11
- Takano, Y., Chikaraishi, Y., Ogawa, N.O., Nomaki, H., Morono, Y., Inagaki, F., Kitazato, H., Hinrichs, K.-U., Ohkouchi, N., 2010. Sedimentary membrane lipids recycled by deep-sea benthic archaea. *Nature Geoscience* 3, 858–861. doi:10.1038/ngeo983
- Taylor, J., Parkes, R.J., 1983. The Cellular Fatty-Acids of the Sulfate-Reducing Bacteria, *Desulfobacter* Sp, *Desulfobulbus* Sp and *Desulfovibrio-Desulfuricans*. *Journal of General Microbiology* 129, 3303–3309.
- Teske, A.P., Durbin, A.M., Durbin, A., Ziervogel, K., Cox, C., Arnosti, C., 2011. Microbial Community Composition and Function in Permanently Cold Seawater and Sediments from an Arctic Fjord of Svalbard. *Applied and Environmental*

- Microbiology 77, 2008–2018. doi:10.1128/aem.01507-10
- Teske, A.P., Sorensen, K.B., 2008. Uncultured archaea in deep marine subsurface sediments: have we caught them all? *ISME J* 2, 3–18. doi:10.1038/ismej.2007.90
- Tully, B.J., Heidelberg, J.F., 2016. Potential Mechanisms for Microbial Energy Acquisition in Oxidic Deep Sea Sediments. *Applied and Environmental Microbiology* AEM.01023–16. doi:10.1128/AEM.01023-16
- Turner, J., Colwell, S.R., Marshall, G.J., Lachlan Cope, T.A., Carleton, A.M., Jones, P.D., Lagun, V., Reid, P.A., Iagovkina, S., 2005. Antarctic climate change during the last 50 years. *International Journal of Climatology* 25, 279–294. doi:10.1002/joc.1130
- Vaughan, D.G., Marshall, G.J., Connolley, W.M., Parkinson, C., Mulvaney, R., Hodgson, D.A., King, J.C., Pudsey, C.J., Turner, J., 2003. Recent Rapid Regional Climate Warming on the Antarctic Peninsula. *Climatic Change* 60, 243–274. doi:10.1023/a:1026021217991
- Veit-Köhler, G., Guilini, K., Peeken, I., Sachs, O., Sauter, E.J., Würzberg, L., 2011. Antarctic deep-sea meiofauna and bacteria react to the deposition of particulate organic matter after a phytoplankton bloom. *Deep Sea Research Part II: Topical Studies in Oceanography* 58, 1983–1995. doi:10.1016/j.dsr2.2011.05.008
- Venkatesan, M.I., 1988. Organic geochemistry of marine sediments in Antarctic region - Marine lipids in McMurdo Sound. *Org Geochem* 12, 13–27. doi:10.1016/0146-6380(88)90111-8
- Venkatesan, M.I., Kaplan, I.R., 1987. The Lipid Geochemistry of Antarctic Marine-Sediments - Bransfield Strait. *Mar Chem* 21, 347–375. doi:10.1016/0304-4203(87)90056-9
- Venkatesan, M.I., Kaplan, I.R., 1982. Distribution and transport of hydrocarbons in surface sediments of the Alaskan outer continental shelf. *Geochim Cosmochim Acta* 46, 2135–2149. doi:10.1016/0016-7037(82)90190-9
- Venkatesan, M.I., Ruth, E., Kaplan, I.R., 1986. Coprostanols in Antarctic marine sediments: A biomarker for marine mammals and not human pollution. *Marine Pollution Bulletin*.
- Venkatesan, M.I., Santiago, C.A., 1989. Sterols in ocean sediments: novel tracers to examine habitats of cetaceans, pinnipeds, penguins and humans. *Mar Biol* 102, 431–437. doi:10.1007/BF00438343
- Vick-Majors, T.J., Achberger, A.M., Santibáñez, P., Dore, J.E., Hodson, T., Michaud, A.B., Christner, B.C., Mikucki, J., Skidmore, M.L., Powell, R., Adkins, W.P., Barbante, C., Mitchell, A., Scherer, R., Prisco, J.C., 2016. Biogeochemistry and microbial diversity in the marine cavity beneath the McMurdo Ice Shelf, Antarctica. *Limnol Oceanogr* 61, 572–586. doi:10.1002/lno.10234
- Viso, A.-C., Marty, J.-C., 1993. Fatty acids from 28 marine microalgae. *Phytochemistry* 34, 1521–1533. doi:10.1016/S0031-9422(00)90839-2
- Volkman, J.K., 2003. Sterols in microorganisms. *Applied Microbiology and*

- Biotechnology 60, 495–506. doi:10.1007/s00253-002-1172-8
- Volkman, J.K., 1986. A Review of Sterol Markers for Marine and Terrigenous Organic-Matter. *Org Geochem* 9, 83–99.
- Volkman, J.K., Barrett, S.M., Blackburn, S.I., Mansour, M.P., Sikes, E.L., Gelin, F., 1998. Microalgal biomarkers: A review of recent research developments. *Org Geochem* 29, 1163–1179. doi:10.1016/s0146-6380(98)00062-x
- Volkman, J.K., Barrett, S.M., Dustan, G.A., 1994. C25 and C30 Highly Branched Isoprenoid Alkenes in Laboratory Cultures of Two Marine Diatoms. *Org Geochem* 21, 407–413.
- Volkman, J.K., Burton, H.R., Everitt, D.A., Allen, D.I., 1988. Pigment and Lipid Compositions of Algal and Bacterial Communities in Ace Lake, Vestfold Hills, Antarctica. *Hydrobiologia* 165, 41–57.
- Volkman, J.K., Jeffrey, S.W., Nichols, P.D., Rogers, G.I., Garland, C.D., 1989. Fatty-Acid and Lipid-Composition of 10 Species of Microalgae Used in Mariculture. *J Exp Mar Bio Ecol* 128, 219–240.
- Volkman, J.K., Johns, R.B., Gillan, F.T., Perry, G.J., Bavor, H.J., Jr, 1980. Microbial lipids of an intertidal sediment—I. Fatty acids and hydrocarbons. *Geochim Cosmochim Acta* 44, 1133–1143. doi:10.1016/0016-7037(80)90067-8
- Wakeham, S.G., 1995. Lipid biomarkers for heterotrophic alteration of suspended particulate organic matter in oxygenated and anoxic water columns of the ocean. *Deep-Sea Research Part I* 42, 1749–1771.
- Wakeham, S.G., Canuel, E.A., 2006. Degradation and Preservation of Organic Matter in Marine Sediments, in: Volkman, J.K. (Ed.), *The Handbook of Environmental Chemistry, Marine Organic Matter, The Handbook of Environmental Chemistry*. Springer-Verg, Berlin/Heidelberg, pp. 295–321. doi:10.1007/698_2_009
- Wakeham, S.G., Hedges, J.I., Lee, C., Peterson, M.J., Hernes, P.J., 1997. Compositions and transport of lipid biomarkers through the water column and surficial sediments of the equatorial Pacific Ocean. *Deep Sea Research Part II: Topical Studies in Oceanography* 44, 2131–2162.
- Wakeham, S.G., Lee, C., 1993. Production, Transport, and Alteration of Particulate Organic Matter in the Marine Water Column, in: *Organic Geochemistry, Topics in Geobiology*. Springer US, Boston, MA, pp. 145–169. doi:10.1007/978-1-4615-2890-6_6
- Warton, D.I., Hui, F.K.C., 2011. The arcsine is asinine: the analysis of proportions in ecology. *Ecology* 92, 3–10. doi:10.1890/10-0340.1
- Wefer, G., Fischer, G., Fütterer, D.K., Gersonde, R., 1988. Seasonal particle flux in the Bransfield Strait, Antarctica. *Deep Sea Research* 35, 891–898. doi:10.1016/0198-0149(88)90066-0
- Weijers, J.W.H., Panoto, E., van Bleijswijk, J., Schouten, S., Rijpstra, W.I.C., Balk, M., Stams, A.J.M., Sinninghe Damsté, J.S., 2009. Constraints on the Biological Source(s) of the Orphan Branched Tetraether Membrane Lipids. *Geomicrobiology Journal* 26,

- 402–414. doi:10.1080/01490450902937293
- Weijers, J.W.H., Schouten, S., Hopmans, E.C., Geenevasen, J.A.J., David, O.R.P., Coleman, J.M., Pancost, R.D., Sinninghe Damsté, J.S., 2006a. Membrane lipids of mesophilic anaerobic bacteria thriving in peats have typical archaeal traits. *Environmental Microbiology* 8, 648–657. doi:10.1111/j.1462-2920.2005.00941.x
- Weijers, J.W.H., Schouten, S., Spaargaren, O.C., Sinninghe Damsté, J.S., 2006b. Occurrence and distribution of tetraether membrane lipids in soils: Implications for the use of the TEX86 proxy and the BIT index. *Org Geochem* 37, 1680–1693. doi:10.1016/j.orggeochem.2006.07.018
- Westrich, J.T., Berner, R.A., 1984. The Role of Sedimentary Organic-Matter in Bacterial Sulfate Reduction - the G Model Tested. *Limnol Oceanogr* 29, 236–249.
- Williams, T.J., Wilkins, D., Long, E., Evans, F., DeMaere, M.Z., Raftery, M.J., Cavicchioli, R., 2013. The role of planktonic Flavobacteria in processing algal organic matter in coastal East Antarctica revealed using metagenomics and metaproteomics. *Environmental Microbiology* 15, 1302–1317. doi:10.1111/1462-2920.12017
- Witte, U., Wenzhofer, F., Sommer, S., Boetius, A., Heinz, P., 2003. In situ experimental evidence of the fate of a phytodetritus pulse at the abyssal sea floor. *Nature*.
- Wuchter, C., Abbas, B., Coolen, M.J.L., Herfort, L., van Bleijswijk, J., Timmers, P., Strous, M., Teira, E., Herndl, G.J., Middelburg, J.J., Schouten, S., Sinninghe Damsté, J.S., 2006. Archaeal nitrification in the ocean. *proceedings of the National Academy of Sciences* 103, 12317–12322. doi:10.1073/pnas.0600756103
- Wuchter, C., Schouten, S., Coolen, M.J.L., Sinninghe Damsté, J.S., 2004. Temperature-dependent variation in the distribution of tetraether membrane lipids of marine Crenarchaeota: Implications for TEX86 paleothermometry. *Paleoceanography* 19. doi:10.1029/2004pa001041
- Yanagawa, K., Morono, Y., de Beer, D., Haeckel, M., Sunamura, M., Futagami, T., Hoshino, T., Terada, T., Nakamura, K.-I., Urabe, T., Rehder, G., Boetius, A., Inagaki, F., 2013. Metabolically active microbial communities in marine sediment under high-CO₂ and low-pH extremes. *ISME J* 7, 555–567. doi:10.1038/ismej.2012.124
- Yoon, H., Park, B.-K., Kim, Y., Kang, C.Y., Kang, S.-H., 2003. Origins and paleoceanographic significance of layered diatom ooze interval from the Bransfield Strait in the northern Antarctic Peninsula around 2500 yrs BP. *Antarctic Research Series* 79, 225–238. doi:doi:10.1029/AR079p0225
- Yoon, J., Matsuo, Y., Adachi, K., Nozawa, M., Matsuda, S., Kasai, H., Yokota, A., 2008. Description of *Persicirhabdus sediminis* gen. nov., sp. nov., *Roseibacillus ishigakijimensis* gen. nov., sp. nov., *Roseibacillus ponti* sp. nov., *Roseibacillus persicus* sp. nov., *Luteolibacter pohnpeiensis* gen. nov., sp. nov. and *Luteolibacter algae* sp. nov., six marine members of the phylum “Verrucomicrobia,” and emended descriptions of the class Verrucomicrobiae, the order Verrucomicrobiales and the

- family Verrucomicrobiaceae. INTERNATIONAL JOURNAL OF SYSTEMATIC AND EVOLUTIONARY MICROBIOLOGY 58, 998–1007. doi:10.1099/ijs.0.65520-0
- Yoshinaga, M.Y., Sumida, P.Y.G., Wakeham, S.G., 2008. Lipid biomarkers in surface sediments from an unusual coastal upwelling area from the SW Atlantic Ocean. *Org Geochem* 39, 1385–1399. doi:10.1016/j.orggeochem.2008.07.006
- Yunker, M.B., Belicka, L.L., Harvey, H.R., Macdonald, R.W., 2005. Tracing the inputs and fate of marine and terrigenous organic matter in Arctic Ocean sediments: A multivariate analysis of lipid biomarkers. *Deep Sea Research Part II: Topical Studies in Oceanography* 52, 3478–3508. doi:10.1016/j.dsr2.2005.09.008
- Zegouagh, Y., Derenne, S., Largeau, C., Bardoux, G., Mariotti, A., 1998. Organic matter sources and early diagenetic alterations in Arctic surface sediments (Lena River delta and Laptev Sea, Eastern Siberia), II. *Org Geochem* 28, 571–583. doi:10.1016/S0146-6380(98)00020-5

Biography

Megumi S. Shimizu

Born: November 16, 1987, Osaka, Japan

Education

Doctor of Philosophy, Marine Science and Conservation (2017)

Duke University, Nicholas School of the Environment, Durham, North Carolina USA

Bachelor of Arts, Biology (2010)

International Christian University, Tokyo, Japan

Publications

McCormick, M.L., Seraichick, A.D., Bucceri, E.M., Huebner, E.J., Shimizu, M., Antonopoulos, D.A., Koval, J.C., Cape, M.R., Vernet, M., Grange, L., Smith, C.R., Domack, E.W., Leventer, A., 2013. Impact of ice-shelf loss on geochemical profiles and microbial community composition in marine sediments of the Larsen A embayment, Antarctic Peninsula. American Chemical Society Meeting 245.

Sakaue, H., Dan, R., Shimizu, M., Kazama, H., 2012. Note: in vivo pH imaging system using luminescent indicator and color camera. Rev Sci Instrum 83, 076106. doi:10.1063/1.4737875

Sakaue, H., Morita, K., Goto, M., Shimizu, M., Hyakutake, T., Nishide, H., 2008. Chemical Flow Control Method Using Combination of Hydrophobic and Hydrophilic Coatings, in: Presented at the 46th AIAA Aerospace Sciences Meeting and Exhibit, American Institute of Aeronautics and Astronautics, Reston, Virginia. doi:10.2514/6.2008-632

Fellowships and Award

Student Exchange Support Program for Long-Term Study Abroad 2010 – 2015

Japan Student Services Organization (JASSO)

Summer Research Fellowship, Duke University Graduate School, 2015

Travel Scholarship, European Association of Organic Geochemistry, 2014

Dissertation Research Travel Award, Duke University Graduate School, 2013

Graduate Student and Postdoctoral Research Exchange, 2012

Center for Dark Energy Biosphere Institute

Joseph S. Ramus Endowment Fund, Duke University 2011-2013